Institut für Biologische Chemie und Ernährungswissenschaft
Universität Hohenheim

Role of reactive oxygen species in anti-cancer treatment: Investigations in 2-methoxyestradiol chemotherapy and 5-aminolevulinic acid based photodynamic therapy combined with hyperthermia

Dissertation
zur Erlangung des Grades eines Doktors
der Naturwissenschaften

der Fakultät Naturwissenschaften
der Universität Hohenheim

vorgelegt von
Christine Lambert
aus Schwäbisch Gmünd
2002

Tag der mündlichen Prüfung: 30.01.2003

Dekan: Prof. Dr. rer. nat. K. Bosch

Berichterstatter, 1. Prüfer: PD Dr. rer. nat. J. Frank

Mitberichterstatter, 2. Prüfer: Prof. Dr. med. H.K. Biesalski

3. Prüfer: HD Dr. med. O. Thews

The best way to predict future

is to create it.

Peter F. Drucker

The present work has in part been published as follows:

Lambert C., Thews O., Biesalski H.K., Vaupel P., Kelleher D.K., and Frank J.
2-Methoxyestradiol Enhances Reactive Oxygen Species Formation andIncreases the Efficacy of Oxygen Radical Generating Tumor Treatment, EurJ Med Res 7, 404-414, 2002

Lambert C., Apel K., Biesalski H.K., and Frank J.
Apoptosis signaling by 2-methoxyestradiol in DS-sarcoma cells, Eur J Cancer. 38 (Supplement 7), S169, 2002
(Poster presentation at 14th EORTC-NCI-ACCR Symposium on Molecular Targets and Cancer Therapeutics, November 19th-22th, 2002, Frankfurt, Germany)

Lambert C., Thews O., Kelleher D.K., Biesalski H.K., Vaupel P., and Frank J.
2-methoxyestradiol in combination with oxidative stress inhibits proliferation of sarcoma cells in vitro and in vivo. Proceeding Book of 12th international congress on anti-cancer treatment 2002, S233
(Poster presentation at 12th international congress on anti-cancer treatment, Februrary 4th-7th, 2002, Paris, France)

Frank J., Lambert C., Thews O., Kelleher D.K., Vaupel P., Biesalski H.K.
Anti-tumorigenic effects of 2-methoxyestradiol in DS-sarcoma cells in vitro and in vivo. FASEB J., 16(5). A965, 2002
(Poster presentation at Experimental Biology 2002, April 20th-24th, 2002, New Orleans, Louisiana)

Frank J., Kelleher D.K., Lambert C., Thews O., Vaupel P., Biesalski H.K.
Involvement of oxidative injury in the enhancement of the antitumor effects of ALA-based photodynamic therapy by hyperthermia. FASEB J., 16(5). A1204, 2002
(Poster presentation at Experimental Biology 2002, April 20th-24th, 2002, New Orleans, Louisiana)

Index

Acknowledgements

First of all, I sincerely thank Dr. rer. nat. habil. J. Frank, University of Hohenheim, for the initiation, his steady interest and the constructive suggestions. I greatly appreciate his friendly and motivating disposition. Of course, I would like to thank him for his great help in writing the publication representing parts of this thesis.

I am indebted to Prof. Dr. med. H.K. Biesalski, who had the basic idea to investigate 2-methoxyestradiol due to its SOD inhibiting activity and also encouraged me to publish these data.

My special thanks also go to Dr. med. habil. O. Thews, University of Mainz, for his cooperation, scientific support and accepting to be my third examiner and Dr. rer. nat. D.K. Kelleher, University of Mainz, who performed the *in vivo* experiments of the ALA-PDT project.

I am grateful to Andrea Flaccus for her patience in answering my endless practical questions, for being my living dictionary and for sharing the "Kaiserschmarn" with me. I appreciate the time we spent together.

I am particularly thankful to Katrin Apel for her help in determining caspase-8 activity, Bcl-proteins und FasL/TNF? for the 2-ME experiment.

Special thanks to the PHD "students" of the old school, especially to Dr. rer. nat. Inka Pfitzner, who assisted me with the administrative questions of this thesis. I also want to thank Gundel Essig for her friendly help in histology and for the nice "cutting sessions" in the cellar. A big "Thank you" for the pleasant atmosphere in the lab to all my co-workers, particularly to those not specifically mentioned.

And finally I want to thank my friend, Klaus Betz, and my parents for their steady support and patience, without which, I could not have accomplished this work.

Abbreviations

A	adenine
7-AAD	7-aminoactinomycin D
AIF	apoptosis inducing factor
ALA	5-aminolevulinic acid
AP	alkaline phosphatase
APAF-1	apoptotic protease activating factor 1
BHT	butylated hydroxy toluene
BSO	buthionine sulfoximine
C	cytosine
CCCP	carbonyl cyanide m-chlorophenylhydrazone
CFE	colony forming efficiency
$\Delta\Psi_m$	mitochondrial membrane potential
DAPI	4´,6´-diamino-2-phenylindole dihydrochloride
DCF	2´,7´-dichlorofluorescein
DDC	diethyldithiocarbamate
DFF45/ICAD	DNA fragmentation factor-45/inhibitor of caspase-activated DNase
DHE	dihydroethidium
DISC	death initiating signalling complex
DOX	doxorubicin
FADD	Fas-associated death receptor
FITC	fluoresceinisothiocyanat
FSC	forward light scatter
G	guanine
GAPDH	glyceraldehyde-3-phosphate dehydrogenase
GSH	reduced glutathione
GSSX	total oxidised glutathione
HO-1	heme oxygenase-1
HRP	horseradish peroxidase
HT	hyperthermia
HX	hypoxanthine
IgG	immunoglobuline G
i.p.	intraperitoneal
i.v.	intravenous
2-ME	2-methoxyestradiol
MMP	matrix metalloproteinase
MTPT	mitochondrial transition permeability pore

HSP	heat shock protein
PDT	photodynamic therapy
PARP	poly (ADP-ribose) polymerase
PBS	phosphate buffered saline, pH 7.4
PUFAs	polyunsaturated fatty acids
PVDF	polyvinylidene fluoride
RH	respiratory hyperoxia
ROS	reactive oxygen species
RT-PCR	reverse transcriptase polymerase chain reaction
SD	standard deviation
SDS	sodium dodecyl sulfate
SEM	standard error of the mean
SOD	superoxide dismutase
T	thymine
TBARS	thiobarbituric acid reactive substances
TBE	Tris borate EDTA
tBid	truncated Bid
TBS	Tris-buffered saline
TBST	Tris-buffered saline containing Tween 20
TdT	terminal deoxynucleotidyl transferase
TE	Tris EDTA
VDAC	voltage dependent anion channel
XO	xanthine oxidase

1 Introduction

Free radicals arising from metabolism or environmental sources continuously interact in biological systems and there is evidence that oxidants and antioxidants must be in balance to mimic molecular, cellular and tissue damage. Such damage can arise from our own body metabolism, exposure to environmental stress, infections, micro-organisms, viruses, parasites etc., and of course during ageing. Biological structures, in particular polyunsaturated membrane lipids, DNA and amino acids, are the target molecules reacting with ROS. The cellular effects of free radicals are dependent on their concentration and the target cell type: at low concentrations ROS are involved in signal transduction and thus regulate gene expression, whereas high concentrations of ROS cause malignant transformation or apoptosis depending on cell type [1,2]. Necrotic cell death mainly occures at very high ROS levels [3].

It appears as though the action of free radicals on normal and tumour cells is diametrically opposite: when free radicals attack normal cells, DNA damage can occur, leading to the development of tumours, whereas when the same free radicals are produced in excess in tumour cells, there is a beneficial action, namely elimination of those cells [4]. Oxidative stress leads to inhibition of tumour cell growth by several mechanisms including p53 upregulation, Bcl-2 inactivation and telomere shortening [4-6]. Anti-cancer treatments acting via ROS-formation include radiation, anthracyclines, hyperthermia and photodynamic therapy. But there are also physiological substances like polyunsaturated fatty acides (especially n-3 PUFAs), cytokines and 2-methoxyestradiol, which express anti-cancer action by the mechanisms mentioned above. Fig. 1.1 shows an overview about various factors executing tumour regression by ROS-formation.
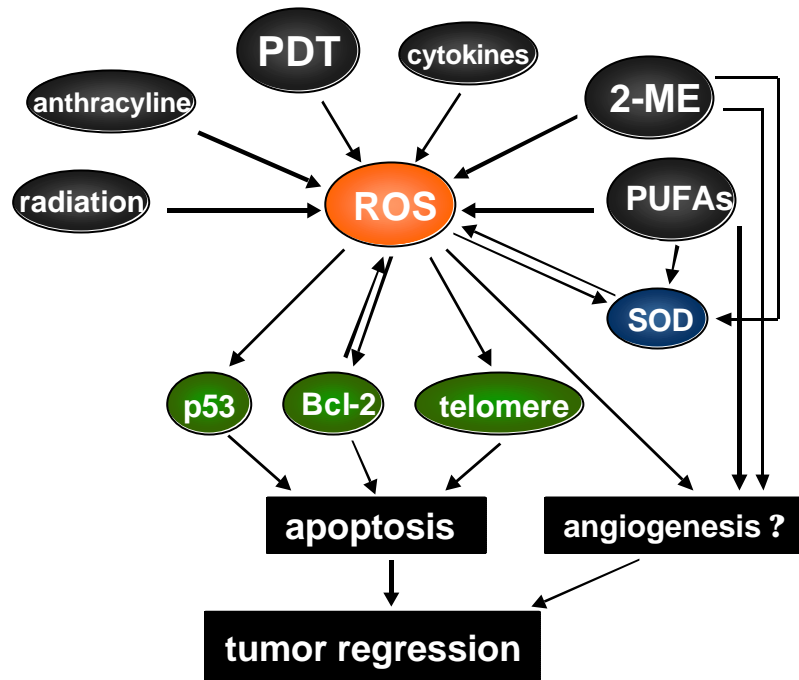
Fig. 1.1: Scheme showing possible interaction of various factors generating ROS on tumour regression. Free radical mediated inhibition of tumour growth can be induced by enhanced expression of p53, inactivation of Bcl-2, telomere shortening and inhibition of angiogenesis (modified [4]).

At the moment ionisating radiation and chemotherapy with anthracyclines (especially doxorubicin) are the most frequently used ROS-generating anti-cancer treatments. Anthracyclines are capable of generating superoxide anions (O_2^-), typically by redox cycling with oxygen. These drugs contain electron-transfer entities that readily accept electrons from biological sources, followed by transfer to oxygen [7], which leads to the production of superoxide anions. Conversion of O_2^- leads to production of other reactive oxygen species like hydrogen peroxide (H_2O_2) or the highly reactive hydroxyl radical ($OH^?$). The following reactions take part in this process:

$2\,O_2^- + 2\,H_2O \quad ? \quad 2\,H_2O_2 + O_2$ \qquad\qquad (catalase reaction)

$Fe(II) + H_2O_2 \quad ? \quad Fe(III) + OH^? + OH^-$ \qquad (Fenton reaction)
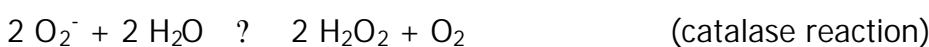
Unfortunately the drug doxorubicin can also undergo redox cycling with cytochrome P-450 species in the endoplasmic reticulum of the liver and the sarcoplasmic reticulum of cardiac muscle [8]. This reaction causes cardiotoxicity, a serious side-effect of doxorubicin. The lower level of antioxidant systems, especially the low catalase activity in heart cells is a contributing factor.

Ionising radiation causes ROS-generation by another mechanism than anthracyclines. Because cells are 80% aqueous, the majority of the energy of radiation is absorbed by water, resulting in ionisation to hydrogen atoms, solvated electrons and most importantly in terms of damage to DNA, hydroxyl radicals.

However, some tumours are resistant to ROS-generating treatments. There are several mechanisms affecting tumour response to these treatments. Enhanced antioxidative capacities of tumour cells, caused by high intracellular levels of antioxidants (e.g. glutathione, vitamin E) or ROS detoxifying enzymes (e.g. superoxide dismutase), are important reasons for this phenomenon [9,10].

Oxygenation of the tumour is another parameter influencing tumour response to anti-cancer therapies. In hypoxic tumours ROS-generating treatments show relatively low response rates due to the fact that the low level of molecular oxygen terminates the formation of superoxide anions, hydroxyl radicals and hydrogen peroxide [11,12]. Development of new, more tumour specific ROS-generating treatments could enhance the efficiency of anti-cancer therapies with lesser side-effects. Furthermore, using these treatments as adjuvant in established anti-cancer regimes may increase the response rate of tumours having poor prognosis at the moment. The studies in this thesis are part of this development by investigating the drug 2-methoxyestradiol (2-ME) and photodynamic therapy with 5-aminolevulinic acid. Both regimes generate ROS by different mechanisms, which lead to the death of tumour cells without any serious side-effects. Apoptotic cell death is mostly the consequence of these treatments, as mitochondria, playing a critical role in the apoptotic process, are damaged easily by ROS [13-15]. ROS induced permeabilisation of mitochondrial membranes results in release of various molecules that are crucial for apoptosis. Such molecules include procaspases, cytochrome c, endonuclease G and apoptosis inducing factor (AIF), which ultimately induce DNA fragmentation, the endpoint of

apoptosis [13,16]. Apoptosis is an energy-requiring process, associated with characteristic changes in cell morphology including condensation of chromatin with nuclear fragmentation, condensation of the cytosol into apoptotic bodies and changes in the cell surface that enable recognition by macrophages. These engulf apoptotic cells enabling them to be destroyed in a non-inflammatory manner. In contrast, necrosis is characterised by swelling of cell organelles and plasma membrane ruptures with the loss of intracellular contents into the surrounding medium. This attracts neutrophils which cause an inflammatory response and secondary damage to the tissue [17].

In this thesis two new anti-cancer treatments, (i) chemotherapy with 2-methoxy-estradiol (2-ME) and (ii) 5-aminolevulinic acid based photodynamic therapy (ALA-PDT), were investigated. Both therapies are known to generate reactive oxygen species. Due to this fact, the two independent studies presented in this thesis determined the anti-cancer effect of 2-ME and ALA-PDT as single therapies and in combination with hyperthermia to assess the possible benefit of these combinations. The following paragraphs briefly describe the supposed mechanisms of 2-ME and ALA-PDT responsible for killing tumour cells. Additionally, the advantages, possible side- effects and the clinical relevance of these therapies will be explained.

2-Methoxyestradiol

The natural estrogen metabolite 2-ME is formed by hydroxylation and methyl group transfer out of 17ß-estradiol or out of the contraceptiva 17-ethylestradiol [18]. Women in the luteal phase or pregnant women have elevated blood levels of 2-methoxyestrogens in a nanomolar range [19].
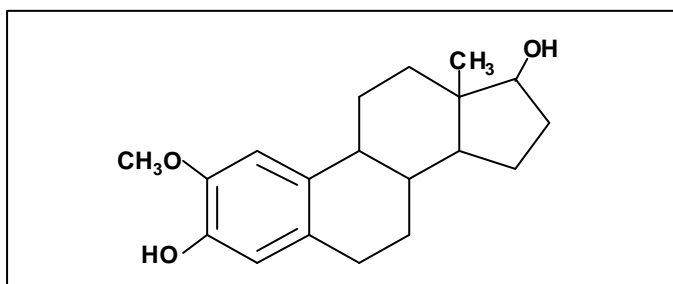
Fig. 1.2: Structure of 2-methoxy-estradiol (2-ME) [20].

The anti-cancer potential of 2-ME is independent of estrogen-receptor binding, because estrogen receptor affinities for 2-ME are extremely weak [21]. Selective growth inhibition of transformed (cancer) cells or tumours by 2-ME is a result of several factors. In 1994 d'Amato et al found that 2-ME inhibits tubulin polymerisation by interacting with the colchicine site [22]. Further investigations showed that 2-ME increases the insoluble polymerised fraction of cellular tubulin similar to the anti-cancer drug taxol [23]. The alteration of microtubuli formation induced by 2-ME can explain the inhibitory effect on cell growth but it does not elucidate the selective inhibition of tumour cells compared to normal cells. One possible explanation of this selective effect could be the inhibition of CuZn-superoxide dismutase (CuZn-SOD) by 2-ME which was recently reported by Huang and colleagues [15]. SOD detoxifies superoxide anions to H_2O_2 in an enzymatic reaction. Due to the high proliferation rates of tumour cells, resulting in enhanced levels of endogenous ROS compared to normal cells, 2-ME may achieve its selective effect by inhibition of SOD.

In recent years effect of 2-ME on many different cell types was assessed, showing growth inhibition in all tested cancer cell lines. Observed differences in sensitivity against 2-ME were dependent on cell line, not on cell type. Investigations on pancreatic cancer cell lines showed, that proliferation of 3 out of 4 cell lines were inhibited at a concentration between 2 and 3 µM 2-ME, whereas growth inhibition of the 4th cell line was achieved at a 4-fold higher concentration [20]. The role of p53 in 2-ME induced cell death is not clear, because p53 dependent and independent mechanisms were described [24,25]. Huober and colleagues reported that cells expressing wild-type p53 are more sensitive to 2-ME than cells with mutated p53 [24]. However this finding could not be validated by Huang [15].

2-ME induced cell death is associated with apoptosis including caspase activation [26], Bcl-2 phosphorylation (inactivation) or down-regulation [20,23] and changes in mitochondrial integrity [15,27]. Significance of reactive oxygen species in this process is presumably dependent on the investigated cell line [15,27].

In vivo 2-ME shows potent inhibition of tumour growth by oral application [24,28]. Responsible for the high tumour response rate *in vivo* are anti-angiogenetic properties of 2-ME in addition to the effects mentioned above [28,29]. These *in vivo*

studies demonstrated that 2-ME is a well tolerated, highly effective anti-cancer drug confirming the findings of cell culture tests.

At the moment, efficacy of 2-ME (Panzem^{TM}) is being investigated in four clinical trials (phase I and II) in USA. Patiens with myeloma, breast or prostate cancer get 2-ME orally as single agent therapy. Combination of 2-ME with the microtubule stabilising drug Taxotere[?] (docetaxel) is also tested. Unfortunately, results are not yet available.

Photodynamic therapy

Photodynamic therapy (PDT) is based on the administration of tumour-localising photosensitisers (generally porphyrin derivates), followed by exposure of the tumour region to light [30,31]. Irradiation of the photosensitiser with a specific wavelength generates reactive oxygen species including singlet oxygen. PDT promises to be more selective than radio- and chemotherapy and can be applied to recurrent tumours that have already received maximal doses of conventional treatment. Since photosensitisers lack toxicity in the absence of light, adverse reactions at other sites of drug accumulation are eliminated and the drug-activating light is harmless in the absence of sensitiser. Some limitations of PDT include light-inaccessible tumours and large tumour masses. [7].

In the last 20 years, several types of photosensitisers were developed and investigated. In the present study 5-aminolevulinic acid (ALA) was used as 'photosensitiser'. ALA is an endogenous precursor of the highly photosensitising protoporphyrin IX (Fig. 1.3). Compared to the first generation photosensitisers like Photofrin II[?], ALA is more tumour specific and has a higher rate of clearance from normal tissue [7]. *In vivo* ALA formation from glycine and succinyl-coenzyme A is the first step in the heme synthesis pathway. Subsequently two ALA molecules are formed to porphobilinogen. Further pathway intermediates are uroporphyrinogen, coproporphyrinogen and protoporphyrinogen. The latter one is oxidised to protoporphyrin IX, which is transformed to heme by incorperation of iron. Under

physiological conditions, ALA synthesis is tightly controlled by feedback regulation by intercellular heme. Exogenous application of ALA (orally or i.v.) bypass this pathway and can therefore lead to higher formation of photosensitive porphyrins in cells [32]. Based on the fact that protoporphyrin IX synthesis is located in the mitochondria and due to the lipophilic properties of protoporphyrin IX, ROS generated by ALA-PDT primarily damage mitochondria, lysosomes and plasma membranes [33].
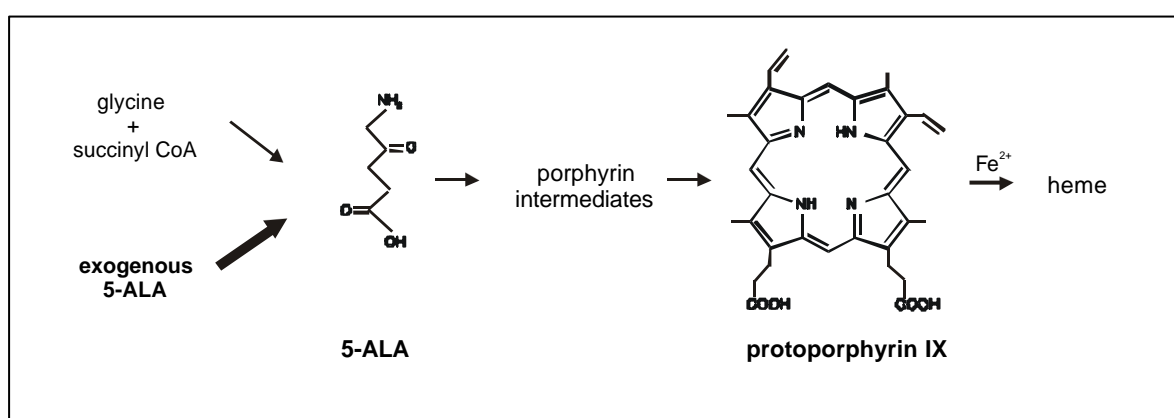
Fig. 1.3: Pathway of porphyrin biosynthesis [32]. First and last two steps of this biochemical pathway are located in the mitochondria, porphyrin intermediates are formed in cytosol.

The mechanism of ALA uptake and accumulation in malignant and regenerative cells are not completely understood. The active transport of the compound through plasma membranes was demonstrated in microorganisms and in cell culture [34,35]. However, a cell-type dependent uptake mechanism cannot be excluded [32]. It has been suggested that cells with higher turnover rates like tumour cells produce more protoporphyrin IX due to decreased ferrochelatase activity [36].

The initiating step of the photosensitising reaction is the absorption of a light photon by protoporphyrin IX, causing a shift of the molecule from its ground state to the extremely unstable excited singlet state. The excited protoporphyrin IX molecule either decays back to the ground state, resulting in the emission of light in the form

of fluorescence, or undergoes intersystem crossing to the more stable triplet excited state by electron spin conversion. The interaction of the triplet sensitiser with surrounding molecules results in two types of photooxidative reaction. Type I pathway involves transfer of electrons or hydrogen atoms producing radical forms of the photosensitiser or the substrate. The intermediates may further react with oxygen to form peroxides, superoxide anions and hydroxyl radicals, which initiate free radical chain reactions. Type II mechanism is mediated by an energy transfer process with ground state oxygen, leading to the formation of singlet oxygen and the return of the sensitiser to its ground state [32]. It is supposed that type II processes predominate in oxygenated systems, whereas type I reactions prevail under hypoxic conditions [36].
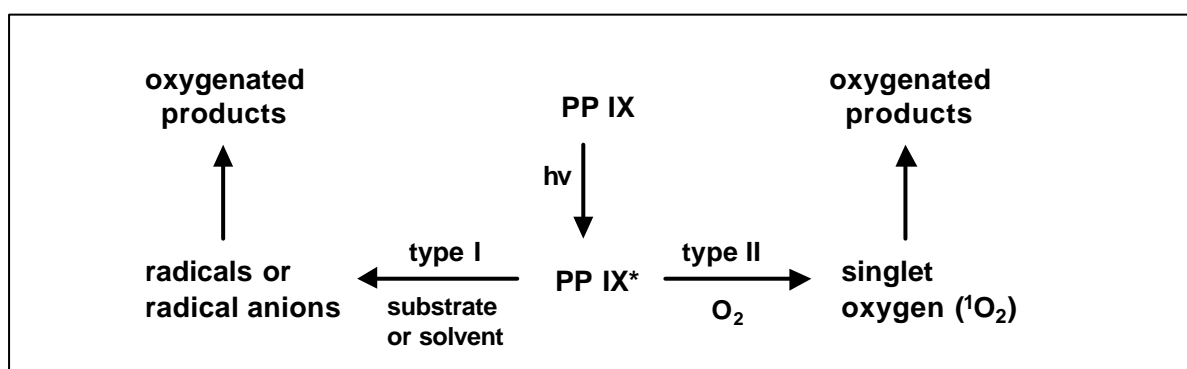
Fig. 1.4: Diagrammatic presentation of type I and type II photosensitised oxidation reactions of protoporphyrin IX (PP IX) [37].

In recent years many clinical trials and phase I-III studies have been carried out to investigate the clinical efficacy of ALA-PDT. The studies have been focused on skin tumours, but there have been also investigation on non skin tumours, e.g. bladder, kidney and colon tumours. High clinical response rates were described in these studies, however tumour size is the limiting factor for ALA-PDT efficacy. Ineffective penetration of ALA in large tumours, hypoxic conditions in the tumour centre and the limited irradiation depth may contribute to low response rates in large tumours [32].

Side-effects of ALA-PDT differ from topical ALA-treatment and systemic admini-stration. If ALA is topical applicated irradiation causes only a stringing and burning [38]. The side-effects associated with the systemic administration of ALA can be more serious. They may include transient liver function abnormalities, nausea and vomiting [39].

Aim of this thesis

Both anti-cancer treatments, chemotherapy with 2-ME as well as ALA-PDT, are highly specific regimes, demonstrated by high response rates and low side-effects. Combination of these regimes with conventional ROS-generating therapies may enhance the cytotoxic effect in a synergistic manner by producing excessive amounts of free radicals. Data have been shown that ?-radiation plus 2-ME treatment resulted in a dramatic increase in cell death compared to single treatments [24,40], whereas the successively followed combination of PDT and ?-radiation showed additive and synergistic effects, dependent on cell type and treatment regime [41-43]. In comparison to these regimes, simultaneous combination of PDT and ?-radiation resulted in increased efficiencies [44].

Interesting findings were observed combining PDT and hyperthermia. PDT followed by hyperthermia caused cytotoxicity in a synergistic manner [45,46], reversing the sequence of the treatments resulted only in additive tumour damage [30,46].

On the basis of above mentioned literature data, the studies of this thesis would like to elucidate the anti-tumour effect of

1. 2-ME in combination with a potent ROS inducing treatment (hyperthermia + hyperoxia + xanthine oxidase) and

2. simultaneous administration of ALA-PDT and hyperthermia.

In addition to point 1 a further objective is to enlighten 2-ME mediated signalling pathways leading to apoptosis. This information may avail to estimate the effect of 2-ME in different therapy regimes. Finally, results of this thesis should help to classify 2-ME and ALA-PDT as adjuvant therapies.

2 Materials and Methods

2.1 Materials

All chemicals were obtained from Sigma (Deisenhofen, Germany) unless otherwise indicated. Cell culture materials were purchased from Biochrom (Berlin, Germany) or Greiner (Frickenhofen, Germany).

2.2 Cell culture

DS-sarcoma cells of the rat were used for *in vitro* experiments. Cells were grown in RPMI medium supplemented with 10% fetal bovine serum and 2 mM glutamine at 37°C in a humidified 5% CO_2 atmosphere. They were passaged twice weekly.

2.3 Drug treatment

2-methoxyestradiol was dissolved in absolute ethanol to give a 20 mM solution and stored at -20°C. Cells were treated with 2-ME for up to 96 h. The concentration of ethanol in the medium of 2-ME treated and control cells was adjusted to 0.1% (v/v). In order to generate additional reactive oxygen species in 2-ME treated cells, the free radical generating system xanthine oxidase/hypoxanthine was used. For DHE-assay cells subsequently treated with 2-ME (48 h) were incubated in KRH^+ buffer (134 mM NaCl, 4.8 mM KCl, 1.2 mM KH_2PO_4, 1.2 mM $MgCl_2$ x 7 H_2O, 2.8 mM glucose, 20 mM HEPES, 1 mM $CaCl_2$ x 2 H_2O, pH 7,4) with or without 1 mM hypoxanthine and 10 mU/ml xanthine oxidase (Roche, Mannheim, Germany) for 50 min at 37°C. For determination of cell viability, cells were grown in medium containing 1 mM hypoxanthine and treated with 2-ME at the indicated doses for 48 h. 24 h after 2-ME addition 1 mU xanthine oxidase per ml medium was added.

2.4 Cell proliferation and viability

Cell numbers were determined by means of a cell counter (Casy[?] TTC, Schärfe System, Reutlingen, Germany).

For colony forming efficiency (CFE)-assay cells were treated with different stimulants for 48 h. Subsequently, cells were washed twice in medium and transferred into a 96-well-plate (dilution series from 1 to 512 cells/well). After 5 days, cell clones per

well were counted and the CFE was calculated as follows:

CFE [%] = clones per well / seeded cells per well x 100

Cell uptake of propidium iodide was used to identify dead cells. Drug-treated cells were stained with propidium iodide (0.2 µg/ml) in PBS for 10 min at room temperature. Thereafter, cells were washed three times in PBS and analysed for propidium iodide uptake by flow cytometry (Coulter Epics XL, Hamburg, Germany).

2.5   SOD activity

The effect of 2-ME on SOD activity was measured by the inhibition of pyrogallol autooxidation [47]. Here, bovine CuZn-SOD (25 ng/ml; Roche, Mannheim, Germany) was incubated with or without 0.01, 0.1 or 1 mM 2-ME for 5 min at room temperature. 4 µl of this mixture were added to 986 µl assay buffer (50 mM Tris/cacodylic acid, 1 mM diethyltriamine pentoacetic acid, 1200 U/ml catalase, pH 8.2). The reaction was started by the addition of 10 µl pyrogallol stock solution (20 mM pyrogallol in 0.01 N HCl). Pyrogallol autooxidation was measured as the rate of change of absorbance at 420 nm over 5 min. SOD inhibitor diethyldithiocarbamate (DDC) was used as a positive control for this test system. The amount of SOD inhibiting the reaction rate by 50% in the given assay conditions was defined as one SOD unit [48].

2.6   Determination of superoxide anion radicals (DHE-assay)

To measure the production of superoxide anion radicals dihydroethidium (DHE; Molecular Probes, Leiden, The Netherlands) was used. Superoxide radicals oxidise DHE to ethidium which intercalates into DNA producing a red fluorescence [49].
Cells were washed in PBS and resuspended in PBS with 20 ng DHE/ml for 1h at room temperature. After staining, cells were washed twice in ice cold PBS, resuspended and analysed within 1 h by flow cytometry (620 nm).

2.7   Superoxide anion production by Lucigenin chemiluminescence

DS-sarcoma cells were incubated for 24 h with 2-ME, DDC or doxorubicin (DOX). Subsequently, the medium was replaced with physiological buffer (119 mM NaCl, 20 mM HEPES, 4.6 mM KCl, 1 mM $MgSO_4$, 0.15 mM Na_2HPO_4, 0.4 mM KH_2PO_4, 5 mM

$NaHCO_3$, 1.2 mM $CaCl_2$, 11.1 mM glucose, pH 7.4) with a cell density of 4 x 10^6 cells/ml. Lucigenin (200 µM; bis-N-methylacridinium nitrate) was added to the cell suspension and luminescence, measured with a Bioorbit 1251 luminometer (LKB Wallac, Munich, Germany), was integrated for 10 minutes at 37°C. Background luminescence was determined in the presence of the superoxide scavenger Tiron (10 mM, 4,5-dihydroxy-1,3-benzenedisulfonic acid). Superoxide levels are reported as Tiron-inhibited arbitrary units [50].

2.8   Determination of ROS-formation (DCF-assay)

ROS production was assessed by oxidation of 2´,7´-dichlorodihydrofluorescein diacetate (H_2-DCF-DA) (Molecular Probes, Leiden, The Netherlands) to the fluorescent product 2´,7´-dichlorofluorescein (DCF). In the presence of ROS, especially hydrogen peroxides and lipid hydroperoxides, H_2-DCF is rapidly oxidised to highly fluorescent DCF [51].

Cells were stained as previously described [52]. 10^6 cells were incubated in RPMI with 5 µM H_2-DCF-DA for 45 min at 37°C, then incubated in PBS containing 0.2 µg propidium iodide/ml for 10 min at room temperature. Thereafter, cells were washed once and resuspended in 1 ml PBS. Flow cytometric analysis was performed within 1 h (525/620 nm).

2.9   Biochemical assessment of lipid peroxidation (TBARS assay)

High amounts of reactive oxygen intermediates result in lipid peroxidation. Therefore, analysis of malondialdehyde equivalents (TBARS) as a marker of lipid peroxidation end products was carried out as described previously [53,54]. After drug treatment, approx. 3 x 10^6 cells were washed in ice cold PBS, lysed in 260 µl solubilisation buffer [10 mM Tris, pH 7.4, 9 g/l NP40, 1 g/l SDS and 250 U/ml benzonase (Roche, Mannheim, Germany)] and centrifuged at 20.000 x g for 10 min at 4°C. For protein measurement, an aliquot of 50 µl was frozen at –20°C. 200 µl of cell lysate or malondialdehyde standards were mixed with 10 µl butylated hydroxy-toluene (50 mg/ml ethanol) and 200 µl of orthophosphoric acid (0.2 mM). Thereafter, 25 µl of 2-thiobarbituric acid reagent (800 mg of 2-thiobarbituric acid

dissolved in 50 ml of 0.1 M NaOH) were added. The reaction mixture was then incubated at 90°C for 45 min. Formed TBARS were extracted once with 500 µl 1-butanol. 250 µl of the butanol phase was placed into a 96-well-plate. Malondialdehyde equivalents (TBARS) were measured using a fluorescence plate reader (Bio-Tek FL 600, Biotek, Winooski, VT) with excitation at 530 ? 25 nm and emission detection at 590 ? 35 nm. For quantitative determination of TBARS, 200 µl of a malondialdehyde standard solution were used instead of cell lysate. For this, 50 µl of 1,1,3,3,-tetramethoxypropane (10 mM) was hydrolysed in 10 ml of 0.01 M HCl for 10 min at room temperature and then diluted with ultrapure water to suitable concentrations. Protein content was measured spectrophotometrically using the Bio-Rad DC Protein Assay (Bio-Rad, Munich, Germany), according to the manufacturer´s protocol.

2.10 Detection of mitochondrial changes

Mitochondrial injury can lead to depolarisation of the mitochondrial membrane, a frequent early event in apoptosis. The depolarisation is linked to release of pro-apoptotic factors from the mitochondrion, some of which are familiar players in the central apoptosis mechanism [55]. Therefore, the mitochondrial membrane potential ($?? _m$) was determined by using rhodamine 123 as described by Li et al. [56]. Treated cells were washed and resuspended in medium at a concentration of 10^6 cells/ml. After incubation with 5 µM rhodamine 123 for 20 min at room temperature, cells were washed once in medium and resuspended in PBS for flow cytometry analysis (575 nm). Carbonyl cyanide m-chlorophenylhydrazone (CCCP) at a concentration of 50 µM, was used as a positive control.

Swelling of mitochondria is another marker of apoptosis [57]. Relative mitochondrial mass was measured by flow cytometry using 10-nonyl-acridine-orange (NAO) (Moleculare Probes, Leiden, The Netherlands). The fluorescent dye NAO binds specifically to the mitochondrial inner membrane independent of energetic state [58]. 10^6 cells were washed once in PBS and stained with 10 µM NAO in 1 ml PBS for 10 min at room temperature. Thereafter, cells were washed in PBS and underwent flow cytometry analysis (525 nm).

2.11 Caspase activity assay

The activation of caspases, intracellular cysteine proteases, play a central role in the apoptotic process. Once activated, executor caspase-3 -6 and -7 cleave cytoskeletal and nuclear proteins and induce apoptotic cell death [59].

4×10^6 cells or 7 tumour sections of 40 µm were cut at –20°C in a cryostat and lysed in 300 µl ice cold HEPES buffer (10 mM HEPES pH 7.4, 2 mM EDTA, 1 g/l CHAPS, 2 mM Pefabloc (Biomol, Hamburg, Germany). The solution was centrifuged at 20,000 x g at 4°C for 30 min and 200 µl of the supernatant were mixed with 22 µl 50 mM DTT and stored at –80°C for caspase-3 and caspase-8 activity assay. The aliquot of the supernatant was used for protein content determination with Bio-Rad DC Protein Assay (Bio-Rad, München, Germany). For caspase-3-like activity measurement 100 µl of the supernatant were incubated with the fluorogenic caspase-3 tetrapeptide substrate Ac-DEVD-amino-4-methylcoumarin [60] (Calbiochem, Bad Soden, Germany) at a final concentration of 20 µM. For caspase-8 activity measurement the fluorogenic caspase-8 substrate Ac-IETD-amino-4-methylcoumarin [61] (Bachem, Heidelberg, Germany) at a final concentration of 50 µM was used. Cleavage of the substrates was followed by determination of emission at 460 ? 40 nm after excitation at 360 ? 40 nm using the fluorescence plate reader FL600 (Biotek, Winooski, VT).

Relative caspase-3 and caspase-8 cleavage activity was expressed as a function of protein content. Activity of control cells or control tumours were set at 100%.

2.12 Western blot analysis

4×10^6 cells resp. 7 tumour sections (40 µm) were lysed with 10 mM Tris (pH 7.4), 9 g/l NP-40, 1 g/l SDS and 5 µl/ml protease inhibitor cocktail and centrifuged at 20,000 x g for 10 min at 4°C. Generating cell fractions 20×10^6 cells were washed and resuspended in 1 ml of a hypotonic buffer (20 mM HEPES-KOH (pH 7.5), 10 mM KCl, 1.5 mM MgCl2, 1 mM EDTA, 1 mM DTT, 5 µl protease inhibitor cocktail/ml, 250 mM sucrose), and incubated for 20 min on ice. They were then homogenised in a tissue grinder. The homogenate was centrifuged at 100 x g for 10 min at 4°C, and the resulting supernatant was then centrifuged at 10,000 x g for 30 min at 4°C. The

second pellet containing mitochondria was suspended in 10 mM Tris (pH 7.4), 0.9% NP-40, 0.1% SDS and 5 µl/ml protease inhibitor cocktail. The supernatant contained the cytosolic cell fraction [62].

Equal protein amounts were run on a 10-12% polyacrylamide gel and blotted onto PVDF membranes by semidry electroblotting. Membranes were stained with Ponceau S to verify equal protein loading per lane.

Following antibodies were used for Western blot detection:

antibody	source	dilution
rabbit polyclonal anti PARP antibody	Santa Cruz Biotechnologies, CA	1:200
goat polyclonal anti-AIF antibody	Santa Cruz Biotechnologies, CA	1:150
goat polyclonal anti-cytochrome c antibody	Santa Cruz Biotechnologies, CA	1:100
mouse monoclonal anti-Bax antibody	Santa Cruz Biotechnologies, CA	1:100
mouse monoclonal anti-Bcl-2 antibody	Santa Cruz Biotechnologies, CA	1:100
mouse monoclonal anti-Bcl-xL antibody	Santa Cruz Biotechnologies, CA	1:100
goat polyclonal anti-HSP70 antibody	Santa Cruz Biotechnologies, CA	1:200
rabbit polyclonal anti-HO1 antibody	Stress Gene Biotechnologies, Victoria, Canada	1:20 000
goat anti-rabbit IgG HRP-conjugated	Cell signaling, Beverly, MA	1:2000
rabbit anti-goat IgG HRP-conjugated	DAKO, Glostrup, Denmark	1:6000
rabbit anti-mouse IgG HRP-conjugated	Calbiochem, San Diego, CA	1:5000
goat anti-rabbit IgG AP-conjugated	Boehringer Mannheim, Mannheim, Germany	1:3000

Tab. 2.12.1: Characterisation of antibodies used in Western blot analysis.

After blocking (3% milk powder and 0.05% Tween 20 in TBS) the membranes for 1 h, blots were probed for 1 h with primary antibody and rinsed twice with TBST. The membranes then were probed with horseradish peroxidase-conjugated

secondary antibody for 1 h. After three washes in TBST the detection was performed with chemiluminescence system LumiGLO[TM] (Cell signaling, Beverly, MA). Colorimetric detection was used to determine HO-1 expression as described previously [63].

2.13 Real time PCR

The mRNA expression of FasL and TNF?, two ligands of death receptors (Fas and TNF-R1) were measured quantitatively by real-time PCR (iCycler, Bio-Rad, Munich, Germany). GAPDH expression served as a control for cDNA amount.

Total RNA isolation was done with RNeasy mini kit (Qiagen, Hilden, Germany). 2 µg of total RNA were transcribed into cDNA using Omniscript RT Kit (Qiagen) and oligo dT-primers (end volume: 20 µl) as indicated in manufacturer's instructions .

Primers listed below were used for transcription and RT-PCR:

reaction	sequence
reverse transcriptase reaction	5′-TTT TTT TTT TTT TTT TVN-3′ V= A or G or C, N= A or G or C or T
RT-PCR: GAPDH	5′-GTG TTC CTA CCC CCA ATG TAT-3′ 5′-CCTGTTGCT GTA GCC ATA TTC-3′
RT-PCR: TNF?	5′-CAG ATG GGC TGT ACC TTA TC-3′ 5′-GGA CTC CGT GAT GTC TTA GTA-3′
RT-PCR: FasL	5′-TCT GGA ATG GGA AGA CAC ATA-3′ 5′-ACC AGA TCC CCA GGA TAC TT-3′

Tab. 2.13.1: Primers used for reverse transcriptase reaction and quantification of TNF?, FasL and GAPDH mRNA by real-time RT-PCR.

Real time RT-PCR was performed using QuantiTec[TM] SYBR? Green PCR Kit (Qiagen) following manufacturer's instructions. Briefly, 1 µl of cDNA were added to the master mix (25 µl 2x QuantiTec SYBR Green PCR Master Mix, 1 µl 500 nM Fluorescein, 1 µl of each primer [50 pmol/µl], 21 µl RNAse-free water). A calibration curve was run in parallel and in duplicate with each analysis, using PCR fragments of the target cDNA

in a concentration of 10^1-10^9 copies per sample. Negative water blanks were included in every analysis. A 15 min denaturation at 95°C activated the Taq Polymerase, which was followed by 40 PCR cycles, in accordance with the following protocol: denaturation at 95°C (30 seconds), annealing at 57°C for FasL and GAPDH and at 61°C for TNF? (30 seconds), and elongation at 72°C (30 seconds). At the end of the PCR, a melting curve analysis was performed by gradually increasing the temperature to 95°C. This was to detect possible formation of primer-dimers. Data acquisition was performed during elongation step.

After PCR was completed the SYBR Green fluorescent signal was transformed into a relative number of copies of target molecules. Differences in cDNA amount were equalised by expression of the house keeping gene GAPDH.

2.14 Identification of apoptotic cells with 7-AAD

Staining cells with 7-aminoactinomycin D is a previously described method used to identify apoptotic cells in a given cell population [64]. Here, 10^6 cells were washed in HEPES buffer (10 mM HEPES, pH 7.4, 140 mM NaCl, 2.4 mM $CaCl_2$) and stained with 22 µM 7-aminoactinomycin D (7-AAD) for 20 min at 4°C in the dark. Cells were washed once and resuspended in an HEPES buffer. Flow cytometric analysis was performed within 1 h (FSC versus fluorescence at 675 nm).

2.15 DNA fragmentation

A late biochemical hallmark of apoptosis is the fragmentation of genomic DNA. It is an irreversible event that commits the cell to die and occurs prior to changes in plasma membrane permeability.

Approx. 1.5 x 10^6 cells or 4 tumour sections of 40 µm were resuspended in 500 µl lysis buffer [10 mM Tris (pH 8.0), 100 mM NaCl, 25 mM EDTA, 5 g/l SDS). The solution was incubated sequentially with 50 µg/ml RNase A (Qiagen) for 60 min at RT, and 100 µg/ml proteinase K (Qiagen) at 50°C over night. Subsequently the solution was cooled down to RT und gently extracted with 500 µl Roti Phenol/Chloroform (Roth, Karlsruhe, Germany). The mixture was transferred to a Phase Lock Gel^{TM} light tube (Eppendorf, Hamburg, Germany). After centrifugation at

14,000 x g for 5 min the upper aqueous phase was decanted and 0.1 volume 3 M sodium acetate and 2.2 volumes of absolute ethanol were added. The tube was kept at −20°C for 2 h. After centrifugation, the DNA precipitate was washed with 70% ethanol and dried for 20 min at RT. DNA was dissolved in TE buffer (pH 8.0) overnight at 4°C. To detect DNA fragments, 2 µg of isolated DNA were separated on a 1.8% agarose gel in TBE buffer and stained with ethidium bromide. DNA fragments were visualized under ultraviolet light.

2.16 RNA fragmentation

RNA was isolated from tumour sections (40 µm) cut at −20°C in a cryostat with Qiagen RNeasy Mini Kit (Qiagen) according to the manufacturer's instructions. 1 µg of total RNA was analysed on a 1% agarose gel in TBE buffer containing 0.5 µg ethidium bromide per ml.

2.17 Glutathione determination with HPLC

Approx. 40 µg tumour tissue (cut in 40 µm sections) was transferred to a tissue grinder, extracted with 2 ml of ice-cold 60 g/l sulfosalicylic acid containing 1 mM EDTA, and rapidly homogenised while the protein was directly precipitated. After centrifugation (21,000 x g for 5 min at 4°C), aliquots of the clear supernatant and protein precipitate were stored at −80°C. Protein precipitate was resolved in 0.1 N NaOH, afterwards protein content was assessed by the method of Bradford. Reduced and oxidised glutathione levels were determined as described previously by Kuhn and colleagues [65].

2.18 Histochemical determination of apoptosis (TUNEL-assay)

Apoptosis associated DNA single and double strand breaks were detected using the 'Apoptosis Detection System Fluorescein´ (Promega, Mannheim, Germany) according to the manufacturer's protocol for frozen tissue sections. Tumour sections of 10 µm were cut at −20°C in a cryostat and subsequently fixed with 4% freshly prepared methanol-free formaldehyde for 30 min at RT. Specimens were washed in phosphate buffered saline and permeabilised in 0.1% Triton X-100 in 0.1% sodium citrate

solution for 30 min at RT. Positive controls were prepared by incubating tissue sections with 0.2 U/µl DNAse I (Boehringer-Mannheim, Mannheim, Germany) in 40 mM Tris-HCl (pH 7.4), 10 mM NaCl, 6 mM $MgCl_2$ and 10 mM $CaCl_2$ for 10 min at RT. Specimens were equilibrated and incubated with the nucleotide mix and the TdT enzyme (terminal deoxynucleotidyl transferase) according to the manufacturer´s protocol at 37°C for 1 h. Negative controls were treated identically, but in the absence of the TdT enzyme. Specimens were washed in 2 changes of sodium citrate-buffered saline and counter-stained with 4´,6-diamidino-2-phenylindole dihydro-chloride (DAPI). Samples were mounted in embedding medium (SlowFade Light, Molecular Probes, MoBiTec, Goettingen, Germany) and analysed immediately under a fluorescence microscope (Axioplan, Zeiss) using a standard fluorescein and DAPI filter set.

2.19 Histochemical detection of nitrosative stress

The analysis of nitrosylated proteins as a marker of the formation of the toxic oxidant peroxynitrite anion ($ONOO^-$) [66] was carried out as follows: tumour sections (5-10 µm) were cut at –20°C in a cryostat, air dried and subsequently fixed in freshly prepared 4% paraformaldehyde for 20 min. Thereafter, specimens were washed twice in PBS for 5 min. Non-specific primary and secondary antibody binding sites were blocked by incubation of specimens with PBS containing 2% BSA and 10% normal donkey serum for 1 h at RT. Excess blocking solution was removed and sections were covered with 6 µg/ml anti-nitrotyrosine rabbit polyclonal antiserum (Upstate Biotechnology, Lake Placid, NY) diluted in PBS, 2% BSA and incubated overnight at 4°C. Sections were rinsed twice for 5 min in PBS and covered with 1:25 diluted FITC labeled anti-rabbit IgG from donkey for 1 h at RT. Specimens were washed in two changes of PBS and counterstained with DAPI. In the cases in which sections were stained simultaneously for nitrosylated proteins and blood vessels, anti-rat von Willebrand factor sheep polyclonal antiserum (Technically, Ontario, Canada) was given (1:500) into the diluted anti-nitrotyrosine polyclonal antiserum and detected by Cy3^{TM} labeled anti-sheep IgG from donkey (Dianova, Hamburg, Germany).

Samples were mounted in embedding medium (SlowFade Light; Molecular Probes, MoBiTec, Goettingen, Germany) and analysed immediately under a fluorescence microscope (Axioplan, Zeiss, Germany) using standard fluorescein, rhodamine and DAPI filters. The specificity of the staining of nitrosylated proteins was verified by incubating the diluted anti-nitrotyrosine polyclonal antiserum with 10 mM nitro-tyrosine in PBS for h at RT. This solution was used in place of the primary antibody and should result in no staining (negative control).

2.20 Matrix metalloproteinase activity

MMPs are associated with tumour growth, invasion and metastasis. They are responsible for the degradation of extracellular matrix proteins, whereby tumour angiogenesis and tumour invasion in healthy tissue is submitted [67]. Two members of the MMP family, the gelatinases MMP-2 and MMP-9, were investigated by zymography.

Samples were prepared from tissue sections as described in the chapter `Western blot analysis', but the lysis buffer did not contain any protease inhibitors. Zymography was performed in 10% SDS-polyacrylamide gels containing 1 mg/ml gelatin. Samples (30 µg protein) were mixed with Laemmli sample buffer without a reducing agent and subjected to electrophoretic analysis without boiling. Gels were washed in 50 mM Tris (pH 7.5) containing 2.5% Triton X-100 for 1 h and were then incubated at 37°C overnight in 50 mM Tris (pH 7.5) containing 150 mM NaCl, 10 mM $CaCl_2$, and 0.1% Triton X-100. Gels were stained with Coomassie Brilliant Blue [68].

2.21 In vivo studies

All *in vivo* studies were kindly performed by Dr. med. habil. Oliver Thews and Dr. rer. nat. Debra K. Kelleher, Institute of Physiology and Pathophysiology, University of Mainz, Germany.

2.21.1 Animals

Male Sprague-Dawley rats (Charles River Wiga, Sulzfeld, Germany; body weight 160 to 195 g) housed in a animal care facility were used in the study. Animals were allowed access to food and acidified water ad libitum before and throughout the investigation. All experiments had previously been approved by the regional animal ethics committee and were conducted in accordance with the German Law for Animal Protection and the UKCCCR Guidelines [69].

2.21.2 Tumours

Solid DS-sarcomas were induced by injecting DS-sarcoma cells (0.4 ml approx. 10^4 cells/µl) subcutaneously into the dorsum of the left hind foot. Tumours grew as flat, spherical segments and replaced the subcutis and corium completely. Volumes were determined by measuring the three orthogonal diameters of the tumours and using an ellipsoid approximation with the formula: $V = d_1 \times d_2 \times d_3 \times ?/6$.

2.21.3 ROS-generating treatment and 2-ME administration

A previous study demonstrated that 44°C-hyperthermia (HT) for 60 min markedly induced the generation of reactive oxygen species, an effect which was even more pronounced when HT was combined with xanthine oxidase application and the animals allowed to breath pure oxygen [70]. For this reason, the same treatment protocol was used to induce oxygen radicals in tumours *in vivo* in the present study. Tumours were treated when they reached a volume of 0.5 to 0.75 ml, approx. 5 to 7 days after implantation.

HT was performed by heating the tumour in a saline (9 g/l NaCl) bath set to a temperature of 44.3°C. For this, animals were anaesthetised with pentobarbital (40 mg/kg, i.p., Narcoren™, Merial, Hallbergmoos, Germany) and placed on a poly-styrene board in a ventral position above the saline bath. The tumour-bearing leg was immersed into the saline through a hole in the polystyrene layer so that the tumour was completely submerged for 60 min. The saline bath temperature was set at 44.3°C in order to obtain a temperature of 44.0°C in the center of the tumour as has been confirmed in previous studies [70].

Fifteen min prior to HT, animals received an i.v. injection of 15 U/kg body weight of xanthine oxidase (XO). XO was previously dissolved in distilled water at a concentration of 7.5 U/ml. In contrast to the *in vitro* experiments, the addition of hypoxanthine (substrate of XO) was not necessary because larger amounts of hypoxanthine will be formed within tumour tissue by the partial degradation of ATP into hypoxanthine (ATP ? ADP ? AMP ? IMP ? inosin ? hypoxanthine).

Additionally during HT, animals breathed pure oxygen spontaneously (respiratory hyperoxia; RH) which was flushed around the nose and mouth of the animal at a flow rate of 2 l/min by using a loosely fitting face mask.

Control animals were also anaesthetised but, not treated with HT, XO or oxygen breathing.

2-ME was dissolved in absolute ethanol at a concentration of 10 mg/ml and injected at a dose of 17.5 mg/kg 2 h prior to HT treatment. For i.p. injection, the stock solution was diluted with 1ml of peanut oil and the mixture vortexed to obtain a stable emulsion. Animals in the control groups received equivalent volumes of the vehicle (ethanol + peanut oil) 120 min prior to HT.

The experimental groups can be described as follows:

Group 1 (control, n = 17 tumours): Animals were neither treated with ROS-inducing HT nor with 2-ME.

Group 2 (HT+RH+XO-treated, n = 13 tumours): Animals received ROS-inducing treatment (HT + XO injection + oxygen breathing) but no 2-ME.

Group 3 (2-ME-treated, n = 11 tumours): Animals were treated with a single injection of 2-ME but no HT was applied.

Group 4 (HT+RH+XO + 2-ME-treated, n = 17 tumours): Animals received a single i.p. injection of 2-ME 2 h prior to the ROS-inducing treatment.

On the day of treatment (day 5 to 7 after implantation) tumours in the different groups were size-matched to exclude systematic differences in tumour size.

2.21.4 ALA-PDT and hyperthermia

Tumours were heated to a set temperature of 43°C using a infrared-A irradiator (Fig. 2.21.4.1), containing a halogen lamp (24V/150W, type HLX6443, Osram, Munich, Germany), a waterfilter (Maxs, Sachseln, Switzerland) and a long wave pass filter of 420 nm [71]. The waterfilter absorbs practically all energy ? 1400 nm and is responsible for two strong, distinct absorption bands at 944 and 1180 nm [72]. Without the waterfilter, this absorption would be performed by water in the most superficial skin layers, which can lead to painful sensations and exsiccosis. Using a feedback control system involving measurement of temperature in the tumour centre with 250 µm needle-thermocouples (type 2ABAc, Philips, Kassel, Germany) tumour temperature was maintained at 43°C for 60 min, by continuous regulation of the radiation source, which switched on and off intermittently. Animals which were selected for PDT-treatment received 3 h before irradiation 375 mg/kg 5-amino-levulinc acid i.v.. Irradiation was performed with the infrared-A irradiator described above in combination with a barrier filter of 800 nm to blind out infrared light, which is responsible for heat generation in the irradiated tumour. The tumour was irradiated with an energy density of 200 mW/cm^2 and a power density of 370 J/cm^2.
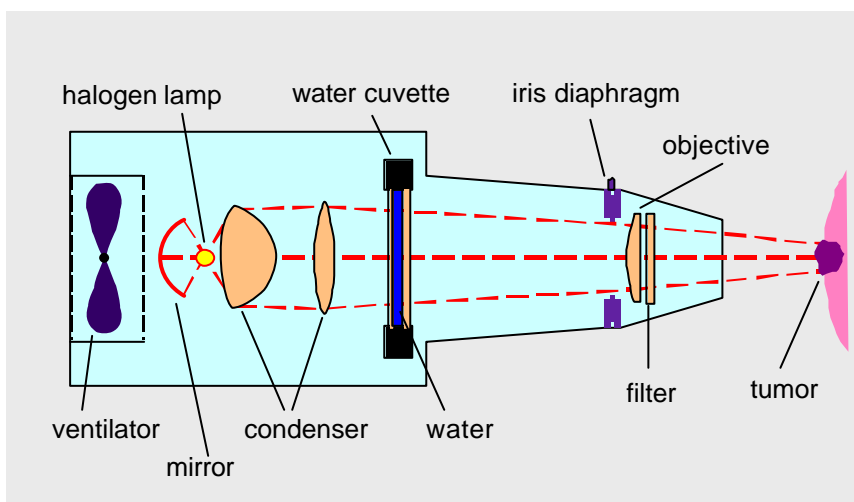
Fig. 2.21.4.1: Longitudinal section through the IR-A irradiation source used for simultaneously inducing HT and ALA-PDT [71].

The experimental groups can be described as follows:

Group 1 (control, $n_{0h} = 7$, $n_{18h} = 4$ tumours): Animals were neither treated with HT nor ALA-PDT.

Group 2 (HT, $n_{0h} = 6$, $n_{18h} = 4$ tumours): Animals received hyperthermia 43°C.

Group 3 (ALA-PDT, $n_{0h} = 6$, $n_{18h} = 5$ tumours): Animals were treated with ALA-PDT.

Group 4 (ALA-PDT+HT $n_{0h} = 6$, $n_{18h} = 4$ tumours): Animals received ALA-PDT treatment in combination with hyperthermia.

Group 5 (ALA alone, $n_{0h} = 7$, $n_{18h} = 5$ tumours): Animals received ALA injection, but the tumour was not illuminated. This treatment group was added due to the fact, that ALA and porphyrins at higher concentrations can generate ROS in absence of activating light [73].

Group 6 (light alone, $n_{0h} = 6$, $n_{18h} = 4$ tumours) Animals were irradiated without ALA administration.

Tumour were excised with a scalpel blade immediately or 18 h after treatment, placed in tissue embedding medium (GSV 1, Slee Technik, Mainz, Germany), rapidly cooled in liquid nitrogen, and stored at −80°C until further investigation.

2.21.5 Statistical analysis

Results are expressed as means ± standard error of the mean (SEM) or standard deviation (SD). Differences between the groups were assessed by the two-tailed Wilcoxon test for unpaired samples. The significance level was set at ? = 5% for all comparisons. For comparing the tumour growth in the *in vivo* experiments, the time taken to reach a previously defined tumour volume of 3.5 ml was determined. These time intervals were analysed using Kaplan-Meier statistics and differences between the probability curves were assessed using the log-rank test.

3 Results

3.1 2-Methoxyestradiol

3.1.1 2-Methoxyestradiol induces cell death by apoptosis

DS-sarcoma cells were treated with various 2-ME concentrations between 0.5 and 10 µM. Control cells were incubated with 0.1% ethanol. Over a period of 4 days proliferation was determined by cell counting. High concentrations of 2-ME (5 and 10 µM) stopped cell proliferation immediately, whereas low concentrations (0.5 and 1 µM) showed an increasing inhibitory effect on cell proliferation during the first 3 days, resulting in growth arrest.
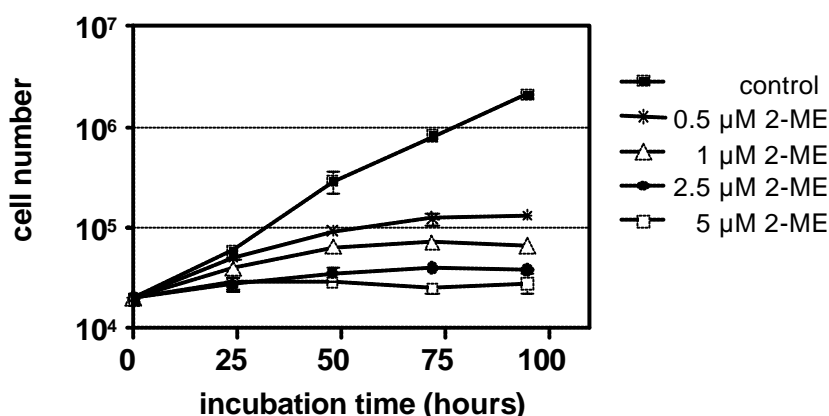
Fig. 3.1.1.1: Inhibition of cell proliferation by 2-ME. DS-sarcoma cells were treated with the indicated 2-ME concentrations for 96 h. Cells were counted 24, 48, 72 and 96 h after treatment. Values are means ? SD of three independent experiments.

Uptake of propidium iodide was used to measure cytotoxicity of 2-ME. Therefore, cells were incubated with 0.5, 1, 5 and 10 µM 2-ME for 72 h. The proportion of propidium iodide positive cells increased substantially from 41% (0.5 µM) to 59% (1 µM) and reached a plateau at 5 µM with 71%.
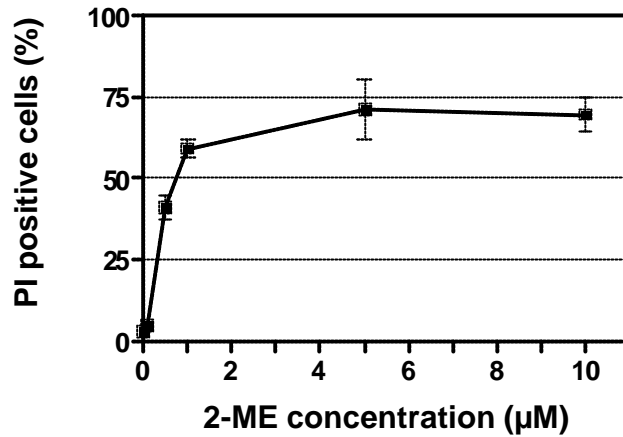
Fig. 3.1.1.2: 2-ME effectively damaged DS-sarcoma cells. Cells were incubated with 0.5, 1, 5 and 10 µM 2-ME. After 72 h they were stained with propidium iodide (PI) measuring membrane integrity. PI uptake was determined by flow cytometry. Data are means ? SD of three independent experiments.

The influence of 2-ME on the mitochondrial integrity was determined by flow cytometry. Cells were treated with 0.5, 1 and 5 µM 2-ME for 24 h. Measuring mitochondrial mass cells were stained with acridine orange. For determining changes of mitochondrial inner membrane potential ($? ?_m$) cells were stained with rhodamine 123. Cells treated with 5 µM 2-ME showed a clear increase in mitochondrial mass of 66% compared to sham treated cells. After correcting the mitochondrial transmembrane potential for the corresponding mitochondrial mass a concentration-dependent decrease in mitochondrial membrane potential was observed in 2-ME treated cells (Tab. 3.1.1.1).

treatment	mitochondrial mass	$\Delta\Psi_m$	$\Delta\Psi_m$/ mitochondrial mass
control	1	1	1
0.5 µM 2-ME	1.05 ± 0.10	0.84 ± 0.06	0.82 ± 0.06
1 µM 2-ME	1.02 ± 0.13	0.80 ± 0.06	0.84 ± 0.19
5 µM 2-ME	1.66 ± 0.34	1.25 ± 0.14	0.78 ± 0.18

Tab. 3.1.1.1: Effect of 2-ME on mitochondrial mass and membrane potential. DS-sarcoma cells were incubated with 0.1% (v/v) ethanol (control) or the indicated 2-ME concentrations for 24 h. Thereafter, cells were stained with acridine orange to determine mitochondrial mass or stained with rhodamine 123 for measurement of the inner mitochondrial membrane potential $\Delta\Psi_m$ by flow cytometry. The quotient of $\Delta\Psi_m$/mitochondrial mass was calculated to correct $\Delta\Psi_m$ for differences in mitochondrial mass. Results presented are mean fluorescence values relative to vehicle control of at least three independent experiments ± SD.

Permeability of mitochondrial membrane is influenced by Bcl-2 family members. Pro-apoptotic members like Bax and Bid localise to cytosol or cytoskeleton prior to a death signal whereas anti-apoptotic members, e.g. Bcl-2 and Bcl-xL, are initially integral membrane proteins found in the mitochondria, endoplasmic reticulum or nuclear membrane. Following a death signal, the pro-apoptotic members undergo a conformational change that enables them to target and integrate into membranes, especially the mitochondrial outer membrane [74]. Apoptotic stimuli can induce translocation of monomeric Bax to the mitochondria where it becomes an integral membrane protein and cross-linkable as a homodimer [75]. It is a fact that some Bcl-2 members can form ion channels in artificial membranes [76]. Additionally modulation of mitochondrial permeability transition pore (PTP) by Bax and Bak was proposed [77].

Due to the important role of Bcl-2 proteins in the apoptotic process of mitochondria, expression of pro-apoptotic Bax and anti-apoptotic proteins Bcl-2 and Bcl-xL were

determined by Western blot analysis. Expression of these proteins was measured in whole cell lysates as well as in mitochondrial fractions. Therefore, DS-sarcoma cells were treated with 1 or 5 µM 2-ME for different time intervals. Cells were harvested and whole cell lysates were prepared. Additionally, mitochondria were isolated to check the localisation of the three investigated apoptosis influencing proteins. Western blot analysis of whole cell lysates showed that protein expression of Bax, Bcl-2 and Bcl-xL was not modulated by 2-ME (data not shown). However, in mitochondria 2-ME increased the fraction of Bax molecules compared to the anti-apoptotic molecules Bcl-2 and Bcl-xL. Six hours after incubating cells with 1 or 5 µM 2-ME, the Bax to Bcl-2 ratio in mitochondria increased 2.2-fold compared to the control cells. Similar results were observed in the Bax-to Bcl-xL ratio indicating apoptotic changes at the outer mitochondrial membrane. At later time points (48 and 72 h) ratios of the investigated pro- and anti-apoptotic proteins in mitochondrial fraction normalised to control level (data not shown).
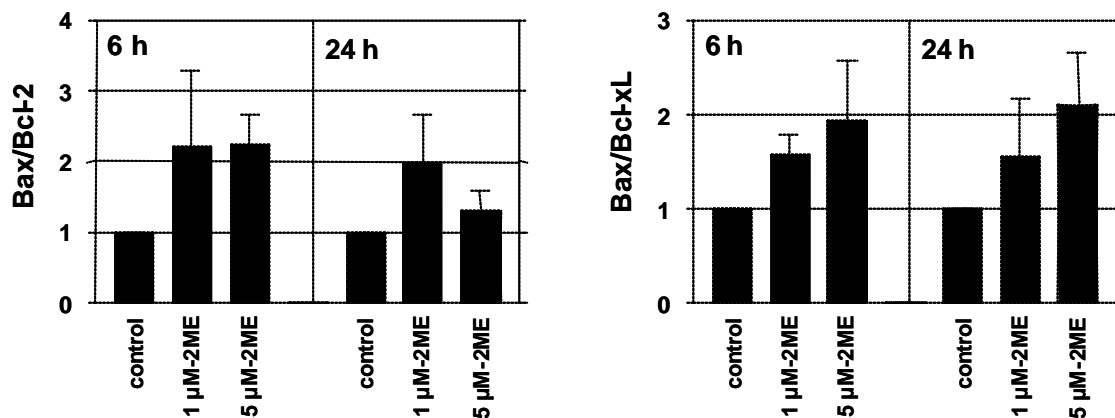
Fig. 3.1.1.3: 2-ME treatment increased portion of pro-apoptotic Bax in comparison to anti-apoptotic Bcl-2 and Bcl-xL. DS-sarcoma cells were incubated with ethanol (control), 1 or 5 µM 2-ME for the indicated periods. Mitochondria were then isolated and Western blotting was performed (10 µg protein). Relation of densitometric values of Bax and Bcl-2, and Bax and Bcl-xL was calculated. Ratio of control cells was set at 1. Data presented are means ? SEM of three independent experiments.

Two marker proteins for mitochondrial associated apoptosis are cytochrome c and AIF. Both proteins can be released out of mitochondria in apoptotic events. Cytochrome c release leads to the cytosolic assembly of the apoptosom caspase activation complex involving Apaf-1 and caspase-9 [78]. AIF, a caspase-independent DNase can translocate from the mitochondrial intermembrane space to the nucleus, where it causes chromatin condensation and large scale DNA fragmentation of approximately 50 kbp [79]. For determining the protein content of cytochrome c and AIF in cytosolic cell fractions, cells were treated with 1 and 5 µM 2-ME for 24, 48 and 72 h. Western blotting showed that cytochrome c was not released into cytosol but a 3.6-fold increase in cytosolic AIF was observed after 2-ME treatment with 1 µM for 48 h. Treatment for 72 h resulted in a 5.8- (1 µM) and 9.0-fold (5 µM) increase in cytosolic AIF content.
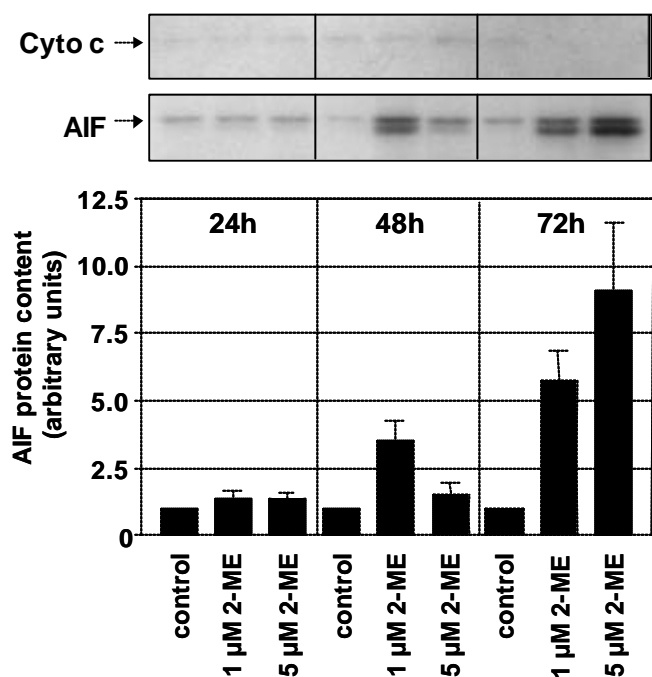
Fig. 3.1.1.4: Time course of the mitochondrial release of cytochrome c and AIF into cytosol. Cells were incubated with ethanol (control), 1 or 5 µM 2-ME for 24, 48 and 72 h. The cytosolic fractions of the cells were then separated and Western blotting was performed. Data represent means ? SEM of three independent experiments. Representative Western blots for cytochrome c and AIF at each time point are also shown.

Due to the very important role of caspases in the apoptotic pathway, activity of effector caspases was investigated. Caspase-3, -6 and −7 are counted among effector (or downstream) caspases, which finally lead to apoptotic cell death. In this study caspase-3-like activity (activity of effector caspases) was determined with the fluorogenic substrate Ac-DEVD-AMC. Three different 2-ME concentrations, 0.5, 1 and 5 µM 2-ME, were tested for caspase-3-like activation in DS-sarcoma cells. Treatment with 1 µM 2-ME strongly increased caspase-3-like activity. This concentration resulted in a 2.8-fold increase 24 h after 2-ME treatment. After 48 h caspase-3-like activity was raised 5.6-fold compared to control cells. Assessment of activity after 72 h showed a regression in activation (data not shown).
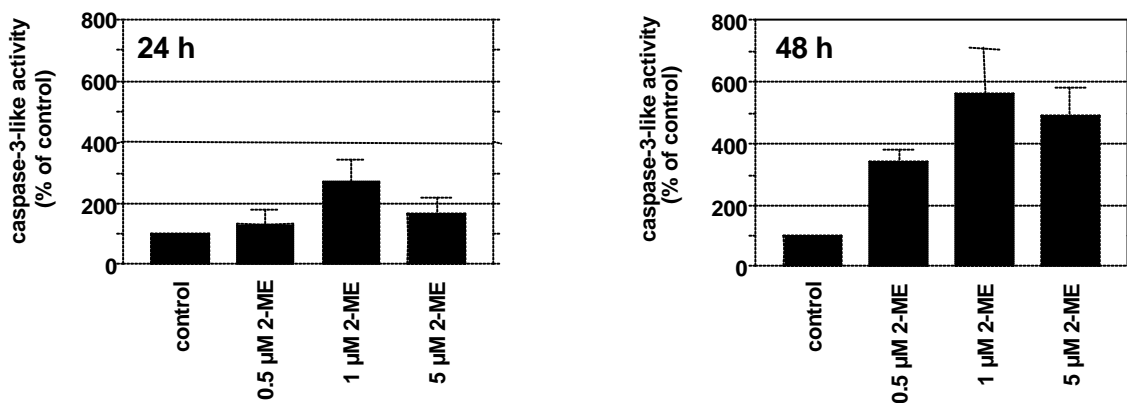
Fig. 3.1.1.5 Increased caspase-3-like activity after 2-ME treatment. Cells were incubated with the indicated 2-ME concentrations. 24 and 48 h after exposure , cells were washed and lysed. The lysate was then centrifugated at 21,000 x g for 30 min and the supernatants was incubated with the fluorogenic substrate Ac-DEVD-AMC. Cleavage of this substrate was detected in a fluorescence reader. Bars represent means ? SD of three independent experiments.

A consequence of caspase-3-like activation is cleavage of poly-ADP-ribose-poly-merase (PARP), a DNA repairing enzyme. After activation of effector caspases PARP will be cleaved into a 29 and 85 kDa fragment [80]. In this study PARP cleavage was investigated 24, 48 and 72 h after 2-ME treatment by Western blot analysis. The

occurrence of a second band at 85 kDa indicates partial PARP deavage 48 h after 2-ME treatment. The major part of PARP was not cleaved.
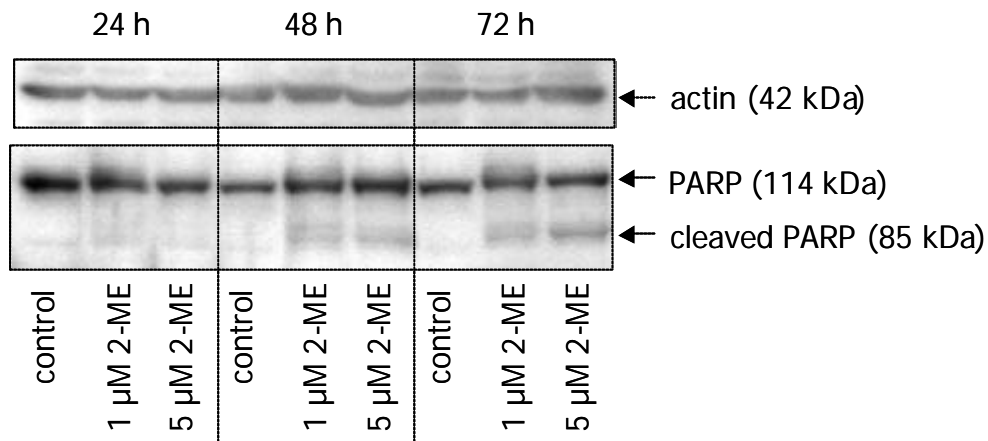
Fig. 3.1.1.6: Time course of PARP cleavage after 2-ME treatment. Cells were treated with ethanol (control), 1 or 5 μM 2-ME for 24, 48 and 72 h. Cells were then harvested and analysed for PARP cleavage by Western blotting. Protein load was verified by actin expression. Blots shown are representatives of two independent experiments.

Beside the important role of mitochondria in the apoptotic process, activation of death receptors like Fas, TNFR1 and TRAIL-R1/2 can also induce apoptosis. Death receptor mediated apoptosis of tumour cells could be induced either by autocrine production of FasL or TNF? by the tumour or by release of these factors out of lymphocytes. Upregulation of death receptors on tumour cell surface could be another mechanism to sensitise tumour cells against FasL or TNF? .

Fas-ligand binding initiates trimerisation of the Fas (CD95) receptor and this permits the immediate recruitment of several proteins that form a complex around the cytoplasmic moiety of the receptor - the death initiating signalling complex (DISC). DISC proteins bind to each other and CD95 through a series of homologous domains. Thus the C-terminus of CD95 binds a DISC protein called FADD, which can activate caspase-8 [81]. TNF? binding to TNFR1 engages similar mechanisms. But the DISC complex of TNFR1 contains several proteins, which can activate JNK, NF-?B and caspase-2 [82]. Accordingly TNFR1 is involved in pro- and anti-apoptotic pathways [83], which applies to Fas as well [84].

To investigate the role of death receptors in 2-ME induced cell death autocrine production of FasL and TNF? after 2-ME administration was determined. DS-sarcoma cells were treated with 1 or 5 µM 2-ME for different periods, cells were then harvested, RNA was isolated and transcribed into cDNA. Quantification of FasL and TNF? mRNA was done by real time RT-PCR using SYBR^TM Green as fluorophore.

2-ME treatment of DS-sarcoma cells induced upregulation of FasL and TNF? mRNA expression after 24 h. An increased expression of both investigated parameters was determined 24 h after 2-ME addition (1 and 5 µM 2-ME), with 1 µM enhancing expression more potently than 5 µM 2-ME. Cells treated with 1 µM 2-ME for 24 h had a 3.0-fold higher TNF? expression compared to control cells. Treatment with 5 µM 2-ME resulted only in a 1.9-fold increase. Similar results were observed in FasL expression. 1 µM 2-ME caused a 3.1-fold, 5 µM a 2.3-fold upregulation.
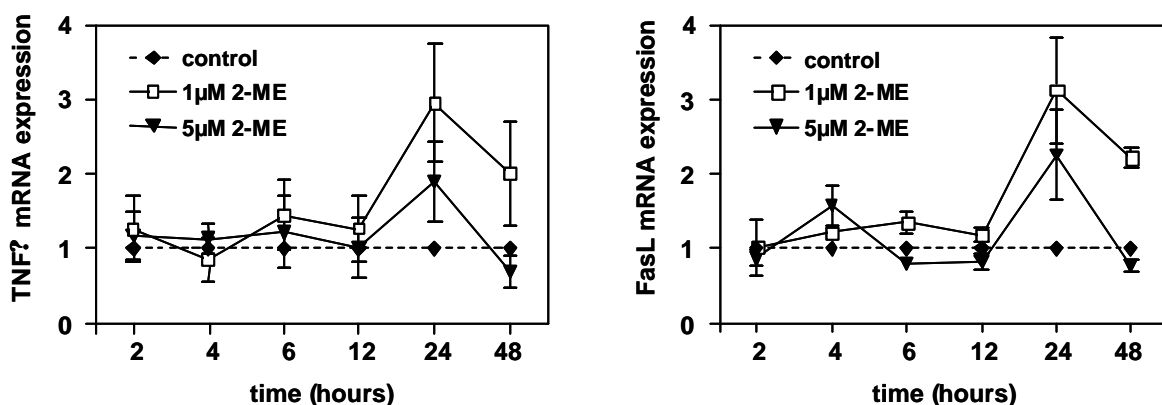
Fig. 3.1.1.7: Time course of FasL and TNF? mRNA expression after 2-ME treatment. Cells were treated with ethanol (control), 1 or 5µM 2-ME for the indicated periods. Subsequently, total RNA was isolated and transcribed into cDNA. FasL and TNF? mRNA expression was quantified by real time RT-PCR. GAPDH expression was used to correct the cDNA amount. Data shown are means ? SEM of three independent experiments. PCR analysis of each experiment was performed twice.

Ligand binding to Fas or TNFR1 results in cleavage of caspase-8 leading to the activation of effector caspases. 2-ME treatment for 24 h increased caspase-8 activity in DS-sarcoma cells only marginal (data not shown). Yet, caspase-8 activity of cells

treated with 1 μM or 5 μM 2-ME for 48 h showed a 1.6-fold increase compared to control cells.
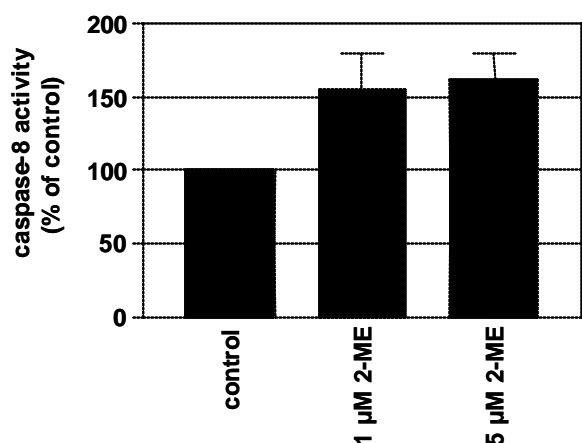
Fig. 3.1.1.8: Slight increase in caspase-8 activity 48 h after 2-ME treatment. Cells were incubated with the indicated 2-ME concentrations. 48 h after exposure , cells were washed and lysed. Caspase-8 activity was determined using the fluorogenic substrate Ac-IETD-AMC. Cleavage of this substrate was detected in a fluorescence reader. Bars represent means ? SD of three independent experiments.

DNA fragmentation is associated with the endpoint of the apoptotic process. Caspase-3 can induce DNA fragmentation by inactivating DFF45/ICAD, which results in the formation of the active enzyme DFF40/CAD [85]. Specific cleavage of nucleosomes generates the typical 180-200 bp DNA fragments [86]. Mitochondrial endonuclease G and AIF are also involved in DNA fragmentation, whereby AIF induces large scale fragmentation [16,87].

2-ME induced DNA fragmentation occurred 72 h after drug administration in a dose dependent manner. Control cells did not show any DNA degradation. After 96 h, DNA laddering reached the same level in 0.5, 1 and 5 μM 2-ME treated cells. The observed DNA fragmentation is a clear sign of apoptotic cell death.
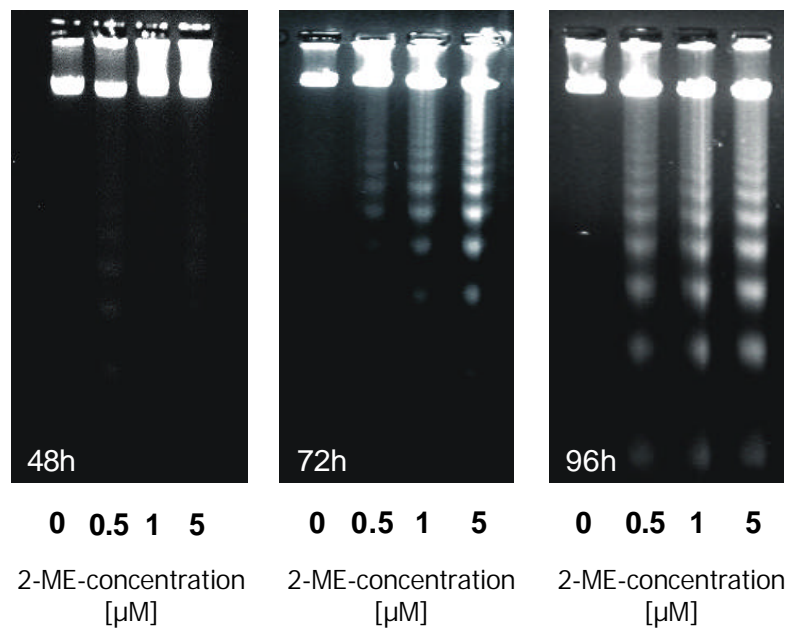
Fig. 3.1.1.9: Time course of DNA fragmentation after 2-ME treatment. DS-sarcoma cells were incubated with indicated 2-ME concentrations. After 48, 72, and 96 h cells were harvested and genomic DNA was isolated by chloroform/phenol extraction. 2 µg DNA were analysed on a 1.8% agarose gel. Gels are representatives of two independent experiments.

3.1.2   ROS-generation after 2-ME administration

The postulated effect of 2-ME inhibiting superoxide dismutase (SOD) was verified with the cell free pyrogallol-assay. Different concentrations of 2-ME (0.01, 0.1 and 1 mM) were preincubated with recombinant CuZn-SOD for 5 min. Then the SOD activity of these mixtures was determined, measuring the rate of pyrogallol autooxidation compared to SOD without 2-ME preincubation. Non of the investigated 2-ME concentrations had an inhibitory effect on SOD activity. In contrast, CuZn-SOD inhibitor diethyldithiocarbamate (DDC), which was used as positive control, decreased SOD activity in a concentration-dependent manner.
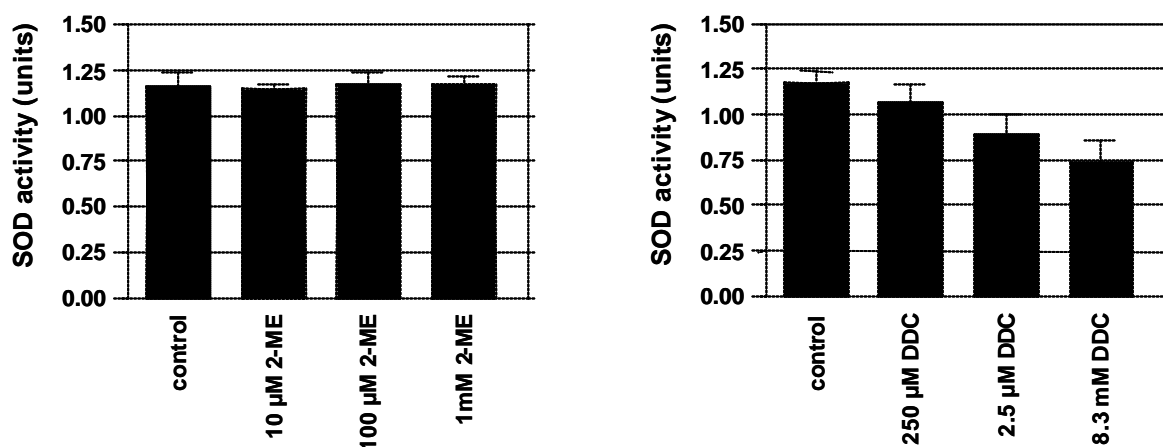
Fig. 3.1.2.1: 2-ME did not inhibit SOD activity. 2-ME or SOD-inhibitor DDC (positive control) were preincubated with SOD (25 ng/ml) in the indicated concentrations for 5 min. SOD activity was then determined by measuring the autooxidation rate of pyrogallol at 420 nm. Bars indicate the means ? SD of three independent experiments.

Notwithstanding the lack of a SOD inhibitory action of 2-ME, the induction of ROS by 2-ME was analysed by different methods. Superoxide anion formation in DS-sarcoma cells incubated with 1 or 5 µM 2-ME for 24 h were determined by dihydroethidium (DHE) oxidation or by Lucigenin chemiluminescence production. Both analysis showed an obvious increase in O_2^- formation in cells treated with 5 µM, whereas cells treated with 1 µM 2-ME had similar O_2^- levels as control cells. Flow cytometric analysis of DHE oxidation of 5 µM 2-ME treated cells (24 h) resulted in a 2.10-fold increase in O_2^- level compared to ethanol treated cells (control). Determining the superoxide anion formation by Lucigenin chemiluminescence cells incubated with 5 µM 2-ME showed a 1.96-fold increase compared to sham treated cells. For comparison cells were treated with SOD-inhibitor DDC and doxorubicin, a ROS-generating drug, which resulted in a similar increase in Lucigenin chemiluminescence as observed in 5 µM 2-ME treated cells.
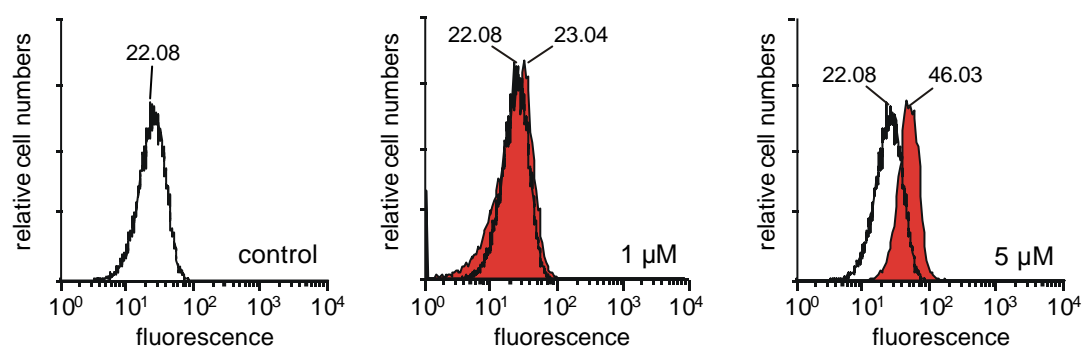
Fig. 3.1.2.2: Enhanced superoxide anion production in cells treated with 5 µM 2-ME for 24 h. Cells were treated with ethanol (control), 1 and 5 µM 2-ME for 24 h. Afterwards cells were washed and stained with dihydroethidium. Flow cytometric quantification of the oxidised product ethidium was done subsequently. Filled curves describe the fluorescence of 2-ME treated cells compared to control cells (empty curve). Histograms shown are representatives of three independent experiments.

treatment	Lucigenin chemiluminescence (Tiron inhibited arbitrary units)
control (ethanol)	1
1 µM 2-ME	1.00 ? 0.44
5 µM 2-ME	1.96 ? 0.59
25 µM DDC	1.69 ? 0.19
5 nM DOX	1.86 ? 0.40

Tab. 3.1.2.1: Increase in superoxide anion formation after treatment with 5 µM 2-ME measured by Lucigenin chemiluminescence. Cells were treated with the indicated substances for 24 h. Afterwards cells were counted and transferred to physiological buffer. Chemiluminescence was determined after administration of Lucigenin or Lucigenin + Tiron. DOX and DDC were used as positive controls. Values are means ? SD of three independent experiments.

Another method detecting reactive oxygen species is based on the oxidation of H_2-DCF to the fluorescent product DCF. Using this method a concentration dependent increase in ROS-formation was observed in cells exposed to 1 and 5 μM 2-ME for 24 h. Compared to data obtained from DHE- or Lucigenin-assays, this result showed a clear concentration-dependent enhancement in ROS-generation, whereas the increase was more modest.

treatment	DCF fluorescence (arbitrary units)
control	1
1 μM 2-ME	1.21 ? 0.07
5 μM 2-ME	1.29 ? 0.08
5 nM DOX	1.45 ? 0.17

Tab. 3.1.2.2: Concentration dependent increase in ROS production after 2-ME treatment. DS-sarcoma cells were treated with ethanol (control) and the indicated 2-ME concentrations. After 24 h cells were washed and stained with H_2-DCF. Cells were then washed and analysed within 1 h by flow cytometry. DOX was used as a positive control. Values are means ? SD of three independent experiments.

Lipid peroxidation is a result of enhanced ROS-formation. To determine this indirect marker of oxidative stress, cells were treated with 1 μM and 5 μM 2-ME for 48 h. Control cells were supplemented with 0.1 % (v/v) ethanol. Afterwards, lipid peroxidation was measured fluorometrically by formation of thiobarbituric reactive substances (TBARS). Cells treated with 1 μM 2-ME showed a 1.5-fold increase in lipid peroxidation compared to control cells. TBARS in cells, incubated with 5 μM 2-ME, increased 2.2-fold.
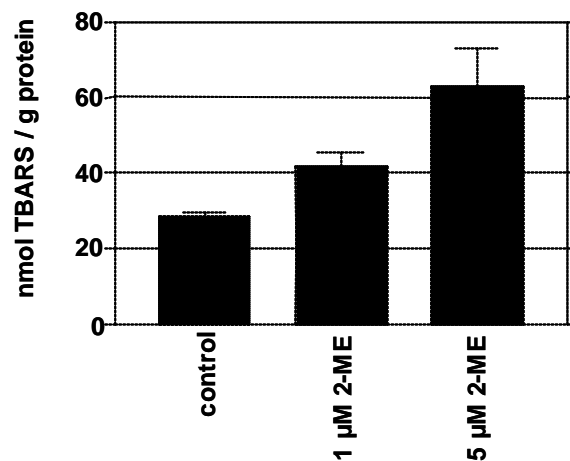
Fig. 3.1.2.3: Enhanced lipid peroxidation after 2-ME treatment. Cells were treated with ethanol (control) or the indicated 2-ME concentrations for 48 h. Lipid peroxidation end products were determined as thiobarbituric acid reactive substances (TBARS) as described in material and methods. Bars indicate the mean ? SD of at least three independent experiments.

Combination of 2-ME with a further ROS-generating treatment

For further increase of oxidative cell damage 2-ME treatment was combined with the ROS-generating system hpoxanthine/xanthine oxidase. This system is widely used to generate ROS, especially superoxide anions and hydrogen peroxides, in *in vitro* models [88]. Therefore, cells were grown in medium containing hypoxanthine (1 mM). ROS-production was induced by addition of xanthine oxidase (1 mU/ml). DS sarcoma cells received four different treatments for 48 h, proliferation activity was then determined by colony forming efficiency (CFE): control cells proliferated very well which resulted in a CFE of 100%, cells treated with hypoxanthine/xanthine oxidase showed a CFE of 89%, 2-ME treated cells had a CFE of 54% and the combination of both treatment resulted in a CFE of 34%. The calculated additive effect of the combined treatment would be about 48%. Thus combination of 2-ME and hypoxanthine/xanthine oxidase showed a synergistic effect on cell growth inhibition.

treatment	CFE in %
control	100 ? 6.1
oxidative stress	89 ? 10.8
0.25 µM 2-ME	54 ? 12.8
0.25 µM 2-ME + oxidative stress	34 ? 10.7

Tab. 3.1.2.3: Effective inhibition of cell proliferation by combining 2-ME administration and induction of oxidative stress. Cells were treated with 0.25 µM 2-ME, oxidative stress or a combination of both. Oxidative stress was generated by hypoxanthine (1 mM) + xanthine oxidase (1 mU/ml). Control cells were incubated with 0.1% (v/v) ethanol. After 48 h cells were washed and transferred to drug free medium and seeded at low cell concentrations. Colony forming efficiency (CFE) was determined after a period of 5 days. Values are means ? SD of three independent experiments.

In addition cellular ROS-formation after treatment with 2-ME, hypoxanthine/xanthine oxidase or the combination of both was determined by flow cytometry (oxidation of dihydroethidium). No increase in intracellular superoxide anion levels were observed in cells treated with hypoxanthine/xanthine. In contrast, cells receiving both treatments had higher O_2^- levels compared to cells treated with 2-ME alone (Tab. 3.1.2.4).

treatment	O_2^--formation (arbitrary fluorescence units)
control	1
1 µM 2-ME	1.65 ? 0.35
5 µM 2-ME	2.58 ? 0.00
ox. stress	1.01 ? 0.02
1 µM 2-ME + ox. stress	1.73 ? 0.12
5 µM 2-ME + ox. stress	2.89 ? 0.18

Tab. 3.1.2.4: Enhanced superoxide anion production by combining 2-ME and oxidative stress treatment. Cells were treated with 1% (v/v) ethanol (control), 1 µM or 5 µM 2-ME for 48 h. Cells were then treated with oxidative stress (1 mM hypoxanthine/ 10 mU xanthine oxidase/ml) for 45 min. Afterwards the superoxide anion formation was determined in the cells by flow cytometry (DHE staining). Data represent means ? SD of three independent experiments

3.1.3   Effect of antioxidants on 2-ME induced cell death

For later clinical application it is very useful to know if antioxidants can reduce the response to 2-ME chemotherapy. The effect of six different antioxidants on 2-ME induced proliferation inhibition was determined by CFE. The fatsoluble vitamin ? -tocopherol (vitamin E) and the watersoluble vitamin L-ascorbic acid (vitamin C) were used in concentrations which are common in the plasma of healthy persons [89]. Butylated hydroxy toluene (BHT), a synthetic fatsoluble ROS-quencher and N-acetyl-L-cysteine, a thiol based antioxidant was also tested. Further the effect of the hydroxyl radical scavenger mannitol [90] and the drug ambroxol, which detoxifies superoxide anions were investigated [91]. Therefore, cells were preincubated with the respective antioxidant for 4 h, 2-ME at a concentration of 0.35 µM was then added. This concentration has been chosen because higher 2-ME

doses killed nearly all cells. After 48 h the cells were seeded in 96-well-plates to determine colony formation.

Antioxidants tested did not reduce 2-ME induced proliferation inhibition. Only a marginal increase in CFE of antioxidant treated cells could be observed.

treatment	CFE ? SD (%)
control	100
0.35 µM 2-ME	5.4 ? 3.95
25 µM ?-tocopherol + 0.35 µM 2-ME	11.3 ? 5.20
10 µM ascorbic acid + 0.35 µM 2-ME	11.3 ? 6.45
25 µM BHT + 0.35 µM 2-ME	13.0 ? 10.20
5 mM N-acety-L-cysteine + 0.35 µM 2-ME	6.6 ? 3.15
3 mM mannitol + 0.35 µM 2-ME	10.0 ? 5.39
0.1 mM ambroxol + 0.35 µM 2-ME	7.3 ? 3.23

Tab. 3.1.3.1: Influence of antioxidants on 2-ME induced growth inhibition. DS-sarcoma cells were preincubated with different antioxidants for 4 h. Subsequently 0.35 µM 2-ME was added for another 48 h. Cells were then washed, transferred to medium without antioxidants and seeded at low cell concentrations. Colony forming efficiency (CFE) was determined after a period of 5 days. Values are means ? SD of three independent experiments.

Beside the influence of antioxidants on proliferation inhibition, the effect of these antioxidants on 2-ME induced caspase-3-like activation was investigated as well. Cells were incubated with the antioxidants described above, then 1 µM 2-ME was added to the medium for 48 h. Determination of caspase activity showed, that preincubation with antioxidants did not significantly reduce 2-ME induced caspase-3-like activation (Data not shown).

3.1.4   Role of caspases in 2-ME induced apoptosis

To elucidate the role of caspases in 2-ME induced apoptosis, DS-sarcoma cell were incubated with the pan caspase inhibitor Z-VAD-FMK (40 µM) for 1 h prior to 2-ME addition. Due to an aspartate residue mimicking cleavage site and a fluoromethyl-ketone (FMK) group forming a covalent inhibitor/enzyme complex, the inhibitor instantly and irreversibly binds to the catalytic site of caspases [92]. In order to prove the effectiveness of this inhibitor, caspase-3-like activity was measured in 2-ME treated cells with or without pan caspase inhibitor. Results presented in Fig. 3.1.4.1 demonstrate that pan caspase inhibitor could completely block caspase-3-like activation by 1 or 5 µM 2-ME.
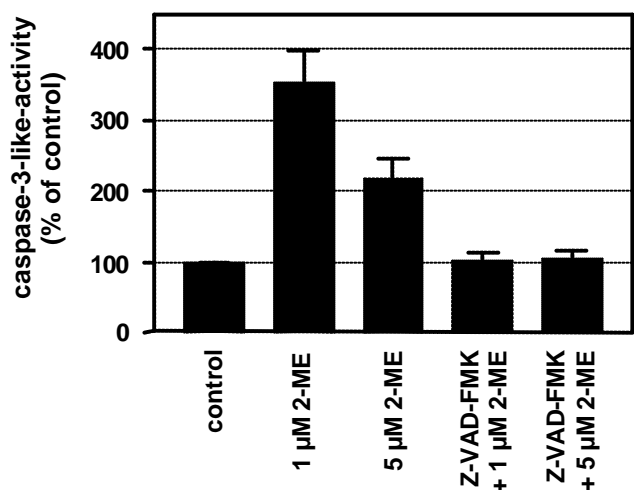
Fig. 3.1.4.1: Complete inhibition of 2-ME induced caspase-3-like activation by pan caspase inhibitor Z-VAD-FMK. Cells were treated with 2-ME alone or the combination of pan caspase inhibitor Z-VAD-FMK and 2-ME. Caspase inhibitor was given 1 h prior to 2-ME administration. After 48 h cells were harvested, lysed and caspase-3-like activity was determined using the fluorogenic substrate Ac-DEVD-AMC. Cells receiving no caspase inhibitor were treated with DMSO (0.4%), control cells got ethanol (0.1%) additionally. Data are means ? SD of three independent experiments.

Cell permeable caspase-8 inhibitor was utilised for a better understanding of caspase-3-like activation by 2-ME. Both caspase-8 activation and mitochondrial changes occurred after 2-ME treatment. On this account caspase-8 inhibitor

Z-IETD-FMK was used to estimate the role of caspase-8 in activation of the effector caspases-3, -6 and -7. Therefore, cells were incubated with 15 µM Z-IETD-FMK one hour before 2-ME was added. After 48 h caspase-3-like activity was determined. In 1 µM 2-ME treated cells 83% of 2-ME induced caspase-3-like activation could be inhibited by preincubation with caspase-8 inhibitor. Cells treated with 5 µM 2-ME showed lower caspase-3-like activation, which could only be halved by caspase-8 inhibitor (data not shown).

Pointing to the high efficiency of used pan caspase inhibitor, cleavage of DNA re-pairing enzyme PARP was investigated. As described in chapter 3.1.1 effector caspases cleave PARP in order to inactivate it. 2-ME treatment resulted in partial PARP cleavage shown in Fig. 3.1.4.2. Cells which were preincubated with the pan caspase inhibitor Z-VAD-FMK showed minimal amounts of cleaved PARP after 72 h. These results evidence the nearly complete inhibition of caspases and caspase-dependent response reactions by the inhibitor Z-VAD-FMK.

1 µM 2-ME	-	+	-	+	-
5 µM 2-ME	-	-	+	-	+
40 µM Z-VAD-FMK	-	-	-	+	+
DMSO	+	+	+	-	-
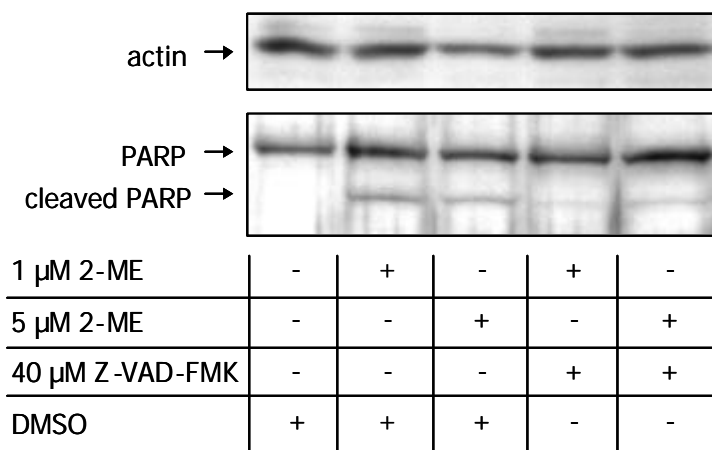
Fig. 3.1.4.2: Pan caspase inhibitor Z-VAD-FMK blocked 2-ME induced PAPR cleavage. Cells were preincubated with 40 µM pan caspase inhibitor Z-VAD-FMK or DMSO. After 1 h 2-ME was added at the indicated concentrations for further 72 h. Control cells were treated with DMSO (0.4%) and ethanol (0.1%). Cells were harvested and analysed for PARP cleavage by Western blotting. Protein load was verified by actin expression. Blots shown are representative.

Surprisingly, no effect on proliferation and apoptosis was observed in cells treated with 2-ME and pan caspase inhibitor in comparison to cells receiving 2-ME treatment alone. Fig. 3.1.4.3 shows electrophoretical analysis of genomic DNA of cells treated with 1 or 5 µM 2-ME with or without Z-VAD-FMK preincubation. DNA laddering could not be blocked by pan caspase inhibitor administration, only a slight reduction in DNA fragmentation was observed. Furthermore, cells treated with Z-VAD-FMK and 2-ME had a larger cell diameter compared to cell receiving 2-ME alone (data not shown).
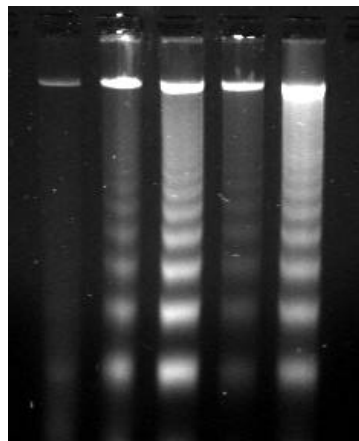
1 µM 2-ME	-	+	-	+	-
5 µM 2-ME	-	-	+	-	+
40 µM Z-VAD-FMK	-	-	-	+	+
DMSO	+	+	+	-	-

Fig. 3.1.4.3: Pan caspase inhibitor Z-VAD-FMK did not block 2-ME induced DNA laddering. Cells were preincubated with 40 µM pan caspase inhibitor Z-VAD-FMK. After 1 h 2-ME was administered at the indicated concentrations for additional 72 h. Cells were then harvested and genomic DNA was isolated. 2 µg DNA were loaded to a 1.8% agarose gel and separated by electrophoresis.

Quantification of apoptotic cells in 2-ME treated cells with or without Z-VAD-FMK preincubation was assessed by staining cells with 7-aminoactinomycin D. Late apoptotic or necrotic cells show a bright 7-AAD fluorescence, whereas apoptotic cells, which retain membrane integrity, show a 7-AAD fluorescence between dead and alive cells. 72 h after addition of 1 µM 2-ME only 12% of DS-sarcoma cells showed

an apoptotic staining pattern. Inhibition of caspases reduced the proportion of apoptotic cells to 9%. The fraction of dead cells could also be decreased to a low extent by pan caspase inhibition. Scatter diagrams point to apoptotic involvement in cell death, which is not caspase-dependent. Due to the fact that the fraction of apoptotic cells is not increased 24 h after 2-ME treatment (data not shown), apoptosis is probably not the only way for 2-ME induced cell death.
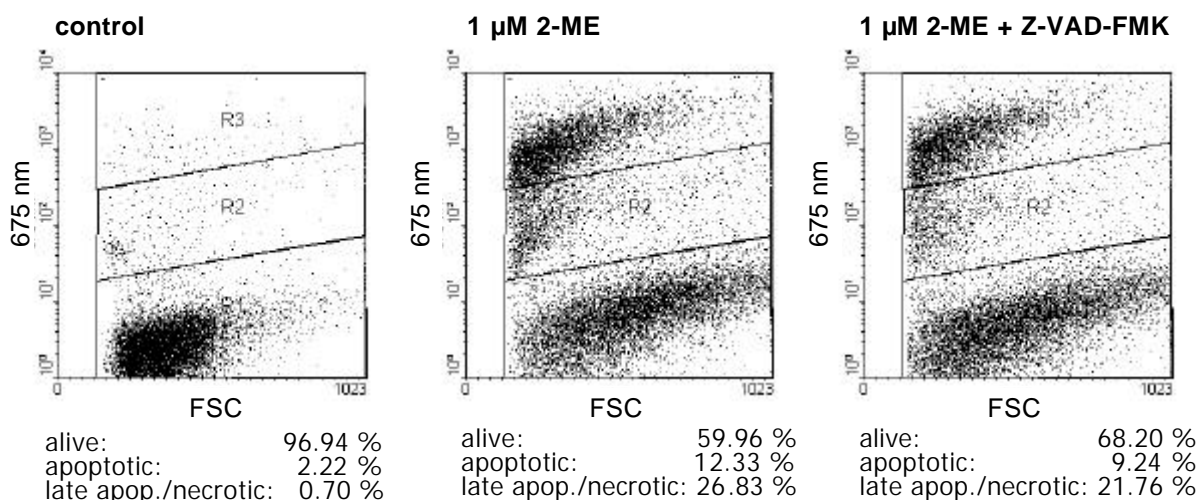
Fig. 3.1.4.4: Scatter diagrams of 7-AAD stained cells. Cells were incubated with 40 µM pan caspase inhibitor Z-VAD-FMK or 0.4% DMSO. After 1 h 1 µM 2-ME was added for 72 h. Thereafter, cells were stained with 7-AAD, washed and analysed by flow cytometry. Control cells were treated with DMSO (0.4%) and ethanol (0.1%). Scatter diagrams presented are representatives of three independent experiments.

3.1.5   In vivo experiments

In order to verify the *in vitro* data, anti-tumour efficacy of 2-ME and the combination of 2-ME and the ROS-generating treatment, hyperthermia/hyperoxia/xanthine oxidase, was investigated *in vivo* (by Dr. med. habil. O. Thews, Institute of Physiology and Pathophysiology, University of Mainz, Germany). Solid DS-sarcomas were induced in the hind feet of Sprague-Dawley rats. The tumours showed an exponential growth behaviour up to a volume of 3.5 ml with a volume doubling time of approx. 1.9 days. 2-ME treatment (without ROS-generating hyperthermia) slightly

slowed down the tumour growth rate to a volume doubling time of 2.5 days. However, the mean tumour volume was not significantly different between the control group and those treated solely with 2-ME. No tumours were cured in any of the animals treated with 2-ME alone. All tumours reached the set volume limit of 3.5 ml within 9 days (8 days in control animals). Treating animals with the combination of 44°C-hyperthermia (HT), xanthine oxidase (XO) and respiratory hyperoxia (RH) led to a growth delay of approx. 5 days with a subsequent regrowth of the tumour. The regrowth rate after this period was slower compared to controls with a volume doubling time of 5.9 days. In three cases, tumours were cured showing no regrowth over a period of 30 days. When the ROS-generating HT treatment was combined with a single injection of 2-ME the growth delay lasted approx. 7 days, with 6 tumours being cured and a probability of local tumour control of 51%. The difference in inhibition of tumour growth was significant between both treatment modalities (log-rank test p=0.0458). These results demonstrate that 2-ME improves the antitumoural efficacy of ROS-generating hyperthermia (HT+XO+RH).
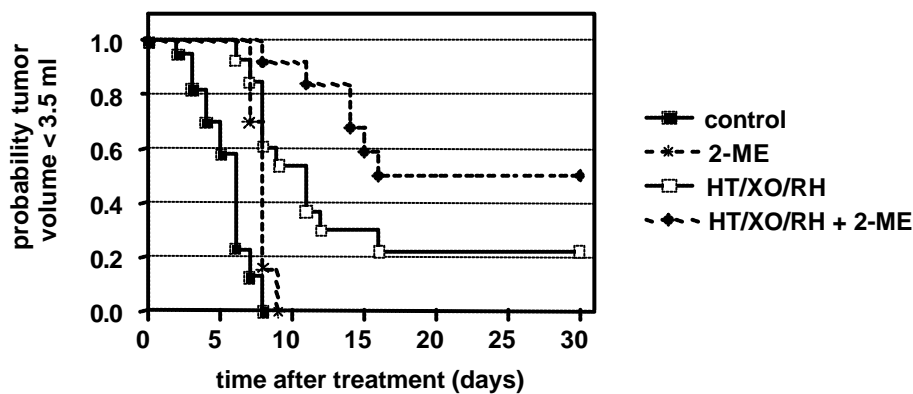
Fig. 3.1.5.1: Combination of 2-ME treatment and ROS-generating therapy reduced tumour growth *in vivo*. Kaplan-Meier analysis showing the probability of tumour volume being less than 3.5 ml as a function of time after sham-treatment (control) or administration of 2-ME (17.5 mg/kg body weight) or following ROS-generating treatment (HT/RH/XO) alone or combined with 2-ME. At least 11 tumours per treatment group were investigated.

3.2   ALA-PDT

In this study anti-tumour efficacy of ALA-PDT and hyperthermia was investigated *in vivo* in the rat DS-sarcoma model. For this purpose ROS-formation, apoptosis induction and expression of prognostic relevant proteins were determined in tumour tissue.

3.2.1   Induction of apoptosis

Induction of apoptosis was visualised by immunohistochemical detection of DNA single and double strand breaks using the TUNEL-assay (Fig. 3.2.1.1). A clear increase of apoptotic cells was found in HT and ALA-PDT treated tumours compared with control tumours. Apoptotic cells were rarely observed in control tumours, as well as in the two additional control groups, which received either ALA (without irradiation) or irradiation alone. The latter two groups were not pictured in Fig. 3.2.1.1. In contrast, an extensive increase in the fraction of apoptotic cells in tumour tissue was observed after treatment with ALA-PDT or ALA-PDT+HT. These treatments resulted in a expression of distinct areas containing several hundred apoptotic cells. In comparison to the 0 h time values, the amount of apoptotic cells increased once more 18 h after treatment within the PDT treated groups. HT alone also resulted in an increased fraction of apoptotic cells but to a much lesser extent. In both time points the greatest amount of apoptotic cells was determined in ALA-PDT+HT treated tumours.

In addition, so called apoptotic bodies could be observed immediately after ALA-PDT (Fig. 3.2.1.2) or ALA-PDT+HT treatment (not pictured).
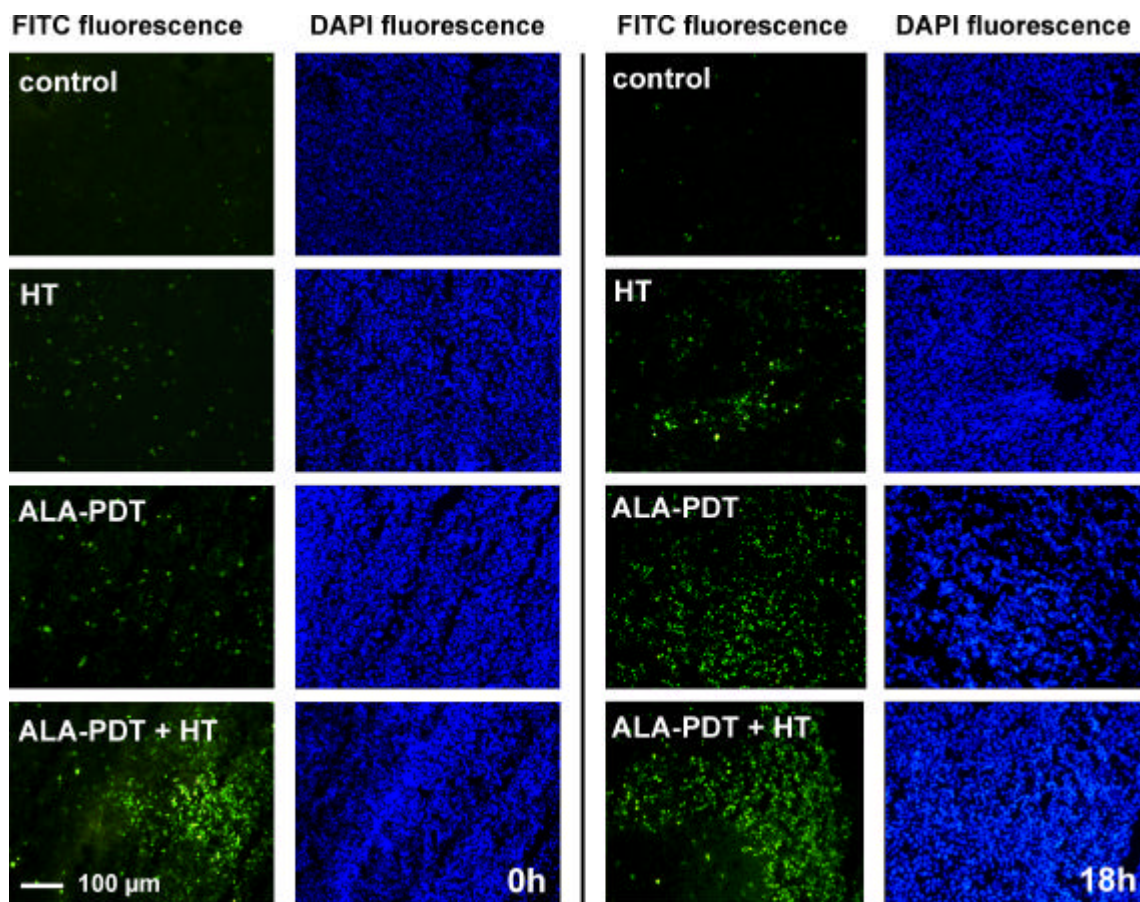
Fig. 3.2.1.1: Induction of apoptosis visualised by TUNEL-assay. DS-sarcomas exposed to sham-treatment, HT, ALA-PDT, ALA-PDT+HT, ALA application without irradiation and irradiation alone were analysed for DNA strand breaks using the TUNEL-assay (green fluorescence) as described in materials and methods. Nucleoli were stained with DAPI (blue fluorescence). Pictures shown are representative.
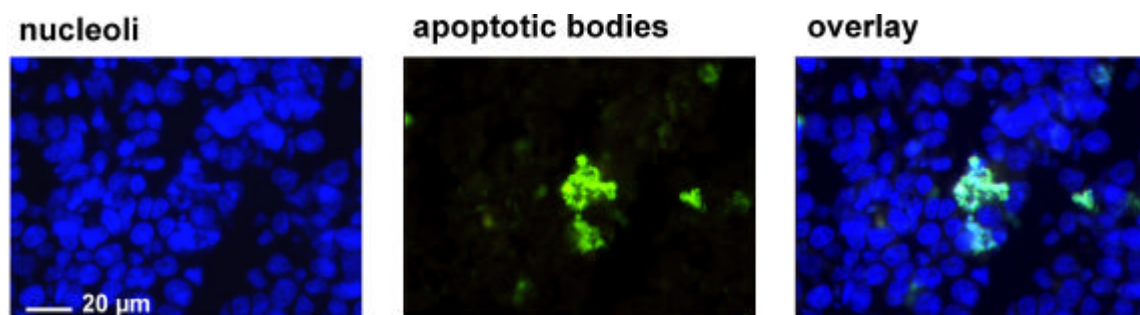
Fig. 3.2.1.2: Formation of apoptotic bodies after ALA-PDT treatment. Tumour tissue immediately excised after ALA-PDT treatment was stained with DAPI (blue fluorescence) visualising nucleoli and analysed for DNA strand breaks by TUNEL-assay (green fluorescence). TUNEL positive cells showed clear staining pattern of apoptotic bodies. Picture on the right shows the overlay of DAPI and TUNEL-staining.

Further clear signs of apoptosis are activation of caspases and DNA fragmentation. They occur at different time points during the programmed cell death and are so called "hallmarks" of apoptosis. As shown in Fig. 3.2.1.3 the occurrence of DNA fragmentation matched well with the extent of apoptosis observed in immuno-histochemistry. Because DNA fragmentation is one of the late events taking place in apoptosis, immediately after treatment (0 h) no DNA fragmentation could be observed, but 18 h after treatment, clear signs of DNA fragmentation were detected. DNA fragmentation was completely absent in control tumour tissues and increased upon treatment, whereby the effect was greatest in ALA-PDT+HT treated tumours.
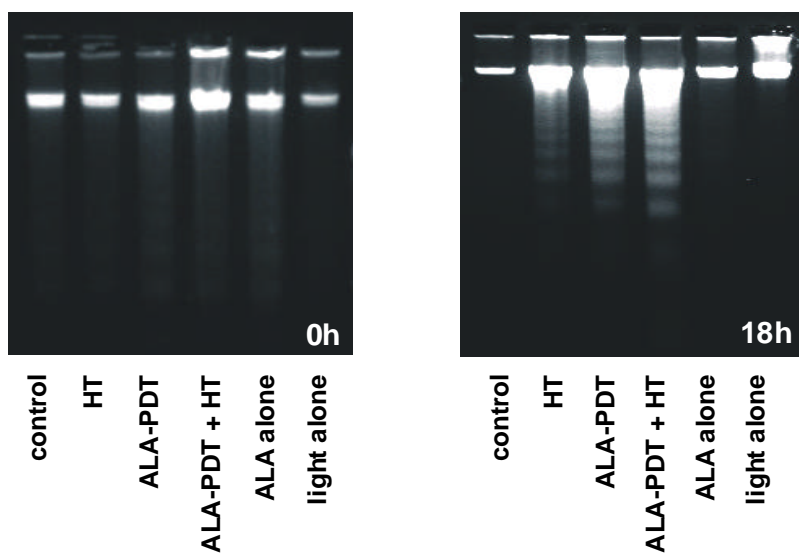
Fig. 3.2.1.3: DNA laddering after hyperthermic and photodynamic treatment. Tumours were treated with HT (43°C), ALA-PDT, ALA-PDT+HT, ALA application without irradiation and irradiation alone. Control tumours were sham treated. The tumours were resected directly or 18 h after treatment. Genomic DNA was isolated by chloroform/phenol extraction. 2 µg DNA was loaded on a 1.8% agarose gel and electrophoresis was performed. DNA preparations of at least two different tumours per treatment group were analysed. Gels presented are representatives.

Interestingly, not only DNA but also RNA fragmentation could be observed upon treatment. In contrast to DNA fragmentation, the fragmentation of RNA occurred very early, already immediately after treatment (0 h), whereby RNA fragmentation seemed to occur only in the PDT treated groups.
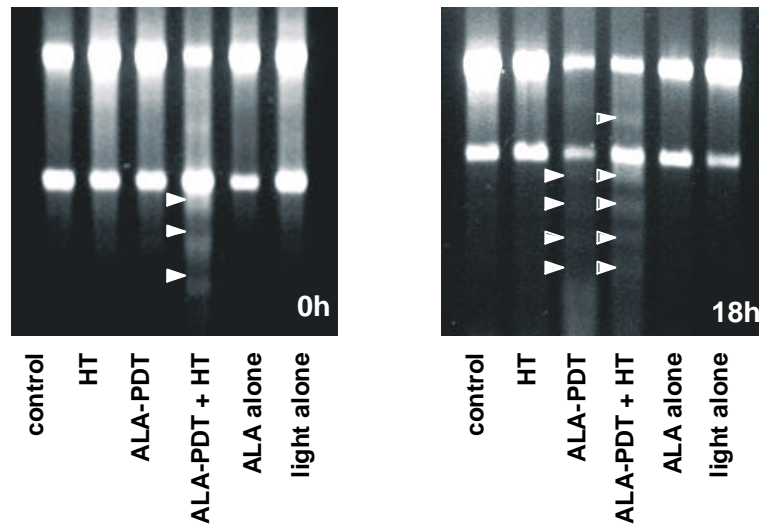
Fig. 3.2.1.4: Specific RNA digestion in tumours treated with ALA-PDT and ALA-PDT+HT. Tumours were treated as described in Fig. 3.2.1.3. Total RNA was isolated out of cryostat sections with RNAwiz[?]. 1 µM RNA was analysed on a TBE-gel. Gels shown are representative.

To identify whether activated caspases are involved in HT and ALA-PDT induced apoptosis, caspase-3 and caspase-8 activities in tumour tissues were investigated. A clear activation of caspase-3-like and caspase-8 activity (Fig. 3.2.1.5) could be demonstrated immediately after treatment. 18 h later caspase activities were normalised and an increase was no longer detectable (data not shown). Clear increases of caspase-3-like and caspase-8 activity were found after HT, ALA-PDT, and ALA-PDT+HT, whereby the effect was greatest with HT. Surprisingly, light alone also increased the activity of caspase-3 and caspase-8 marginally.
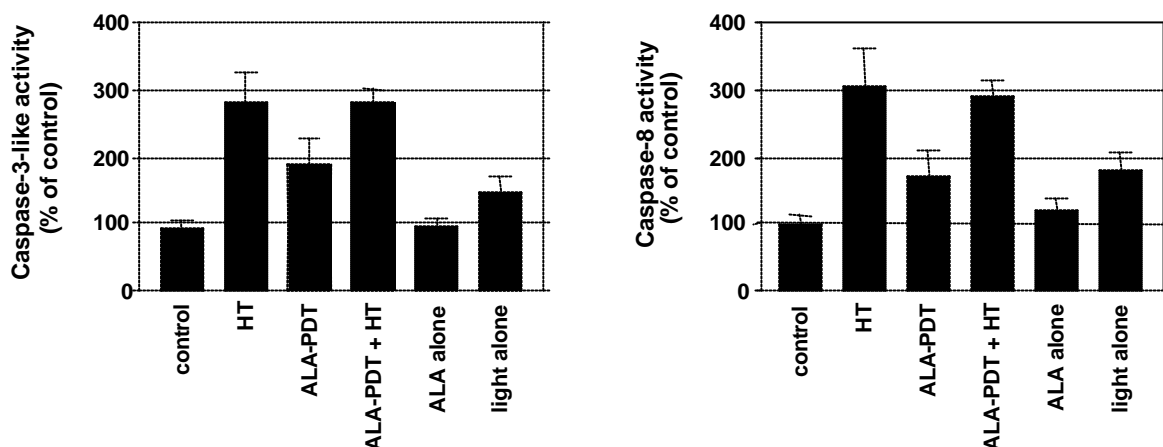
Fig. 3.2.1.5: Enhanced caspase-3-like and caspase-8 activity in tumours exposed to hyperthermia and hyperthermia + ALA-PDT. Tumours resected immediately after treatment (sham-treatment, HT, ALA-PDT, ALA-PDT+HT, ALA application without irradiation and irradiation alone) were lysed and caspase-3-like and caspase-8 activity were determined measuring the cleavage activity of the fluorogenic substrates Ac-DEVD-AMC and Ac-IETD-AMC. Data are means ? SEM of at least five tumour samples per treatment group.

3.2.2   Investigations of tumour defence mechanisms ("rescue response")

Expression of heat shock proteins affects response to anti-cancer treatments. The ability of heat shock proteins protecting biological structures against denaturation can decrease the efficiency of anti-cancer therapies. Heat shock protein 70 (HSP70) inhibits apoptosis by antagonising AIF [93], activation of SAPK/JNK [94] and inhibition of Apaf-1 apoptosom formation [95]. In contrast, it heme oxygenase-1 (HO-1 or HSP32) detoxifies ROS, because the reaction products of HO-1 activity, biliverdin, and its subsequent metabolite bilirubin, have antioxidant properties [96].

The expression of HSP70 and HO-1 were investigated by Western blot analysis. Immediately after treatment, HSP70 expression did not differ between the treatment groups. At time point two (18 h) hyperthermia treated tumours showed a 2.1-fold increase in HSP70 protein level. However, the combination of HT with ALA-PDT abrogated the HT induced increase of HSP70. PDT alone resulted in a moderate downregulation of HSP70 protein expression.

In contrast to literature, HO-1 expression was not up-regulated by hyperthermia or PDT in this study [97,98]. At both time points tumours treated with HT, ALA-PDT or the combined therapy showed a decrease in HO-1 protein content. The highest down-regulation in HO-1 expression was assessed in tumours receiving the combination of hyperthermia and ALA-PDT. In this group HO-1 protein levels were lowered to 24% compared to sham treated tumours (100%). Normally, HO-1 is induced by a host of oxidative stress or heat stimuli, and the activation of HO-1 gene expression is considered to be an adaptive cellular survival response to exposure to environmental stress [99].
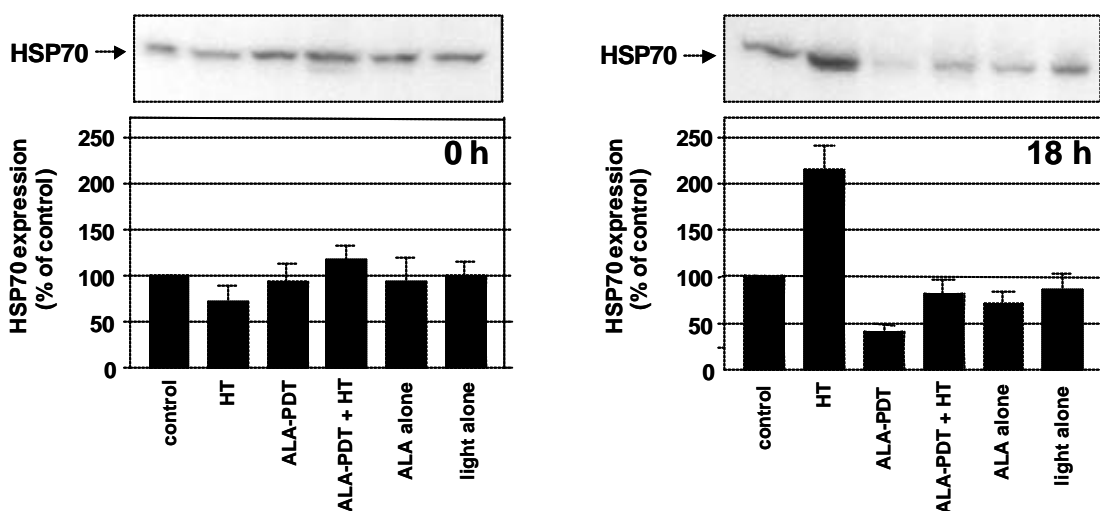
Fig. 3.2.2.1: Modulation of HSP70 expression in hyperthermia and ALA-PDT treated tumours. Sarcomas were exposed to sham-treatment, HT, ALA-PDT, ALA-PDT+HT, ALA application without irradiation and irradiation alone. Immediately or 18 h after treatment tumours were excised. Tissue lysates were prepared and HSP70 protein expression was determined by Western blotting. The graphs display densitometrical analysis of Western blots. HSP70 expression of sham treated tumours (control) were set at 100%. Results presented are means ? SEM of at least 4 tumours per treatment group. In addition, a representative Western blot at each time point is shown.
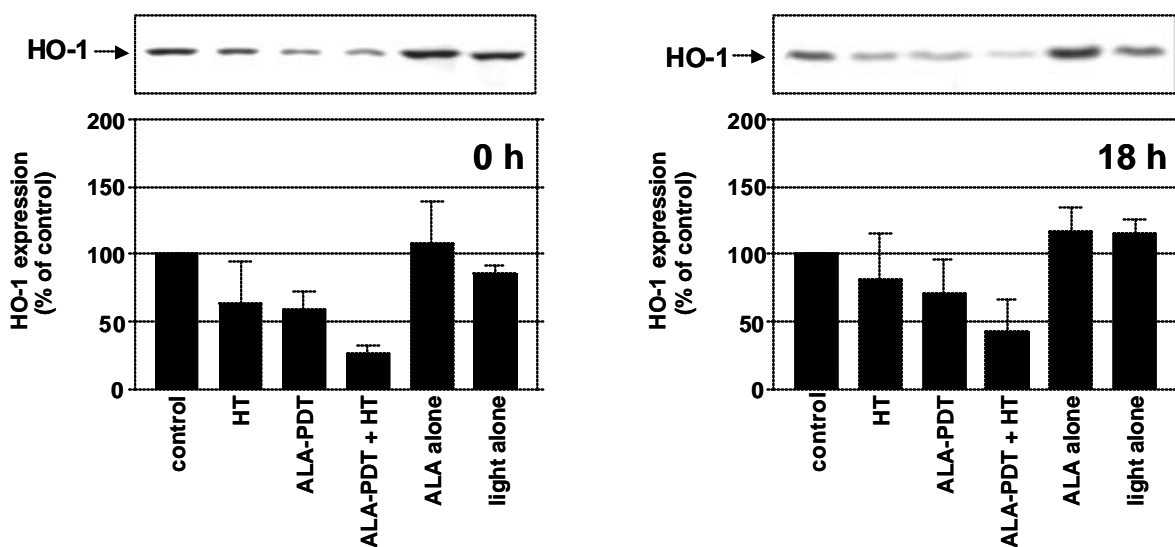
Fig. 3.2.2.2: Decreased HO-1 expression in hyperthermia and ALA-PDT treated tumours. Tumours were treated as described above (see Fig. 3.2.2.1). After tumour resection (immediately or 18 h after treatment) tissue lysates were prepared. HO-1 expression was subsequently analysed by Western blotting using a polyclonal HO-1 antibody. Data are means ? SEM of 4 tumours per treatment group. Blots shown are representatives.

Normally, matrix metalloproteinases (MMPs) are not counted among "rescue response" proteins, but they play an important role in tumour growth, tumour angiogenesis and metastasis by degradation of extracellular matrix [67]. Increased expression of MMPs has been associated with tumour progression [100]. On the base of these facts, activity of MMP-2 and MMP-9, two gelatinases was assessed in tumour tissue. Therefore, tumour lysates were analysed by zymography. Immediately after anti-cancer treatment no changes in MMP-9 and MMP-2 activity were observed between the various treatment groups. In contrast, 18 h after therapy tumours which were treated with ALA-PDT or the combination of ALA-PDT and hyperthermia showed no MMP-9 activity and only slight MMP-2 activity. Comparing these two groups, no benefit of the combined therapy was observed, because PDT alone reached nearly maximal MMP inhibition.
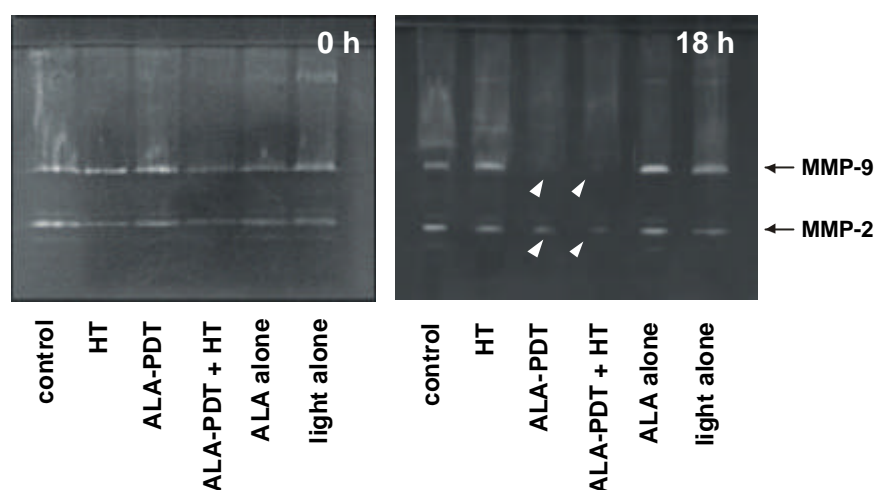
Fig. 3.2.2.3: Photodynamic therapy inhibited MMP-2 and MMP-9 activity 18 h after treatment. Tumours received the indicated treatments. Immediately or 18 h after treatment tumours were excised. Tumour lysates were prepared and MMP activity was determined by SDS-PAGE, gels containing gelatin. Zymographs shown are representatives of three independent experiments.

3.2.3   Detection of oxidative stress

Glutathione is the major water-soluble antioxidant in the cytoplasm, mitochondria and nuclei. It can decrease the efficiency of anti-cancer treatments, due to its antioxidant properties: high glutathione levels in tumours are associated with multidrug resistance [101]. Furthermore, GSH can form chemical interactions between cisplatin or carboplatin, which block their cytotoxic effect [102]. Based on this fact, the reduced form of glutathione was assessed in treated tumours by HPLC. The oxidised form can be generated by the oxidation of two molecules GSH to GSSG, or one molecule GSH and a further thiol containing molecule to GSSX. This reaction detoxifies hydrogen peroxide to water and oxygen (or other peroxides to the corresponding alcohol and oxygen) catalysed by glutathione peroxidase.

Tumours treated with hyperthermia, ALA-PDT and the combination of both resulted in decreased levels of glutathione. Immediately after treatment, tumours exposed to ALA-PDT and hyperthermia showed the highest decrease in GSH content (0.009 µmol GSH/mg protein in contrast to 0.027 µmol GSH/mg protein in control tumours). Single treatment of hyperthermia or ALA-PDT decreased GSH levels as well. 18 h

after treatment, ALA-PDT and the combined therapy of ALA-PDT and HT showed a further decrease in GSH levels, whereas ALA-PDT alone lowered GSH level strongest.
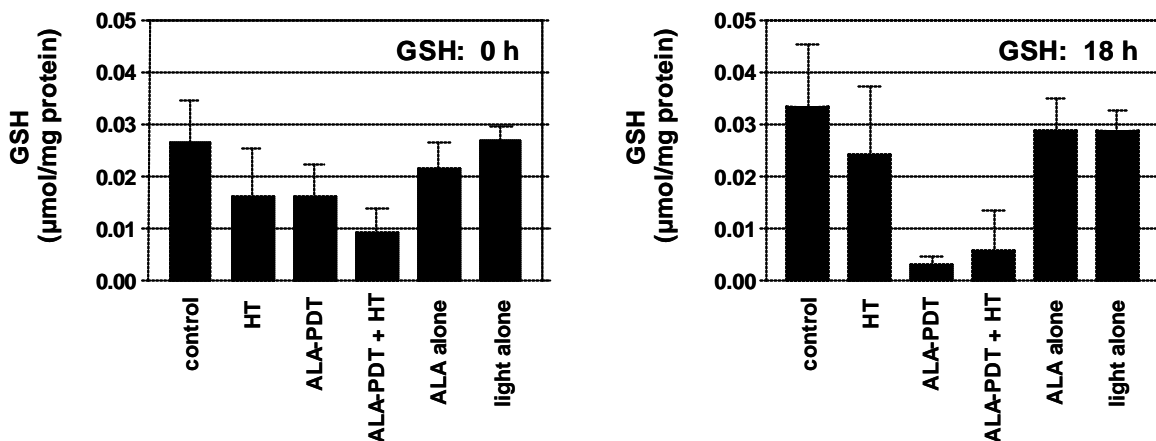
Fig. 3.2.3.2: Levels of reduced glutathione in tumour tissue. Sarcomas were exposed to the indicated treatments. Either immediately or 18 h after treatment tumours were excised and reduced glutathione (GSH) was determined by HPLC after derivatisation with ammonium-7-fluorobenzo-2-oxa-1,3-diazole-4-sulfonate. Data are means ? SD of at least 4 tumours per treatment group.

A subclass of ROS are reactive nitrogen species. This term describes NO radicals and products, which are formed by the reaction of NO with superoxide anions, e.g. peroxynitrite and NO_2 radicals. With the discovery that peroxynitrite can modify a number of biological molecules, including proteins, lipids, and nucleic acids, considerable attention has been given to the role of peroxynitrite in oxidative cellular damage. Among other changes, peroxynitrite has been shown to promote the nitration of tyrosine [103,104]. Besides the oxidation of methionine [105,106] and cysteine [107,108] residues of proteins, tyrosine nitration is a well detectable marker. Therefore, immunohistological detection of "protein nitrosylation" was performed to localise the sites of reactive nitrogen-related damage after the various treatments. Compared with the control groups, an increase was observed in the amount of "protein nitrosylation" in tumours treated with HT. ALA-PDT and the combination of ALA-PDT and HT resulted in a further increase in nitrosylated proteins within the tumour sections, whereby the effect was greatest with ALA-PDT+HT. The amount of nitrosylated proteins formed upon treatment did not substantially increase with time.

No major differences were observed between the first (0 h) and the second time point (18 h) by which nitrosylated proteins were measured. To demonstrate that the formation of nitrosylated proteins may be correlated to endothelial cells (blood vessels), nitrosylated proteins and endothelial cells were stained simultaneously. As shown in Fig. 3.2.3.4, protein nitration corresponded to sites where small vessels were present. This may also explain the focal expression of nitrosylated proteins which was observed upon treatment.
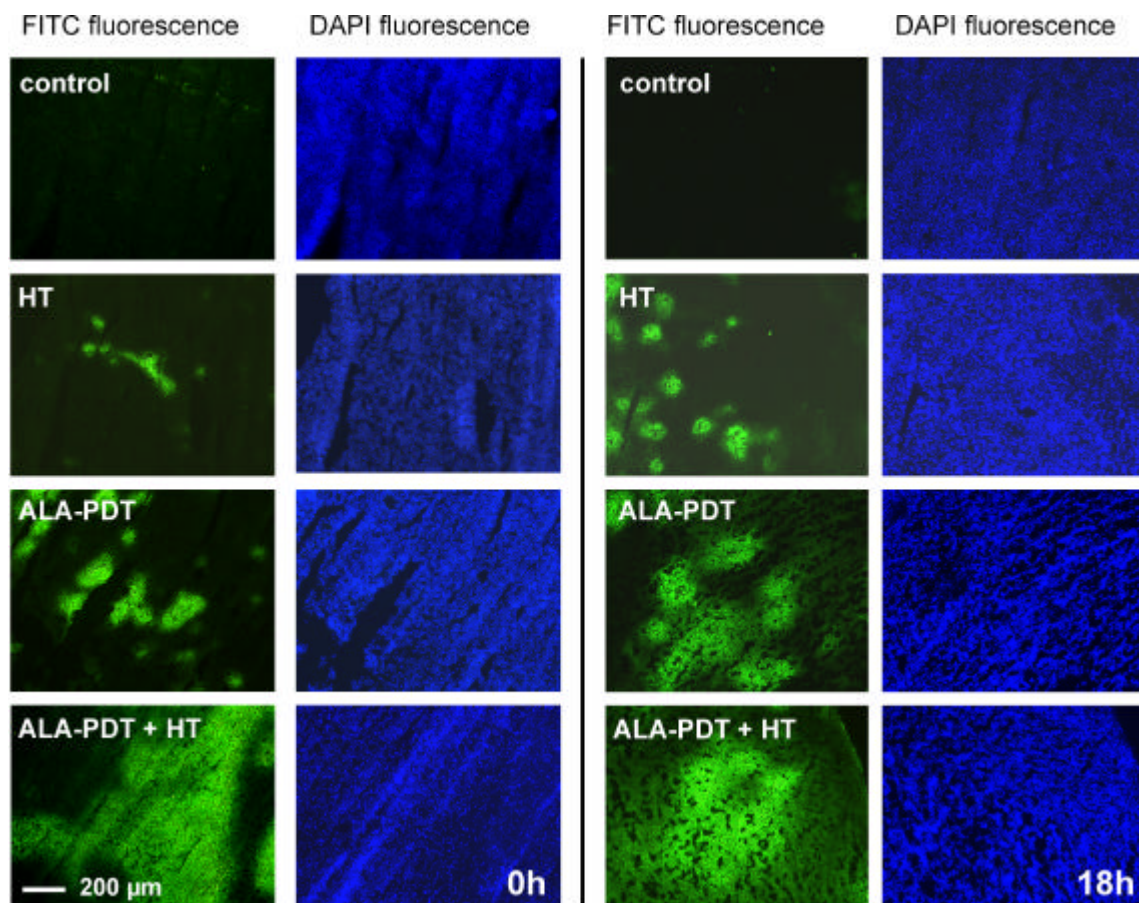
Fig. 3.2.3.3: Enhanced protein nitrosylation in tumours exposed to hyperthermia and PDT. Tissue sections of tumours exposed to sham treatment, hyperthermia, ALA-PDT, ALA-PDT+HT, ALA application without irradiation and irradiation alone were analysed for nitrosylated proteins by immunohistochemistry. Simultaneously, sections were stained with DAPI to visualise nucleoli. Pictures shown are representative.
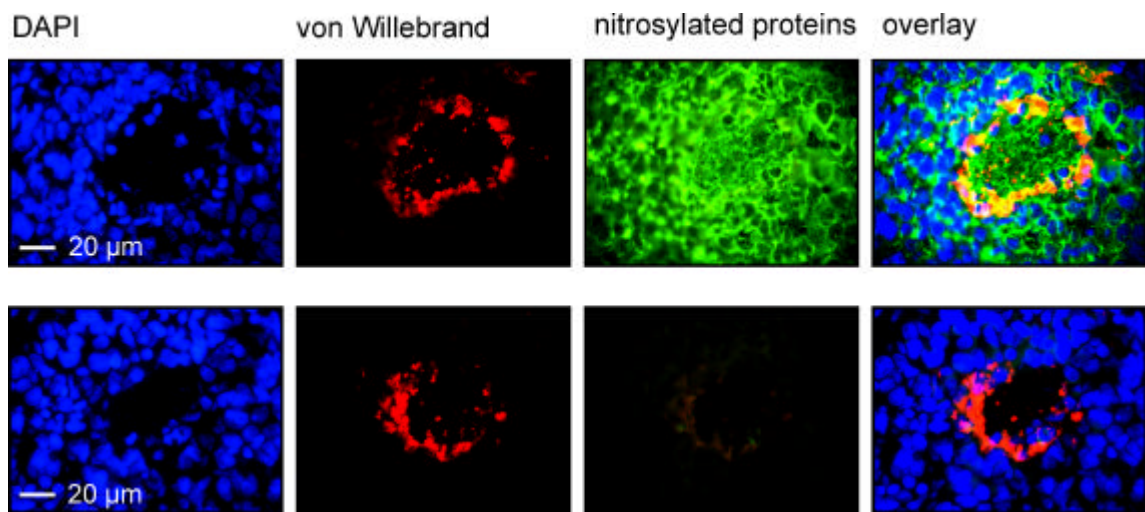
Fig. 3.2.3.4: Localisation of nitrosylated proteins in vessels. Tissue section of a ALA-PDT+HT treated tumour was stained for nitrosylated proteins (green fluorescence), for von Willebrand factor, a marker protein for endothelial cells (red fluorescence) and for nucleoli with DAPI (blue fluorescence). Pictures in the second row demonstrate the specificity of antibody binding. Therefore, primary antibody was blocked with 10 mM nitro-tyrosine for 1 h at RT. Pictures on the right show the overlay of all three stainings.

4   Discussion

4.1   2-Methoxyestradiol

Based on the previous reported finding, that 2-ME inhibits superoxide dismutase activity, 2-ME was chosen to be a perfect candidate for adjuvant anti-cancer therapy with other ROS-generating treatments. At that time mechanisms of 2-ME induced apoptosis and the role of reactive oxygen species in 2-ME cytotoxicity were not elucidated completely. Therefore, apoptotic events like caspase activation, expression of Bcl-2 proteins, mitochondrial and nuclear changes were assessed in the rodent carcinosarcoma cell line DS-sarcoma. These investigations showed, that 2-ME induced apoptosis via mitochondrial injury. Surprisingly, caspases were not essential for the apoptotic process, although they were activated by 2-ME. ROS-formation was increased by 2-ME in a dose-dependent manner. However, supplementation of DS-sarcoma cells with antioxidants did not inhibit 2-ME induced cell death.

The main objective of this study therefore was to determine the anti-cancer effect of 2-ME combined with a further ROS-generating treatment. Both *in vivo* and *in vitro* this treatment regime showed an synergistic anti-cancer effect compared to single treatments, indicating the high therapeutical potential of 2-ME.

Cytotoxicity

This is the first study showing that 2-ME is effective in treating carcinosarcoma cells *in vitro*. Compared to other cell lines, DS-sarcoma cells showed a relatively high sensitivity to 2-ME, starting at 0.25 µM. Cell growth of leukaemia and most of pancreatic cancer cell lines were inhibited at a concentration range of 1-5 µM [15,20] whereas hepatoma cells needed higher concentration (?10 µM) for growth arrest [27]. Proliferation of DS-sarcoma cells stopped short after by addition of ? 3 µM 2-ME, lower 2-ME concentrations caused a decrease in proliferation, growth arrest was observed between 48 and 72 h after 2-ME addition. Induction of apoptosis was independent of growth arrest. These results agree with the data of the antimicro-

tubule agents, docetaxel and paclitaxel, which also induce apoptosis without G2/M arrest at low concentrations [27]. The enhanced production of ROS in cells treated with higher 2-ME concentrations could be involved in inhibition of proliferation which occurred almost immediately after 2-ME addition. Oxidative stress is able to inhibit cell growth by triggering a G2 checkpoint response that results in a delay in the activation of cyclin B/Cdc2 kinase activity at the G2/M border. The cyclin B/Cdc2 kinase activity , as well as entry into mitosis can be suppressed by the ROS-generating agent, tert-butyl hydroperoxide [109]. However, this hypothesis could not be corroborated by the present findings: Preincubation of DS-sarcoma cells with six different antioxidants did not alter the 2-ME induced changes in cell proliferation. Comparable results were obtained by Lin, who investigated the effect of magnolol on 2-ME induced cell death of hepatoma cells [27].

Induction of apoptosis

Investigation of caspase activity, Bax location and nuclear changes in DS-sarcoma cells showed that apoptosis is involved in 2-ME induced cell death. Although caspases were activated by 2-ME, inhibitor studies showed, that 2-ME induced cell death is caspase-independent in DS-sarcoma cells. Caspase-independent apoptosis is a well known phenomenon in the literature [110-112]. Many publications describe, that pan caspase inhibitors can mostly block PARP cleavage and DNA fragmentation, but they are not always able to save cells from dying. Reason for these findings may be the fact that apart from caspases Bcl-2 family members play a prominent role in apoptosis by changing the integrity of the mitochondrial membrane [113]. Probably, 2-ME induced caspase activation is not the initial apoptotic event, it may be rather the consequence of mitochondrial changes, which are induced by translocation or cleavage of proapoptotic Bcl-2 family members. One of these members is Bax, a cytosolic protein, that can translocate to the mitochondrial membrane in the case of apoptosis induction. There, Bax is able to puncture the outer mitochondrial membrane leading to the release of AIF, procaspases, cytochrome c, endonuclease G and other factors [16,114]. The present study shows that 2-ME administration clearly

induces AIF release out of mitochondria. AIF, a mitochondrial intermembrane space protein, migrates to the nucleus and participates in the induction of large scale DNA fragmentation (fragments of approximately 50 kbp) and chromatin condensation in a caspase-independent way [79]. However, AIF is not responsible for the observed low scale DNA fragmentation (~ 200 bp) in DS-sarcoma cells treated with the caspase-inhibitor Z-VAD-FMK and 2-ME. Normally, DNA fragmentation in nucleosome-size is caused by the nuclease DFF40/CAD, that is activated by caspase-3 and −7 [85]. The observed DNA laddering after inhibition of caspases may be explained by another enzyme, that could be released out of mitochondria. Not more than a year ago, Li and coworkers reported on the identification of a mitochondrial nuclease, termed endonuclease G, which can cause low scale fragmentation. Endonuclease G can be released out of mitochondria either by formation of tBid or by action of Bim (Fig. 4.1.2) [115]. Cleavage of Bid to tBid could be induced by caspase-8 [116], granzyme B [117] or by lysosomal proteases [118]. In addition, another caspase-independent mechanism of tBid formation concerning the internalisation of TNF receptor-1 complex is also being discussed at the moment (unpublished data of Prof. S. Schütze, Insitute of immunology, University of Kiel, Germany). The second molecule, modulating the release of endonuclease G is Bim whose apoptotic activity is regulated through its dissociation from microtubular dynein motor complex during apoptosis whereby no caspases are involved [16]. Endonuclease G represents an alternative pathway to DFF40/CAD, which may explain the fact that caspase inhibitor Z-VAD-FMK could not abolish 2-ME induced DNA laddering. Data of Bouillet may confirm the relevance of Bim and therefore of endonuclease G in the cytotoxicity of antimicrotubule agents. He showed that $Bim^{-/-}$ cells treated with the antimicrotubule drug taxol survived 10 to 30 times better than taxol treated wild-type cells [119]. Since 2-ME is known to be a microtubuli destroying drug as well, it is possible that Bim also plays an important role in 2-ME induced apoptosis.

In contrast to AIF, cytochrome c release into cytoplasma could not be observed by 2-ME treatment. Different localisations of these proteins may contribute to this phenomenon: AIF is located in the mitochondrial intermembrane space, whereas

cytochrome c is adsorbed to the inner mitochondrial membrane via weak electro-static interactions [120]. Literature data of Daugas and colleagues showed, that AIF release occurred earlier than cytochrome c release [121,122]. The authors supposed, that AIF release is probably not dependent on the overall release of intermembrane proteins. Moreover, it has been demonstrated that cytochrome c release is not essential for the apoptotic process [123].

A further important questions is: what kind of mitochondrial membrane changes lead to the release of AIF ? Mitochondrial permeability transition pore (MPTP) plays a central role in releasing proteins out of mitochondria. The structure and composition of MPTP include both inner membrane proteins, such as the the adenine nucleotide translocase, and outer membrane proteins, such as the voltage dependent anion channel (VDAC), which operate in concert and create channels through which molecules < 1.5 kDa pass [124]. The three major consequences of MPTP opening are an uncoupling of oxidative phosphorylation, the loss of ions and small molecules from the mitochondrial matrix and extensive swelling of the mitochondria, which could lead to the rupture of the outer membrane [17]. Pro-apoptotic Bcl-2 members, like Bax, Bad and Bid, are involved in membrane permeabilisation. Shimizu and colleagues reported that Bax and Bak bind to the VDAC of the outer membrane and open it [125]. In addition, Bax and Bak probably induce a conformational change in VDAC so that proteins > 1.5 kDa can pass through the channel [125]. Another possibility is that Bax and Bid form selective channels for cytochrome c and other factors from the intermembrane space [126]. In the present study translocation of Bax to the mitochondrial membrane was determined within 24 h after 2-ME treatment. In addition, a decrease in $\Delta\Psi_m$ was assessed. In accordance with the mentioned literature data, these observations may explain the mechanism of AIF release by 2-ME shown in Fig. 4.1.1.

| Bax is located in cytosol | Bax translocates to the mitochondrial membrane | Decrease in mito-chondrial inner membrane potential | Release of AIF (channel impermeable for cytochrome c ?) |
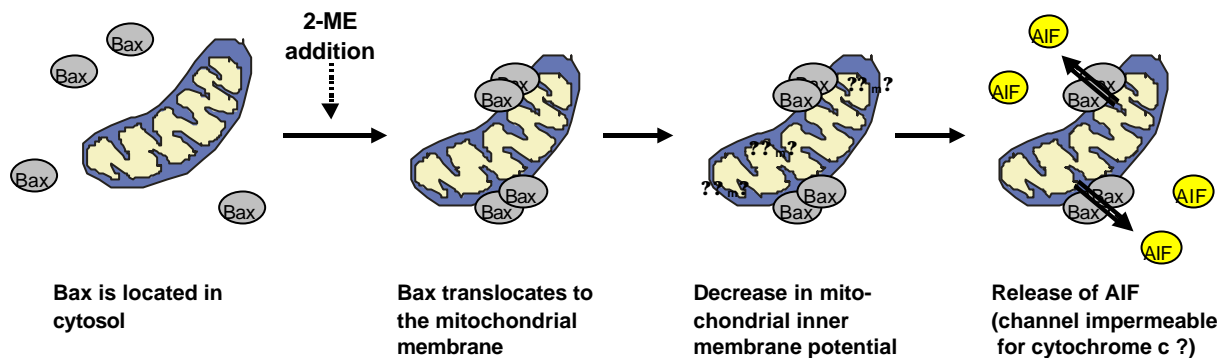
Fig. 4.1.1: Postulated mechanism of 2-ME induced AIF release. Normally, Bax is located in the cytosol. After addition of the apoptosis inducing drug 2-ME, Bax-homodimers translocate to the outer mitochondrial membrane, where they may interact with VDAC. This interaction is probably responsible for the observed decrease in $\Delta\Psi_m$ by 2-ME and the release of AIF.

In DS-sarcoma cells, translocation of Bax to mitochondria by 2-ME may be connected to the inactivation of the anti-apoptotic protein Bcl-2 which was reported by Attalla et al. investigating the effect of 2-ME in leukaemia cells [23]. Inactivation was induced by phosphorylation of Bcl-2, whereas total levels of Bcl-2 protein did not change. The latter finding could be validated in DS-sarcoma cells, yet phosphorylation of Bcl-2 was not determined. The timing of Bcl-2 phosphorylation following 2-ME treatment in leukaemia cells was similar to the Bax upregulation in the present study. Due to these data, we suppose that the pro-apoptotic action of Bax-upregulation is enhanced by Bcl-2 inactivation.

Beside the initial role of mitochondrial changes in 2-ME induced cell death, upregulation of Fas ligand and TNFα was observed 24 h after 2-ME treatment. This increase in death receptor ligands may amplify the mitochondrial alterations by type II reaction (Fig. 4.1.2). Cell response to TNFα treatment is subdivided into two types. Type I cells show strong activation of the DISC and of caspase-8, leading to the activation of caspase-3. Type II cells weakly activate DISC and caspase-8, thus they must amplify their death signal through the mitochondria [127]. Due to the slight

increase in caspase-8 activity after 2-ME exposure, DS-sarcoma cells probably belong to the category of type II cells. Beneath the result of enhanced FasL/TNF? expression by 2-ME, many questions concerning the role of death receptors remain unacknowledged: Does 2-ME also upregulate the expression of Fas and/or TNF-R1? Or is the increased expression of TNF? without effect, as 2-ME may down-regulate TNF-R1 which was discussed by Purohit [128]? Additionally, it would be interesting to know, whether 2-ME stimulates cells of the immune system to produce FasL/TNF?, increasing the anti-tumour effect in a paracrine fashion? Unfortunately at the moment there are no answers to these questions because no data about the effect of 2-ME on death receptors or their ligands in tumour cells have been published. Only Yue and colleagues showed that 2-ME upregulates CD95 (Fas) in endothelial cells [129]. Further investigations, for example, the use of inhibitory antibodies against Fas and TNF-R1, could clarify the role 2-ME in this pathway.

In addition to the previous presented data of this study, the involvement of p53 in 2-ME treated DS-sarcoma cells was taken into consideration (Fig. 4.1.2). Several publications described the involvement of p53 in 2-ME induced apoptosis [25,130]. However, p53 is not generally needed for the cytotoxic effect of 2-ME. Both p53-dependent and independent mechanisms were reported. Determination of p53 protein expression in DS-sarcoma cells exposed to 1-5 µM 2-ME resulted in a decrease in p53 levels (data not shown) which was not expected, but the finding is in accordance with literature data of Kumar et al., who described the same phenomenon in human prostate cancer cells [131]. As p53 status of DS-sarcoma cells has not yet been investigated it is not clear whether the observed p53 down-regulation is related to mutations in the p53 gene or not.
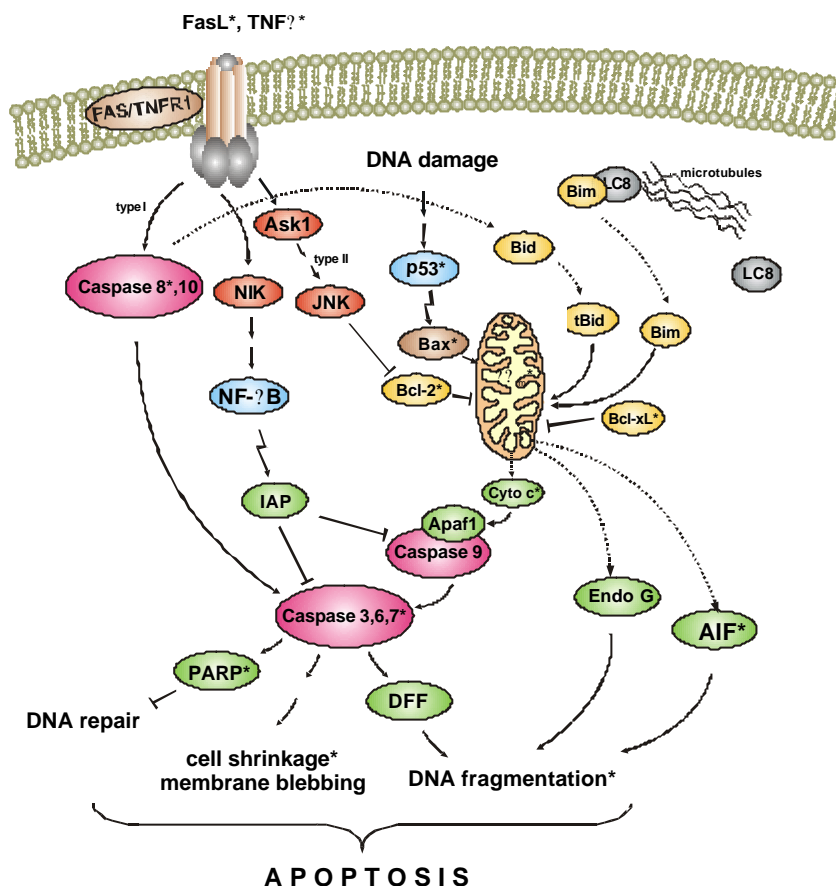
Fig. 4.1.2: Overview showing regulation of apoptosis (simplified). Apoptotic events marked with an asterisk were investigated in this study.

2-ME generally induces apoptosis by the mitochondrial pathway. Translocation of Bax to mitochondria, depolarisation of mitochondrial transmembrane potential ($??_m$) and release of AIF were observed after 2-ME treatment in DS-sarcoma cells. Although caspase-3-like activity was 5-fold increased by 2-ME treatment, pan-caspase inhibitor Z-VAD-FMK could not block DNA fragmentation. Upregulation of FasL and TNF? probably supports the ongoing apoptotic process.

Considering the results of 7-AAD staining, apoptosis is not the only mechanism responsible for 2-ME induced cell death. The small fraction of apoptotic cells in 1 µM and in 5 µM 2-ME treated cells indicate an involvement of necrosis in 2-ME cytotoxicity. The observed swelling of cells exposed to high 2-ME concentration (? 5 µM), may support this presumption. Simultaneous induction of apoptosis and necrosis by anti-cancer drugs as well as shifting from apoptosis to necrosis at higher drug concentrations is a well known phenomenon in anti-cancer therapy [132,133]. In the past, cell death was divided into apoptosis and necrosis, though they may

represent only two extremes of a continuum of intermediate forms of cell demise. There is also a type of cell death, termed aponecrosis, which shares dynamics, molecular and morphological features with both apoptosis and necrosis [134]. The measured DNA fragmentation and Bax translocation in the present study clearly confirm the involvement of apoptosis in 2-ME induced cell death. However, decrease in mitochondrial transmembrane potential, which was determined after 2-ME treatment, is discussed controversially in the literature; both apoptosis and necrosis could be associated with decreased $\Delta\Psi_m$ [17,135]. In contrast to the observed DNA laddering, staining of 2-ME treated cells with 7-AAD did not show a clear staining pattern of apoptotic cell death. Based on these facts, we can state that 2-ME induces apoptosis in DS-sarcoma cells, in which caspases are not necessary for cell death. Supplementary necrosis is probably involved in 2-ME cytotoxicity, especially at higher concentration.

ROS-formation

A dose-dependent increase in ROS-formation in 2-ME treated DS-sarcoma cells could be assessed by four different methods, although the present study could not demonstrate that ROS are initially involved in 2-ME induced apoptosis. Only slight ROS-formation was observed in cells treated with 1 µM 2-ME, whereby caspase-3-like activation and AIF release were more increased than in cells exposed to 5 µM 2-ME, which showed an obvious increase in ROS-formation. In addition, cytotoxic effect of 2-ME could not be decreased by preincubating the cells with six different antioxidants. This finding is in accordance with data of Lin et al., who reported that 2-ME induced apoptosis in the hepatoma cell line HepG2 was not inhibited by the antioxidant magnolol [27]. In contrast, apoptosis in 2-ME treated leukaemia cells could be blocked by the antioxidants ambroxol and N-acety-L-cysteine [15]. These opposed data may imply a cell-specific action of 2-ME. Assuming that 2-ME generates ROS by inhibition of SOD, cells with high levels of SOD could be damaged more potently by 2-ME than cells with low SOD-levels. There are several publications, which report about elevated SOD levels in leukaemia cells compared to normal

lymphocytes [136,137]. Unfortunately, only rare data of SOD levels in sarcoma and hepatoma cells exists. It would be helpful to elucidate the role of SOD status in 2-ME induced cell death by analysing tumour cell lines, that express different amounts of SOD.

Huang and colleagues were the first and only researchers, who showed, that 2-ME inhibits Mg- and CuZn-SOD. They used a cell free system in order to assess the effect of 2-ME on purified Mn- and CuZn-SOD activity, resulting in a concentration dependent decrease in both SOD activities by 2-ME. To verify this finding, Huang exposed cells to [^{3}H] 2-ME for 5 h. Thereafter, cell lysates were prepared and Mg- and CuZn-SOD were precipitated with antibodies. Radioactivity of SOD precipitates was significantly increased compared to control protein precipitates, confirming the result of the cell free assay. Additionally, Huang showed, that overexpression of SOD in leukaemia cells decreased the cytotoxic effect of 2-ME. In addition, in cells treated with SOD antisense S-oligonucleotides, the 2-ME effect was enhanced [15]. In spite of these well-founded results of Huang, data of Kachadourian and the findings of the present study could not confirm them. Kachadourian investigated the effect of 2-ME on SOD activity by using 3 different *in vitro* methods (epinephrine oxidation, hydroethidine oxidation and pulse radiolysis). None of them showed an inhibitory effect of 2-ME on SOD activity. Kachadourian debated, that catecholestrogens interfered with the assay used by Huang, indicating a SOD inhibition, which was not existent [138]. Our present study could not find a decrease in SOD activity, when SOD was preincubated with 2-ME and activity was analysed by the well established pyrogallol assay [47].

Despite these discrepancies, all research groups involved determined an enhanced superoxide anion production in cells treated with 2-ME [15,138]. Inhibition of SOD is probably not the only explication for O_2^--formation. Other reactions, such as redox cycling [139] or interference with the respiratory chain [140], have been suggested for 2-ME analogues. Both reactions would imply the oxidation of estrogens into semiquinone radicals [140], which can result from reaction with cytochrome P450 [139]. It has been shown that estrogen semiquinone radicals react with oxygen yielding O_2^- and the corresponding quinones, the latter being, in turn, reduced by

cytochrome P450 reductase [139]. But these explanations ignore the results of Huang, which showed in cells, that 2-ME binds to SOD and that SOD overexpressing cells are less sensitive to 2-ME [15]. However, extensive mechanisms responsible for the intracellular binding of 2-ME to SOD may be taken into consideration. It could be possible that apart from 2-ME further substances are needed to form an inhibitory complex with SOD. Such complex formation could explain the discrepancies between findings obtained by SOD activity assays using a cell free system and the results of Huang and colleagues who investigated the role of 2-ME on SOD in cells.

Combination of 2-ME with a further ROS-generating treatment

Both *in vitro* and *in vivo* 2-ME therapy was combined with a further ROS-generating treatment. The O_2^- and H_2O_2 generating system hypoxanthine / xanthine oxidase was used as additive treatment *in vitro.* DS-sarcoma cells treated with 2-ME and hypoxanthine/xanthine oxidase (HX/XO) showed a potent decrease in colony formation. Compared to single agent treatments, the combination resulted in a synergistic anti-tumour effect, underlining the great benefit of 2-ME as adjuvant. However, the used *in vitro* model has some weak points: (1) ROS-generation via HX/XO is located outside the cell, only the less polar substance H_2O_2 can diffuse through the cell membrane. (2) Enzymatic production of O_2^- by HX/XO is temporary, because activity of XO decreases fast in *in vitro* conditions. Due to these facts, the observed *in vitro* results provide only an indication of the actual effect of the combined therapy *in vivo.*

For *in vivo* investigations another ROS-generating treatment was chosen, whose high effectiveness was reported by Frank et al [70]. This treatment includes 44°C hyperthermia, respiratory hyperoxia and injection of xanthine oxidase. The combination of this treatment with a single 2-ME application cured 6 out of 17 tumours, showing no regrowth over a period of 30 days. In contrast to the 2-ME data obtained *in vitro*, only minor effect of 2-ME (i.p. injection) on tumour growth were found *in vivo.* A reduction in tumour growth rate from 1.9 to 2.5 days (volume doubling time) was observed under 2-ME treatment. Tumour cure was not achieved in any of the

animals treated with 2-ME alone and only in 3 out of 13 tumours in the group receiving the ROS-generating treatment. Several other researchers showed, that oral application of 2-ME potently inhibited tumour growth [28,141]. However, oral application of 2-ME had not been considered suitable for analysis of the acute impact of 2-ME as a ROS-generating treatment modality. Therefore, in the present study a schedule was chosen which uses only a single 2-ME dose 2 h prior to the other ROS-generating treatment. This single application of 2-ME may only incur a limited anti-tumour effect but supports the hypothesis that a distinct level of ROS (or downregulation of antioxidative defence mechanisms) must be reached within tumour tissue in order to induce oxidative injury severe enough to cause destruction of tumour tissue. Choosing a single i.p. injection of 2-ME, long-term effects like 2-ME binding to microtubuli and inhibition of angiogenesis, were precluded.

The *in vivo* result point at the therapeutic potential of 2-ME in an adjuvant setting. Hereby, the data of Huober, showing a potentiation of the anti-tumour effect through the combination of radiation and 2-ME administration, could be confirmed by the first time [24]. The high efficiency of treatment regimes including 2-ME application as adjuvant, may be caused by overflowing the tumour cell with reactive oxygen species. These enormous amounts of ROS cannot be quenched by cellular antioxidative defence systems, least of all, if SOD activity is diminished by 2-ME.

4.2   ALA-PDT

The objective of this study was to elucidate cellular mechanisms that are responsible for the high tumour response rate of rat sarcomas, receiving simultaneously hyperthermia and 5-aminolevulinic acid based photodynamic therapy. Therefore, ROS-formation (lipidperoxidation, nitration of proteins), apoptotic events and tumour "rescue response" were investigated. The findings demonstrate that the combination of hyperthermia and ALA-PDT dramatically enhanced protein nitrosylation and apoptosis. Heat shock protein and MMP expression were decreased by this treatment, influencing the anti-cancer therapy positively.

Apoptosis

Unpublished data of Dr. rer. nat. D.K. Kelleher (Institute of Physiology and Pathophysiology, University of Mainz, Germany) showed that synchronous combination of ALA-PDT and HT enhances the anti-tumour effect in a synergistic manner. 90 days after tumour treatment, only 17% of animals exposed to hyper-thermia or to ALA-PDT showed no regrowth of the tumour. At the same time, 60% of animals treated with the combination of ALA-PDT and HT were cured. All sham-treated animals reached the set tumour volume limit of 3.5 ml within 8 days.

Determination of apoptotic related biochemical changes in tumour tissue showed that both treatments, HT and ALA-PDT, induced apoptosis in DS-sarcomas. The combination of these treatments resulted in an enhanced apoptotic effect which was measured by DNA fragmentation analysis and TUNEL-assay. Looking at apoptotic events upstream of nuclear changes like caspase activation, unexpected results have been observed, because caspase activity did not correlate with the observed nuclear changes. Caspase-3-like and caspase-8 activity were greatest in HT and HT + PDT treated tumours. Although ALA-PDT as single treatment activated caspases, the combination of HT + ALA-PDT did not increase caspase activity compared to HT treatment. Massive production of ROS in tumours exposed to HT and ALA-PDT may explain this observation. SH groups of caspases are essential for their catalytic

activity. On exposure to free radicals these SH groups can be inactivated. In M14 melanoma cells, O_2^- and H_2O_2 seem to promote cell survival due to the inactivation of caspases [142]. The fact, that caspase activity did not correlate with the apoptotic end point, may portend that caspases play a secondary role in ALA-PDT induced apoptosis. Unfortunately, there are no published data about the necessity of caspases in apoptosis by ALA-PDT. Using the photosensitiser hypericin for PDT, Vantieghem et al. showed, that the pan caspase inhibitor Z-VAD-FMK could not inhibit apoptosis in hybridoma PC60 cells. Whereas in PC60 cells overexpressing Bcl-2, caspases were needed for the apoptotic process [143]. This finding confirms the key role of mitochondria in photodynamic cell damage. Mitochondrial damage induced by PDT is probably the initial event in apoptosis. Consequence of which is the release of apoptotic factors like cytochrome c, AIF and procaspases, that induce caspase-independent and dependent apoptotic processes. After the release of cytochrome c into the cytosol, activation of caspase-9, followed by caspaspe-3, -6 and −7 has been described for several cell types treated with PDT [144-146]. The results of caspase-3-like and caspase-8 activity assay of this study agree with the data of Granville et al.. They showed that caspase-8 is activated after cytochrome-c has been released during PDT-induced apoptosis, an event which is triggered by caspase-3 [145].

Cleavage of RNA is an uncommonly investigated parameter in apoptosis. Houge and colleagues reported the specific cleavage of 28S rRNA in several cell lines undergoing apoptosis and suspected, that RNA fragmentation may be as general a feature of apoptosis as internucleosomal DNA fragmentation [147]. In tumours exposed to ALA-PDT and HT RNA cleavage appeared immediately after treatment, whereas no RNA fragmentation was observed in the other groups. Analysis of tumours, resected 18 h after treatment, showed, that RNA cleavage progressed after ALA-PDT + HT treatment, and appeared in ALA-PDT treated tumours. However we could not corroborate the hypothesis of Houge et al, due to the fact, that DNA fragmentation was assessed after HT and ALA-PDT, whereas RNA cleavage was only seen after

ALA-PDT. The very fast degradation of RNA in HT + ALA-PDT treated tumours may point up the high efficiency of this therapy to damage the tumour.

ROS-generation

ROS formation was induced by ALA-PDT, as demonstrated by immunohistological assessment of 3-nitrotyrosine. Formation of 3-nitrotyrosine is a convenient marker of reactive nitrogen-centered oxidants like peroxynitrite. Substrates for the generation of peroxynitrite, responsible for tyrosine nitration, are superoxide anion and NO. The latter is mainly synthesised by endothelial cells, neutrophiles and macrophages. The reaction rate of the formation is approximately four times faster than the scavenging of superoxide with CuZn-SOD [148,149]. Because of this fast reaction rate, increase in superoxide anion level results in peroxynitrite formation, if NO molecules are present. Peroxynitrite reacts with a number of biological molecules including small molecular weigth nucleophiles and phenolics, proteins, lipids and DNA [150].
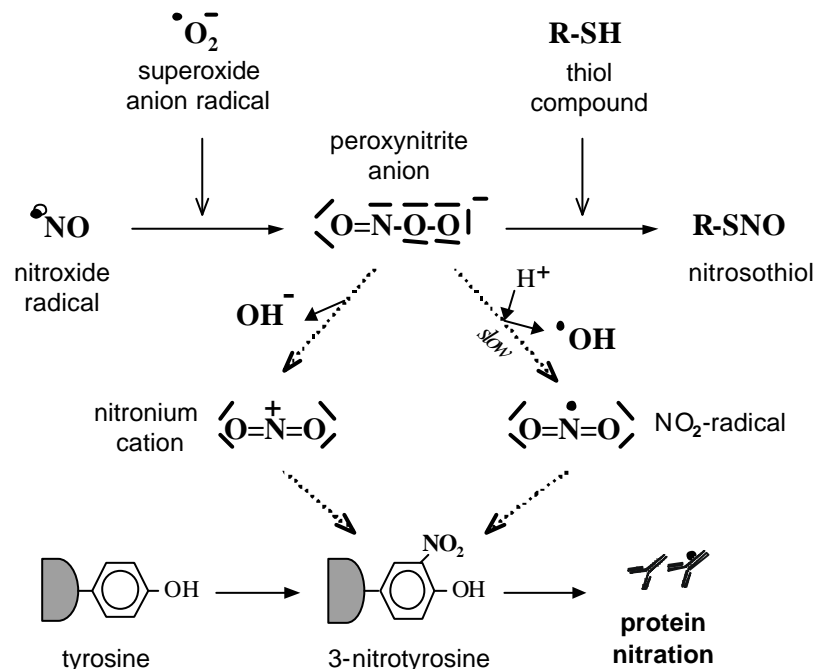
Fig. 4.2.1: Formation of nitrosylated proteins by peroxynitrite. Nitroxide radical and superoxide anion radical react to the highly reactive peroxynitrite anion. Reaction of peroxynitrite with proteins, leading to the formation of 3-nitrotyrosine residues (protein nitration). Intermediate products of this reaction are nitronium cations and NO_2-radicals [66].

In this study a significant increase in protein nitrosylation was observed after HT, ALA-PDT and the combination of both. In tumours treated with the combined therapy, formation of 3-nitrotyrosine was greatest, indicating an enhanced effect of this treatment regime. Nitrosylated proteins were located around vessels, due to the fact, that NO is generally built by the endothelium. Both, an increase in superoxide anion and NO formation could be responsible for the observed protein nitrosylation. Several publications have shown that ALA-PDT as well as hyperthermia induce superoxide anion formation [151-153]. The vasoactive substance NO is also modulated by PDT and HT. Coutier et al. reported, that PDT with the photosensitiser Foscan increased NO release out of macrophages [154] and Gupta and colleagues showed that phthalocyanine PDT enhanced nitrite production in fibrosarcoma and epidermoid carcinoma cells [155]. Hyperthermia also stimulates the release of NO [156]. In recent years many reports related to peroxynitrite and nitrotyrosine have been published. But the consequence of tyrosine nitration on protein function is not yet fully understood. One effect of protein nitrosylation is the advanced degradation of these proteins by the 20S proteasome [157,158]. Additionally, alteration of protein function, mainly enzyme inhibition has been reported by several researchers [157,159]. Beside this „negative" regulation, it is supposed, that protein nitrosylation is involved in signal transduction, comparable to protein phosphorylation [160,161]. Crow supposed, that low levels of peroxynitrite may have signalling function under normal physiological conditions. However, higher concentrations probably activate apoptosis in peroxynitrite sensitive cell types, whereas more resistant cell types may require the peroxynitrite-mediated oxidative damage [162,163].

"Rescue response"

Regarding the results of tumour "rescue response" proteins after HT and ALA-PDT treatment, the enhanced degradation of oxidised proteins discussed above could contribute to these findings. Conversely to literature data [97,164,165], hyperthermia and ALA-PDT treated DS-sarcomas showed decreased HO-1 expression, although HO-1 is generally upregulated by oxidative stress [166]. This phenomenon may be

explained by several mechanisms. (1) Highly oxidised/nitrated HO-1-protein may underlie enhanced proteolysis [157], (2) Structural protein modification by oxidation/nitration may lead to a diminished antibody binding in Western blot detection. (3) Hypoxic tumours (like DS-sarcoma [167]) express constitutive high levels of HO-1 protein [168,169], which may be responsible for no further HO-1 upregulation after tumour treatment. The greatest HO-1 downregulation was observed in tumours simultaneously treated with HT and ALA-PDT, indicating massive alteration in protein metabolism after this treatment.

Results of HSP70 expression are partly in agreement with published data, due to some discrepancies in the literature. As it is well known, hyperthermia upregulates HSP70 expression, which was confirmed by a 2.1-fold increase of HSP70 18 h after HT treatment. Contrary, ALA-PDT treatment notedly decreased HSP70 expression at this time point, which is in good agreement with data of Xue and colleagues. They found that in Chinese hamster V79 cells, treated with aluminum phthalocyanine PDT, HSP70 mRNA and protein expression was decreased [170]. On the other hand, Gomer et al. reported, that Photofrin-PDT induced HSP70 expression *in vivo*, while it failed to induce a cellular HSP response *in vitro* [164]. Additionally, HSP70 response is dependent on the photosensitisers used. Subcellular localisation properties of the photosensitiser that govern the site of singlet oxygen generation may be the critical determinant in whether photosensitiser-mediated PDT activates the heat shock response [164].

Upregulation of HSP70 is an undesired effect of several anti-tumour therapies, due to its ability to inhibit apoptosis [171,172]. This inhibition is provoked by two mechanisms: First, HSP70 can bind to Apaf-1, thereby preventing activation of capspase-9 [95,173]. Furthermore, HSP70 forms a complex with AIF, which leads to the inactivation of AIF [93]. The present study showed that combination of HT and ALA-PDT abolished the upregulation of HSP70 by hyperthermia, indicating no enhanced tumour protection against this combined treatment.

Beside the enhanced formation of heat shock proteins, tumour cells can protect their life by upregulation of antioxidative systems. Glutathione (GSH) is the main water-

soluble cellular antioxidant, which detoxifies hydroperoxides to H_2O and the corresponding alcohol. Determination of reduced glutathione within tumours, showed that ALA-PDT treatment decreased GSH dramatically 18 h after treatment. The combination of ALA-PDT and HT could not enhance the decrease in GSH amount. Specific oxidation of GSH to GSSG/GSSX catalysed by glutathione peroxidase can lead to a decrease in GSH. Furthermore, it is known, that thiol containing molecules are preferred targets for oxidation by peroxynitrite (Fig. 4.2.1) [174]. Unspecific oxidation of GSH may enhance the proteolytic degradation of these peptides. The observed progression of GSH decrease between time point 1 and 2 of tumour resection corroborates this theory. Oxidation, modification and successive degradation of GSH eliminate the GSH-based antioxidative defence system, weakening the tumour defence against ROS-generating anti-cancer treatments. A study with buthionine sulfoximine (BSO), an agent that reduces GSH levels, showed that the efficiency of PDT could be enhanced by lowering intracellular GSH levels [175]. These results concerning glutathione may explain the findings of Chen who showed, that PDT followed by HT evoked a synergistic tumour response, reversing the sequence results only in an additive effect [30].

Further investigations assessing the effect of ALA-PDT on enzyme activity showed that ALA-PDT inhibited enzyme activity in most cases. 18 h after ALA-PDT MMP-9 activity was totally eliminated and MMP-2 activity was significantly decreased. The activity of additional three enzymes, hexokinase, phosphodiesterase-1 and lactate dehydrogenase, were investigated (data not shown). Only phosphodiestrase-1 activity was slightly increased by ALA-PDT, activity of the other enzymes was markedly diminished. The combination of HT + ALA-PDT inhibited enzyme activity in the same range as ALA-PDT alone. These data support the hypothesis, that ALA-PDT modifies proteins, leading to a diminished function and an enhanced proteolysis of these proteins. Prior or simultaneous application of ALA-PDT to a further anti-cancer treatment may result in a synergistic effect due to photodynamic modifications in the tumour cell, which weaken the tumour response against the adjuvant treatment.

5   Summary

The present thesis deals with two different ROS-generating anti-cancer treatments: chemotherapy with the endogenous estrogen metabolite 2-methoxyestradiol and 5-aminolevulinic acid based photodynamic therapy. Both treatments were investigated with the rat DS-sarcoma model, which can be used *in vitro* and *in vivo*.

The first part of this thesis shows that 2-methoxyestradiol induces apoptosis in DS-sarcoma cells. Translocation of the pro-apoptotic protein Bax to the mitochondria was identified as initial apoptotic event, followed by a decrease in mitochondrial transmembrane potential and the release of AIF out of the mitochondria. In addition, upregulation of FasL and TNF? by 2-ME, two death receptor ligands, was observed. Although, 2-ME administration resulted in activation of caspases, pan caspase inhibitor Z-VAD-FMK could not block 2-ME induced apoptotic cell death pointing to a caspase-independent mechanism. Furthermore, an increase in formation of reactive oxygen species was observed after 2-ME treatment. However, supplementation with different antioxidants could not decrease the toxic effect of 2-ME. This finding may indicate, that reactive oxygen species are not involved in apoptosis induction, rather they are a consequence of mitochondrial damage.
In vitro and *in vivo* combination of 2-ME with another ROS-generating treatment resulted in a synergistic anti-tumour effect.

In the second part of the thesis anti-tumour effects of 5-aminolevulinic acid based photodynamic therapy combined with simultaneous hyperthermia was investigated. Analysis of apoptosis associated nuclear changes clearly demonstrated the high efficiency of this treatment regime. Formation of reactive compounds (e.g. ROS, nitrogen monoxide, peroxynitrite) which is mainly responsible for toxicity of PDT, could be assessed in the shape of massive protein nitrosylation in tumours treated with PDT alone or the combined treatment. Detection of decreased amounts of heat shock proteins (HSP70 and HO-1) which protect tumour cells against damaging influences, lowered glutathione levels and reduced MMP-activity indicate an increase

in degradation of proteins. This phenomenon may be caused by excessive generation of ROS.

Taken together, the presented studies could demonstrate the high benefit of combining 2-ME resp. ALA-PDT with hyperthermia (or other ROS-generating therapies), which make them interesting candidates for future clinical applications.

6 Zusammenfassung

Die vorliegende Arbeit befasst sich mit zwei unterschiedliche ROS-generierenden Therapien zur Krebsbekämpfung: zum einen mit der Chemotherapie des endogenen Estrogenmetaboliten 2-Methoxyestradiol, sowie der Photodynamischen Therapie, die auf der Gabe von 5-Aminolaevulinsäure basiert. Beide Behandlungsformen wurden mit Hilfe des DS-Sarkom Modells der Ratte untersucht, das sowohl *in vitro* als auch *in vivo* eingesetzt werden kann.

Im ersten Teil dieser Arbeit konnte gezeigt werden, daß 2-ME Apoptose in DS-Sarkom Zellen induziert. Als initiales apoptotisches Ereignis wurde die Translokation des pro-apoptotischen Proteins Bax an das Mitochondrium nachgewiesen, gefolgt von einer Erniedrigung des mitochondrialen Transmembran-potentials und der Freisetzung von AIF aus dem Mitochondrium. Des weiteren wurde eine erhöhte Expression von FasL und TNF? , zwei „death receptor" Liganden, nach 2-ME Gabe beobachtet. Obwohl nach 2-ME-Verabreichung eine Aktivierung von Caspasen gemessen wurde, konnte die Gabe des Pan-Caspase-Inhibitors Z-VAD-FMK den apoptotischen Zelltod nicht verhindern, was auf einen Caspase-unabhängigen Mechanismus schließen lässt. Außerdem wurde eine erhöhte Bildung von reaktiven Sauerstoffspezies nach 2-ME Administration nachgewiesen, durch die Stimulierung mit verschiedenen Antioxidantien konnte jedoch die toxische Wirkung von 2-ME nicht gemindert werden. Dieses Ergebnis deutet darauf hin, daß reaktive Sauerstoffspezies nicht an der Apoptoseinduktion beteiligt sind, sondern als Folge der mitochondrialen Schädigung auftreten.

Die Kombination von 2-ME mit einer weiteren ROS-erzeugenden Therapie zeigte sowohl *in vitro* also auch *in vivo* eine synergistische Steigerung der antitumoralen Wirkung.

Im zweiten Teil wurde die Tumor-inhibierende Wirkung einer auf 5-Aminolaevulin-säure basierten Photodynamischen Therapie, welche mit Hyperthermie kombiniert wurde, untersucht. Dabei konnte durch Bestimmung von Apoptose-assoziierten Veränderungen des Zellkernes der hohe Wirkungsgrad dieser Behandlungsform

gezeigt werden. Die Bildung von reaktiven Verbindungen (z.B. ROS, Stickstoff-monoxid, Peroxynitrit), die hauptsächlich für die PDT vermittelte Toxizität verantwortlich sind, konnten in Form von nitrosylierten Proteinen in Tumoren bestimmt werden, die mit PDT oder der Kombinationstherapie behandelt wurden. Der Nachweis eines verringerten Gehaltes an Hitzeschockproteinen (HSP70 und HO-1), die das Tumorgewebe vor schädigenden Einflüsssen schützen, sowie ein erniedrigter Glutathionspiegels und eine reduzierte MMP-Aktivität, deuten auf eine gesteigerte Inaktivierung und Degradation von Proteinen hin. Diese wird vermutlich durch die exzessive ROS-Bildung verursacht.

Zusammenfassend kann festgestellt werden, daß beide Kombinationstherapien (2-ME + Hyperthermie und ALA-PDT + Hyperthermie) effektiv das Tumorwachstum gehemmt haben, was sie zu interessanten Kandidaten für eine zukünftige klinische Anwendung macht.

7   References

1. Burdon, R. H., Gill, V., and Alliangana, D. Hydrogen peroxide in relation to proliferation and apoptosis in BHK-21 hamster fibroblasts. Free Radic.Res., *24*: 81-93, 1996.

2. Sundaresan, M., Yu, Z. X., Ferrans, V. J., Irani, K., and Finkel, T. Requirement for generation of H2O2 for platelet-derived growth factor signal transduction. Science, *270*: 296-299, 1995.

3. Hampton, M. B., Fadeel, B., and Orrenius, S. Redox regulation of the caspases during apoptosis. Ann.N.Y.Acad.Sci., *854:328-35.*: 328-335, 1998.

4. Das, U. A radical approach to cancer. Med.Sci.Monit., *8*: RA79-RA92, 2002.

5. Carmody, R. J. and Cotter, T. G. Signalling apoptosis: a radical approach. Redox.Rep., *6*: 77-90, 2001.

6. Ren, J. G., Xia, H. L., Just, T., and Dai, Y. R. Hydroxyl radical-induced apoptosis in human tumor cells is associated with telomere shortening but not telomerase inhibition and caspase activation. FEBS Lett., *488*: 123-132, 2001.

7. Kovacic, P. and Osuna, J. A., Jr. Mechanisms of anti-cancer agents: emphasis on oxidative stress and electron transfer. Curr.Pharm.Des, *6*: 277-309, 2000.

8. Goodman, J. and Hochstein, P. Generation of free radicals and lipid peroxidation by redox cycling of adriamycin and daunomycin. Biochem.Biophys.Res.Commun., *77*: 797-803, 1977.

9. Choi, H. J., Jang, Y. J., Kim, H. J., and Hwang, O. Tetrahydrobiopterin is released from and causes preferential death of catecholaminergic cells by oxidative stress. Mol.Pharmacol., *58*: 633-640, 2000.

10. Hour, T. C., Chen, J., Huang, C. Y., Guan, J. Y., Lu, S. H., Hsieh, C. Y., and Pu, Y. S. Characterization of chemoresistance mechanisms in a series of cisplatin-resistant transitional carcinoma cell lines. Anticancer Res., *20*: 3221-3225, 2000.

11. Hockel, M., Knoop, C., Schlenger, K., Vorndran, B., Baussmann, E., Mitze, M., Knapstein, P. G., and Vaupel, P. Intratumoral pO2 predicts survival in advanced cancer of the uterine cervix. Radiother.Oncol., *26*: 45-50, 1993.

12. Kennedy, K. A. Hypoxic cells as specific drug targets for chemotherapy. Anticancer Drug Des, *2*: 181-194, 1987.

13.   Brenner, C. and Kroemer, G. Apoptosis. Mitochondria--the death signal
      integrators. Science, *289*: 1150-1151, 2000.

14.   Gad, F., Viau, G., Boushira, M., Bertrand, R., and Bissonnette, R.
      Photodynamic therapy with 5-aminolevulinic acid induces apoptosis and
      caspase activation in malignant T cells. J.Cutan.Med.Surg., *5*: 8-13, 2001.

15.   Huang, P., Feng, L., Oldham, E. A., Keating, M. J., and Plunkett, W.
      Superoxide dismutase as a target for the selective killing of cancer cells.
      Nature, *407*: 390-395, 2000.

16.   Li, L. Y., Luo, X., and Wang, X. Endonuclease G is an apoptotic DNase when
      released from mitochondria. Nature, *412*: 95-99, 2001.

17.   Halestrap, A. P., Doran, E., Gillespie, J. P., and O'Toole, A. Mitochondria and
      cell death. Biochem.Soc.Trans., *28*: 170-177, 2000.

18.   Seegers, J. C., Aveling, M. L., Van Aswegen, C. H., Cross, M., Koch, F., and
      Joubert, W. S. The cytotoxic effects of estradiol-17 beta, catecholestradiols
      and methoxyestradiols on dividing MCF-7 and HeLa cells. J.Steroid Biochem.,
      32: 797-809, 1989.

19.   Berg, D., Sonsalla, R., and Kuss, E. Concentrations of 2-methoxyoestrogens in
      human serum measured by a heterologous immunoassay with an 125I-
      labelled ligand. Acta Endocrinol.(Copenh), *103*: 282-288, 1983.

20.   Schumacher, G., Kataoka, M., Roth, J. A., and Mukhopadhyay, T. Potent
      antitumor activity of 2-methoxyestradiol in human pancreatic cancer cell lines.
      Clin.Cancer Res., *5*: 493-499, 1999.

21.   Merriam, G. R., Brandon, D. D., Kono, S., Davis, S. E., Loriaux, D. L., and
      Lipsett, M. B. Rapid metabolic clearance of the catechol estrogen 2-
      hydroxyestrone. J.Clin.Endocrinol.Metab, *51*: 1211-1213, 1980.

22.   D'Amato, R. J., Lin, C. M., Flynn, E., Folkman, J., and Hamel, E. 2-
      Methoxyestradiol, an endogenous mammalian metabolite, inhibits tubulin
      polymerization by interacting at the colchicine site. Proc.Natl.Acad.Sci.U.S.A,
      91: 3964-3968, 1994.

23.   Attalla, H., Westberg, J. A., Andersson, L. C., Adlercreutz, H., and Makela, T.
      P. 2-Methoxyestradiol-induced phosphorylation of Bcl-2: uncoupling from
      JNK/SAPK activation. Biochem.Biophys.Res.Commun., *247*: 616-619, 1998.

24.   Huober, J. B., Nakamura, S., Meyn, R., Roth, J. A., and Mukhopadhyay, T.
      Oral administration of an estrogen metabolite-induced potentiation of radiation
      antitumor effects in presence of wild-type p53 in non-small-cell lung cancer.
      Int.J.Radiat.Oncol.Biol.Phys., *48*: 1127-1137, 2000.

25.   Seegers, J. C., Lottering, M. L., Grobler, C. J., van Papendorp, D. H., Habbersett, R. C., Shou, Y., and Lehnert, B. E. The mammalian metabolite, 2-methoxyestradiol, affects P53 levels and apoptosis induction in transformed cells but not in normal cells. J.Steroid Biochem.Mol.Biol., *62*: 253-267, 1997.

26.   Lin, H. L., Liu, T. Y., Wu, C. W., and Chi, C. W. 2-Methoxyestradiol-induced caspase-3 activation and apoptosis occurs through G(2)/M arrest dependent and independent pathways in gastric carcinoma cells. Cancer, *92*: 500-509, 2001.

27.   Lin, H. L., Liu, T. Y., Chau, G. Y., Lui, W. Y., and Chi, C. W. Comparison of 2-methoxyestradiol-induced, docetaxel-induced, and paclitaxel-induced apoptosis in hepatoma cells and its correlation with reactive oxygen species. Cancer, *89*: 983-994, 2000.

28.   Klauber, N., Parangi, S., Flynn, E., Hamel, E., and D'Amato, R. J. Inhibition of angiogenesis and breast cancer in mice by the microtubule inhibitors 2-methoxyestradiol and taxol. Cancer Res., *57*: 81-86, 1997.

29.   Fotsis, T., Zhang, Y., Pepper, M. S., Adlercreutz, H., Montesano, R., Nawroth, P. P., and Schweigerer, L. The endogenous oestrogen metabolite 2-methoxyoestradiol inhibits angiogenesis and suppresses tumour growth. Nature, *368*: 237-239, 1994.

30.   Chen, Q., Chen, H., Shapiro, H., and Hetzel, F. W. Sequencing of combined hyperthermia and photodynamic therapy. Radiat.Res., *146*: 293-297, 1996.

31.   Kohen, E., Santus, R., and Hirschberg, J.G. Photodynamic therapy. In Photobiology, Academic Press, San Diego 471-489, 1995.

32.   Lang, K., Lehmann, P., Bolsen, K., Ruzicka, T., and Fritsch, C. Aminolevulinic acid: pharmacological profile and clinical indication. Expert.Opin.Investig.Drugs, *10*: 1139-1156, 2001.

33.   Casas, A., Fukuda, H., Riley, P., and del, C. B. A. Enhancement of aminolevulinic acid based photodynamic therapy by adriamycin. Cancer Lett., *121*: 105-113, 1997.

34.   Lopez, R. F., Bentley, M. V., Delgado-Charro, M. B., and Guy, R. H. Iontophoretic delivery of 5-aminolevulinic acid (ALA): effect of pH. Pharm.Res., *18*: 311-315, 2001.

35.   Moretti, M. B., Garcia, S. C., and Batlle, A. Porphyrin biosynthesis intermediates are not regulating delta-aminolevulinic acid transport in Saccharomyces cerevisiae. Biochem.Biophys.Res.Commun., *272*: 946-950, 2000.

36.   Sharman, W. M., Allen, C. M., and van Lier, J. E. Role of activated oxygen
      species in photodynamic therapy. Methods Enzymol., *319:376-400.*: 376-400,
      2000.

37.   Foote, C. S. Definition of type I and type II photosensitized oxidation.
      Photochem.Photobiol., *54*: 659, 1991.

38.   Fritsch, C., Stege, H., Saalmann, G., Goerz, G., Ruzicka, T., and Krutmann, J.
      Green light is effective and less painful than red light in photodynamic therapy
      of facial solar keratoses. Photodermatol.Photoimmunol.Photomed., *13*: 181-
      185, 1997.

39.   Kurwa, H. A., Barlow, R. J., and Neill, S. Single-episode photodynamic therapy
      and vulval intraepithelial neoplasia type III resistant to conventional therapy.
      Br.J.Dermatol., *143*: 1040-1042, 2000.

40.   Kinuya, S., Kawashima, A., Yokoyama, K., Kudo, M., Kasahara, Y., Watanabe,
      N., Shuke, N., Bunko, H., Michigishi, T., and Tonami, N. Anti-angiogenic
      therapy and radioimmunotherapy in colon cancer xenografts. Eur.J.Nucl.Med.,
      28: 1306-1312, 2001.

41.   Allman, R., Cowburn, P., and Mason, M. Effect of photodynamic therapy in
      combination with ionizing radiation on human squamous cell carcinoma cell
      lines of the head and neck. Br.J.Cancer, *83* : 655-661, 2000.

42.   Luksiene, Z., Kalvelyte, A., and Supino, R. On the combination of
      photodynamic therapy with ionizing radiation. J.Photochem.Photobiol.B, *52*:
      35-42, 1999.

43.   Prinsze, C., Dubbelman, T. M., and Van Steveninck, J. Protein damage,
      induced by small amounts of photodynamically generated singlet oxygen or
      hydroxyl radicals. Biochim.Biophys.Acta, *1038*: 152-157, 1990.

44.   Kavarnos, G., Nath, R., and Bongiorni, P. Visible-light and X irradiations of
      Chinese hamster lung cells treated with hematoporphyrin derivative.
      Radiat.Res., *137*: 196-201, 1994.

45.   Henderson, B. W., Waldow, S. M., Potter, W. R., and Dougherty, T. J.
      Interaction of photodynamic therapy and hyperthermia: tumor response and
      cell survival studies after treatment of mice in vivo. Cancer Res., *45*: 6071-
      6077, 1985.

46.   Waldow, S. M., Henderson, B. W., and Dougherty, T. J. Hyperthermic
      potentiation of photodynamic therapy employing Photofrin I and II:
      comparison of results using three animal tumor models. Lasers Surg.Med., *7*:
      12-22, 1987.

47.   Marklund, S. and Marklund, G. Involvement of the superoxide anion radical in the autoxidation of pyrogallol and a convenient assay for superoxide dismutase. Eur.J.Biochem., *47*: 469-474, 1974.

48.   Milhavet, O., McMahon, H. E., Rachidi, W., Nishida, N., Katamine, S., Mange, A., Arlotto, M., Casanova, D., Riondel, J., Favier, A., and Lehmann, S. Prion infection impairs the cellular response to oxidative stress. Proc.Natl.Acad.Sci.U.S.A, *97*: 13937-13942, 2000.

49.   Budd, S. L., Castilho, R. F., and Nicholls, D. G. Mitochondrial membrane potential and hydroethidine-monitored superoxide generation in cultured cerebellar granule cells. FEBS Lett., *415*: 21-24, 1997.

50.   Siwik, D. A., Tzortzis, J. D., Pimental, D. R., Chang, D. L., Pagano, P. J., Singh, K., Sawyer, D. B., and Colucci, W. S. Inhibition of copper-zinc superoxide dismutase induces cell growth, hypertrophic phenotype, and apoptosis in neonatal rat cardiac myocytes in vitro. Circ.Res., *85*: 147-153, 1999.

51.   LeBel, C. P., Ischiropoulos, H., and Bondy, S. C. Evaluation of the probe 2',7'-dichlorofluorescein as an indicator of reactive oxygen species formation and oxidative stress. Chem.Res.Toxicol., *5*: 227-231, 1992.

52.   Mayer, D., Mühlhöfer, A., and Biesalski, H. K. A modified system to evaluate the potency of anti-oxidative compounds in different cell types in vitro. Eur.J.Med.Res., *6*: 1-8, 2001.

53.   Jentzsch, A. M., Bachmann, H., Furst, P., and Biesalski, H. K. Improved analysis of malondialdehyde in human body fluids. Free Radic.Biol.Med., *20*: 251-256, 1996.

54.   Jentzsch, A. M., Bachmann, H., Furst, P., and Biesalski, H. K. Improved analysis of malondialdehyde in human body fluids. Free Radic.Biol.Med., *20*: 251-256, 1996.

55.   Kroemer, G. The proto-oncogene Bcl-2 and its role in regulating apoptosis. Nat.Med., *3*: 614-620, 1997.

56.   Li, L., Lorenzo, P. S., Bogi, K., Blumberg, P. M., and Yuspa, S. H. Protein kinase C delta targets mitochondria, alters mitochondrial membrane potential, and induces apoptosis in normal and neoplastic keratinocytes when overexpressed by an adenoviral vector. Mol.Cell Biol., *19*: 8547-8558, 1999.

57.   Wakabayashi, T. Structural changes of mitochondria related to apoptosis: swelling and megamitochondria formation. Acta Biochim.Pol., *46*: 223-237, 1999.

58.   Leprat, P., Ratinaud, M. H., Maftah, A., Petit, J. M., and Julien, R. Use of nonyl acridine orange and rhodamine 123 to follow biosynthesis and functional

assembly of mitochondrial membrane during L1210 cell cycle. Exp.Cell Res., *186*: 130-137, 1990.

59. Cryns, V. and Yuan, J. Proteases to die for. Genes Dev., *12*: 1551-1570, 1998.

60. Nicholson, D. W., Ali, A., Thornberry, N. A., Vaillancourt, J. P., Ding, C. K., Gallant, M., Gareau, Y., Griffin, P. R., Labelle, M., Lazebnik, Y. A., and . Identification and inhibition of the ICE/CED-3 protease necessary for mammalian apoptosis. Nature, *376*: 37-43, 1995.

61. Harris, J. L., Peterson, E. P., Hudig, D., Thornberry, N. A., and Craik, C. S. Definition and redesign of the extended substrate specificity of granzyme B. J.Biol.Chem., *273*: 27364-27373, 1998.

62. Rao, R. V., Hermel, E., Castro-Obregon, S., del Rio, G., Ellerby, L. M., Ellerby, H. M., and Bredesen, D. E. Coupling endoplasmic reticulum stress to the cell death program. Mechanism of caspase activation. J.Biol.Chem., *276*: 33869-33874, 2001.

63. Obermuller-Jevic, U. C., Francz, P. I., Frank, J., Flaccus, A., and Biesalski, H. K. Enhancement of the UVA induction of haem oxygenase-1 expression by beta-carotene in human skin fibroblasts. FEBS Lett., *460*: 212-216, 1999.

64. Philpott, N. J., Turner, A. J., Scopes, J., Westby, M., Marsh, J. C., Gordon-Smith, E. C., Dalgleish, A. G., and Gibson, F. M. The use of 7-amino actinomycin D in identifying apoptosis: simplicity of use and broad spectrum of application compared with other techniques. Blood, *87*: 2244-2251, 1996.

65. Kuhn, K. S., Krasselt, A. I., and Furst, P. Glutathione and glutathione metabolites in small tissue samples and mucosal biopsies. Clin.Chem., *46*: 1003-1005, 2000.

66. Frank, J., Pompella, A., and Biesalski, H. K. Histochemical visualization of oxidant stress. Free Radic.Biol.Med., *29*: 1096-1105, 2000.

67. Westermarck, J. and Kahari, V. M. Regulation of matrix metalloproteinase expression in tumor invasion. FASEB J., *13*: 781-792, 1999.

68. Leber, T. M. and Balkwill, F. R. Zymography: a single-step staining method for quantitation of proteolytic activity on substrate gels. Anal.Biochem., *249*: 24-28, 1997.

69. United Kingdom Co-ordinating Committee on Cancer Research (UKCCCR) Guidelines for the Welfare of Animals in Experimental Neoplasia (Second Edition). Br.J.Cancer, *77*: 1-10, 1998.

70. Frank, J., Kelleher, D. K., Pompella, A., Thews, O., Biesalski, H. K., and Vaupel, P. Enhancement of oxidative cell injury and antitumor effects of

localized 44 °C hyperthermia upon combination with respiratory hyperoxia and xanthine oxidase. Cancer Res., *58*: 2693-2698, 1998.

71.   Kelleher, D. K., Thews, O., Rzeznik, J., Scherz, A., Salomon, Y., and Vaupel, P. Water-filtered infrared-A radiation: a novel technique for localized hyperthermia in combination with bacteriochlorophyll-based photodynamic therapy. Int.J.Hyperthermia, *15*: 467-474, 1999.

72.   Vaupel, P., Kelleher, D. K., and Kruger, W. Water-filtered infrared-A radiation: a novel technique to heat superficial tumors. Strahlenther.Onkol., *168*: 633-639, 1992.

73.   Monteiro, H. P., Abdalla, D. S., Augusto, O., and Bechara, E. J. Free radical generation during delta-aminolevulinic acid autoxidation: induction by hemoglobin and connections with porphyrinpathies. Arch.Biochem.Biophys., *271*: 206-216, 1989.

74.   Gross, A., McDonnell, J. M., and Korsmeyer, S. J. BCL-2 family members and the mitochondria in apoptosis. Genes Dev., *13*: 1899-1911, 1999.

75.   Wolter, K. G., Hsu, Y. T., Smith, C. L., Nechushtan, A., Xi, X. G., and Youle, R. J. Movement of Bax from the cytosol to mitochondria during apoptosis. J.Cell Biol., *139*: 1281-1292, 1997.

76.   Schlesinger, P. H., Gross, A., Yin, X. M., Yamamoto, K., Saito, M., Waksman, G., and Korsmeyer, S. J. Comparison of the ion channel characteristics of proapoptotic BAX and antiapoptotic BCL-2. Proc.Natl.Acad.Sci.U.S.A, *94*: 11357-11362, 1997.

77.   Zamzami, N., Brenner, C., Marzo, I., Susin, S. A., and Kroemer, G. Subcellular and submitochondrial mode of action of Bcl-2-like oncoproteins. Oncogene, *16*: 2265-2282, 1998.

78.   Joza, N., Susin, S. A., Daugas, E., Stanford, W. L., Cho, S. K., Li, C. Y., Sasaki, T., Elia, A. J., Cheng, H. Y., Ravagnan, L., Ferri, K. F., Zamzami, N., Wakeham, A., Hakem, R., Yoshida, H., Kong, Y. Y., Mak, T. W., Zuniga-Pflucker, J. C., Kroemer, G., and Penninger, J. M. Essential role of the mitochondrial apoptosis-inducing factor in programmed cell death. Nature, *410*: 549-554, 2001.

79.   Lorenzo, H. K., Susin, S. A., Penninger, J., and Kroemer, G. Apoptosis inducing factor (AIF): a phylogenetically old, caspase-independent effector of cell death. Cell Death.Differ., *6*: 516-524, 1999.

80.   Sallmann, F. R., Bourassa, S., Saint-Cyr, J., and Poirier, G. G. Characterization of antibodies specific for the caspase cleavage site on poly(ADP-ribose) polymerase: specific detection of apoptotic fragments and mapping of the

necrotic fragments of poly(ADP-ribose) polymerase. Biochem.Cell Biol., *75*: 451-456, 1997.

81. Algeciras-Schimnich, A., Shen, L., Barnhart, B. C., Murmann, A. E., Burkhardt, J. K., and Peter, M. E. Molecular ordering of the initial signaling events of CD95. Mol.Cell Biol., *22*: 207-220, 2002.

82. Kim, J. W., Joe, C. O., and Choi, E. J. Role of receptor-interacting protein in tumor necrosis factor-alpha -dependent MEKK1 activation. J.Biol.Chem., *276*: 27064-27070, 2001.

83. Kubota, T., Miyagishima, M., Frye, C. S., Alber, S. M., Bounoutas, G. S., Kadokami, T., Watkins, S. C., McTiernan, C. F., and Feldman, A. M. Overexpression of tumor necrosis factor- alpha activates both anti- and pro-apoptotic pathways in the myocardium. J.Mol.Cell Cardiol., *33*: 1331-1344, 2001.

84. Droin, N., Bichat, F., Rebe, C., Wotawa, A., Sordet, O., Hammann, A., Bertrand, R., and Solary, E. Involvement of caspase-2 long isoform in Fas-mediated cell death of human leukemic cells. Blood, *97*: 1835-1844, 2001.

85. Wolf, B. B., Schuler, M., Echeverri, F., and Green, D. R. Caspase-3 is the primary activator of apoptotic DNA fragmentation via DNA fragmentation factor-45/inhibitor of caspase-activated DNase inactivation. J.Biol.Chem., *274*: 30651-30656, 1999.

86. Arends, M. J., Morris, R. G., and Wyllie, A. H. Apoptosis. The role of the endonuclease. Am.J.Pathol., *136*: 593-608, 1990.

87. Daugas, E., Nochy, D., Ravagnan, L., Loeffler, M., Susin, S. A., Zamzami, N., and Kroemer, G. Apoptosis-inducing factor (AIF): a ubiquitous mitochondrial oxidoreductase involved in apoptosis. FEBS Lett., *476*: 118-123, 2000.

88. Lee, M. C., Chung, Y. T., Lee, J. H., Jung, J. J., Kim, H. S., and Kim, S. U. Antioxidant effect of melatonin in human retinal neuron cultures. Exp.Neurol., *172*: 407-415, 2001.

89. Gey, K. F. Optimum plasma levels of antioxidant micronutrients. Ten years of antioxidant hypothesis on arteriosclerosis. Bibl.Nutr.Dieta, 84-99, 1994.

90. Brenneisen, P., Wenk, J., Klotz, L. O., Wlaschek, M., Briviba, K., Krieg, T., Sies, H., and Scharffetterkochanek, K. Central role of ferrous/ferric iron in the ultraviolet b irradiation-mediated signaling pathway leading to increased interstitial collagenase (Matrix-degrading metalloprotease (Mmp)-1) And stromelysin-1 (Mmp-3) Mrna levels in cultured human dermal fibroblasts. CC981314 Journal of Biological Chemistry, *273*: 5279-5287, 1998.

91.   Suzuki, M., Teramoto, S., Matsuse, T., Ohga, E., Katayama, H., Fukuchi, Y., and Ouchi, Y. Inhibitory effect of ambroxol on superoxide anion production and generation by murine lung alveolar macrophages. J.Asthma, *35*: 267-272, 1998.

92.   Garcia-Calvo, M., Peterson, E. P., Leiting, B., Ruel, R., Nicholson, D. W., and Thornberry, N. A. Inhibition of human caspases by peptide-based and macromolecular inhibitors. J.Biol.Chem., *273*: 32608-32613, 1998.

93.   Ravagnan, L., Gurbuxani, S., Susin, S. A., Maisse, C., Daugas, E., Zamzami, N., Mak, T., Jaattela, M., Penninger, J. M., Garrido, C., and Kroemer, G. Heat-shock protein 70 antagonizes apoptosis-inducing factor. Nat.Cell Biol., *3*: 839-843, 2001.

94.   Mosser, D. D., Caron, A. W., Bourget, L., Meriin, A. B., Sherman, M. Y., Morimoto, R. I., and Massie, B. The chaperone function of hsp70 is required for protection against stress-induced apoptosis. Mol.Cell Biol., *20*: 7146-7159, 2000.

95.   Saleh, A., Srinivasula, S. M., Balkir, L., Robbins, P. D., and Alnemri, E. S. Negative regulation of the Apaf-1 apoptosome by Hsp70. Nat.Cell Biol., *2*: 476-483, 2000.

96.   Ryter, S. W. and Tyrrell, R. M. The heme synthesis and degradation pathways: role in oxidant sensitivity. Heme oxygenase has both pro- and antioxidant properties. Free Radic.Biol.Med., *28*: 289-309, 2000.

97.   Ewing, J. F., Haber, S. N., and Maines, M. D. Normal and heat-induced patterns of expression of heme oxygenase-1 (HSP32) in rat brain: hyperthermia causes rapid induction of mRNA and protein. J.Neurochem., *58*: 1140-1149, 1992.

98.   Gomer, C. J., Luna, M., Ferrario, A., and Rucker, N. Increased transcription and translation of heme oxygenase in Chinese hamster fibroblasts following photodynamic stress or Photofrin II incubation. Photochem.Photobiol., *53*: 275-279, 1991.

99.   Dennery, P. A. Regulation and role of heme oxygenase in oxidative injury. Curr Top.Cell Regul.2000.;36.:181.-99., *36:181-99*: 181-199, 2000.

100.   Vacca, A., Ribatti, D., Ria, R., Pellegrino, A., Bruno, M., Merchionne, F., and Dammacco, F. Proteolytic activity of human lymphoid tumor cells. Correlation with tumor progression. Dev.Immunol., *7*: 77-88, 2000.

101.   Kim, W. J., Kakehi, Y., and Yoshida, O. Multifactorial involvement of multidrug resistance-associated [correction of resistance] protein, DNA topoisomerase II and glutathione/glutathione-S-transferase in nonP-glycoprotein-mediated

multidrug resistance in human bladder cancer cells. Int.J.Urol., *4*: 583-590, 1997.

102.   Aamdal, S., Fodstad, O., and Pihl, A. Some procedures to reduce cis-platinum toxicity reduce antitumour activity. Cancer Treat.Rev., *14*: 389-395, 1987.

103.   Beckman, J. S., Ischiropoulos, H., Zhu, L., van der, W. M., Smith, C., Chen, J., Harrison, J., Martin, J. C., and Tsai, M. Kinetics of superoxide dismutase- and iron-catalyzed nitration of phenolics by peroxynitrite. Arch.Biochem.Biophys., *298*: 438-445, 1992.

104.   Kong, S. K., Yim, M. B., Stadtman, E. R., and Chock, P. B. Peroxynitrite disables the tyrosine phosphorylation regulatory mechanism: Lymphocyte-specific tyrosine kinase fails to phosphorylate nitrated cdc2(6-20)NH2 peptide. Proc.Natl.Acad.Sci.U.S.A, *93*: 3377-3382, 1996.

105.   Pryor, W. A., Jin, X., and Squadrito, G. L. One- and two-electron oxidations of methionine by peroxynitrite. Proc.Natl.Acad.Sci.U.S.A, *91*: 11173-11177, 1994.

106.   Pryor, W. A., Squadrito, G. L., and Friedman, M. A new mechanism for the toxicity of ozone. Toxicol.Lett., *82-83:287-93.*: 287-293, 1995.

107.   Karoui, H., Hogg, N., Joseph, J., and Kalyanaraman, B. Effect of superoxide dismutase mimics on radical adduct formation during the reaction between peroxynitrite and thiols--an ESR-spin trapping study. Arch.Biochem.Biophys., *330*: 115-124, 1996.

108.   Mohr, S., Stamler, J. S., and Brune, B. Mechanism of covalent modification of glyceraldehyde-3-phosphate dehydrogenase at its active site thiol by nitric oxide, peroxynitrite and related nitrosating agents. FEBS Lett., *348*: 223-227, 1994.

109.   Shackelford, R. E., Innes, C. L., Sieber, S. O., Heinloth, A. N., Leadon, S. A., and Paules, R. S. The Ataxia telangiectasia gene product is required for oxidative stress-induced G1 and G2 checkpoint function in human fibroblasts. J.Biol.Chem., *276*: 21951-21959, 2001.

110.   Bellosillo, B., Villamor, N., Lopez-Guillermo, A., Marce, S., Esteve, J., Campo, E., Colomer, D., and Montserrat, E. Complement-mediated cell death induced by rituximab in B-cell lymphoproliferative disorders is mediated in vitro by a caspase-independent mechanism involving the generation of reactive oxygen species. Blood, *98*: 2771-2777, 2001.

111.   Carmody, R. J. and Cotter, T. G. Oxidative stress induces caspase-independent retinal apoptosis in vitro. Cell Death.Differ., *7*: 282-291, 2000.

112.   Marzo, I., Perez-Galan, P., Giraldo, P., Rubio-Felix, D., Anel, A., and Naval, J. Cladribine induces apoptosis in human leukaemia cells by caspase-dependent

and -independent pathways acting on mitochondria. Biochem.J., *359*: 537-546, 2001.

113. Borner, C. and Monney, L. Apoptosis without caspases: an inefficient molecular guillotine? Cell Death.Differ., *6*: 497-507, 1999.

114. Granville, D. J., Cassidy, B. A., Ruehlmann, D. O., Choy, J. C., Brenner, C., Kroemer, G., van Breemen, C., Margaron, P., Hunt, D. W., and McManus, B. M. Mitochondrial release of apoptosis-inducing factor and cytochrome c during smooth muscle cell apoptosis. Am.J.Pathol., *159*: 305-311, 2001.

115. van Loo, G., Schotte, P., van Gurp, M., Demol, H., Hoorelbeke, B., Gevaert, K., Rodriguez, I., Ruiz-Carrillo, A., Vandekerckhove, J., Declercq, W., Beyaert, R., and Vandenabeele, P. Endonuclease G: a mitochondrial protein released in apoptosis and involved in caspase-independent DNA degradation. Cell Death.Differ., *8*: 1136-1142, 2001.

116. Li, H., Zhu, H., Xu, C. J., and Yuan, J. Cleavage of BID by caspase 8 mediates the mitochondrial damage in the Fas pathway of apoptosis. Cell, *94*: 491-501, 1998.

117. Heibein, J. A., Goping, I. S., Barry, M., Pinkoski, M. J., Shore, G. C., Green, D. R., and Bleackley, R. C. Granzyme B-mediated cytochrome c release is regulated by the Bcl-2 family members bid and Bax. J.Exp.Med., *192*: 1391-1402, 2000.

118. Stoka, V., Turk, B., Schendel, S. L., Kim, T. H., Cirman, T., Snipas, S. J., Ellerby, L. M., Bredesen, D., Freeze, H., Abrahamson, M., Bromme, D., Krajewski, S., Reed, J. C., Yin, X. M., Turk, V., and Salvesen, G. S. Lysosomal protease pathways to apoptosis. Cleavage of bid, not pro-caspases, is the most likely route. J.Biol.Chem., *276*: 3149-3157, 2001.

119. Bouillet, P., Metcalf, D., Huang, D. C., Tarlinton, D. M., Kay, T. W., Kontgen, F., Adams, J. M., and Strasser, A. Proapoptotic Bcl-2 relative Bim required for certain apoptotic responses, leukocyte homeostasis, and to preclude autoimmunity. Science, *286*: 1735-1738, 1999.

120. Salamon, Z. and Tollin, G. Interaction of horse heart cytochrome c with lipid bilayer membranes: effects on redox potentials. J.Bioenerg.Biomembr., *29*: 211-221, 1997.

121. Daugas, E., Susin, S. A., Zamzami, N., Ferri, K. F., Irinopoulou, T., Larochette, N., Prevost, M. C., Leber, B., Andrews, D., Penninger, J., and Kroemer, G. Mitochondrio-nuclear translocation of AIF in apoptosis and necrosis. FASEB J., *14*: 729-739, 2000.

122. Dumont, C., Durrbach, A., Bidere, N., Rouleau, M., Kroemer, G., Bernard, G., Hirsch, F., Charpentier, B., Susin, S. A., and Senik, A. Caspase-independent

commitment phase to apoptosis in activated blood T lymphocytes: reversibility at low apoptotic insult. Blood, *96*: 1030-1038, 2000.

123. Ghibelli, L., Coppola, S., Fanelli, C., Rotilio, G., Civitareale, P., Scovassi, A. I., and Ciriolo, M. R. Glutathione depletion causes cytochrome c release even in the absence of cell commitment to apoptosis. FASEB J., *13*: 2031-2036, 1999.

124. Petit, P. X., Susin, S. A., Zamzami, N., Mignotte, B., and Kroemer, G. Mitochondria and programmed cell death: back to the future. FEBS Lett., *396*: 7-13, 1996.

125. Shimizu, S., Narita, M., and Tsujimoto, Y. Bcl-2 family proteins regulate the release of apoptogenic cytochrome c by the mitochondrial channel VDAC. Nature, *399*: 483-487, 1999.

126. Susin, S. A., Lorenzo, H. K., Zamzami, N., Marzo, I., Snow, B. E., Brothers, G. M., Mangion, J., Jacotot, E., Costantini, P., Loeffler, M., Larochette, N., Goodlett, D. R., Aebersold, R., Siderovski, D. P., Penninger, J. M., and Kroemer, G. Molecular characterization of mitochondrial apoptosis-inducing factor. Nature, *397*: 441-446, 1999.

127. Johnson, B. W., Cepero, E., and Boise, L. H. Bcl-xL inhibits cytochrome c release but not mitochondrial depolarization during the activation of multiple death pathways by tumor necrosis factor-alpha. J.Biol.Chem., *275*: 31546-31553, 2000.

128. Purohit, A., Singh, A., Ghilchik, M. W., and Reed, M. J. Inhibition of tumor necrosis factor alpha-stimulated aromatase activity by microtubule-stabilizing agents, paclitaxel and 2-methoxyestradiol. Biochem.Biophys.Res.Commun., *261*: 214-217, 1999.

129. Yue, T. L., Wang, X., Louden, C. S., Gupta, S., Pillarisetti, K., Gu, J. L., Hart, T. K., Lysko, P. G., and Feuerstein, G. Z. 2-Methoxyestradiol, an endogenous estrogen metabolite, induces apoptosis in endothelial cells and inhibits angiogenesis: possible role for stress-activated protein kinase signaling pathway and Fas expression. Mol.Pharmacol., *51*: 951-962, 1997.

130. Mukhopadhyay, T. and Roth, J. A. Induction of apoptosis in human lung cancer cells after wild-type p53 activation by methoxyestradiol. Oncogene, *14*: 379-384, 1997.

131. Kumar, A. P., Garcia, G. E., and Slaga, T. J. 2-methoxyestradiol blocks cell-cycle progression at G(2)/M phase and inhibits growth of human prostate cancer cells. Mol.Carcinog., *31*: 111-124, 2001.

132. Pan, J., Simamura, E., Koyama, J., Shimada, H., and Hirai, K. I. Induced apoptosis and necrosis by 2-methylfuranonaphthoquinone in human cervical cancer HeLa cells. Cancer Detect.Prev., *24*: 266-274, 2000.

133. Yeung, T. K., Germond, C., Chen, X., and Wang, Z. The mode of action of taxol: apoptosis at low concentration and necrosis at high concentration. Biochem.Biophys.Res.Commun., *263*: 398-404, 1999.

134. Formigli, L., Papucci, L., Tani, A., Schiavone, N., Tempestini, A., Orlandini, G. E., Capaccioli, S., and Orlandini, S. Z. Aponecrosis: morphological and biochemical exploration of a syncretic process of cell death sharing apoptosis and necrosis. J.Cell Physiol, *182*: 41-49, 2000.

135. Li, Y. Z., Li, C. J., Pinto, A. V., and Pardee, A. B. Release of mitochondrial cytochrome C in both apoptosis and necrosis induced by beta-lapachone in human carcinoma cells. Mol.Med., *5*: 232-239, 1999.

136. Kokoglu, E., Aktuglu, G., and Belce, A. Leucocyte superoxide dismutase levels in acute and chronic leukemias. Leuk.Res., *13*: 457-458, 1989.

137. Yamanaka, N., Nishida, K., and Ota, K. Increase of superoxide dismutase activity in various human leukemia cells. Physiol Chem.Phys., *11*: 253-256, 1979.

138. Kachadourian, R., Liochev, S. I., Cabelli, D. E., Patel, M. N., Fridovich, I., and Day, B. J. 2-methoxyestradiol does not inhibit superoxide dismutase. Arch.Biochem.Biophys., *392*: 349-353, 2001.

139. Liehr, J. G. and Roy, D. Free radical generation by redox cycling of estrogens. Free Radic.Biol.Med., *8*: 415-423, 1990.

140. Roy, D. and Abul-Hajj, Y. J. Estrogen-nucleic acid adducts: guanine is major site for interaction between 3,4-estrone quinone and COIII gene. Carcinogenesis, *18*: 1247-1249, 1997.

141. Banerjeei, S. K., Zoubine, M. N., Sarkar, D. K., Weston, A. P., Shah, J. H., and Campbell, D. R. 2-Methoxyestradiol blocks estrogen-induced rat pituitary tumor growth and tumor angiogenesis: possible role of vascular endothelial growth factor. Anticancer Res., *20*: 2641-2645, 2000.

142. Clement, M. V. and Pervaiz, S. Reactive oxygen intermediates regulate cellular response to apoptotic stimuli: an hypothesis. Free Radic.Res., *30*: 247-252, 1999.

143. Vantieghem, A., Xu, Y., Declercq, W., Vandenabeele, P., Denecker, G., Vandenheede, J. R., Merlevede, W., de Witte, P. A., and Agostinis, P. Different pathways mediate cytochrome c release after photodynamic therapy with hypericin. Photochem.Photobiol., *74*: 133-142, 2001.

144. Carthy, C. M., Granville, D. J., Jiang, H., Levy, J. G., Rudin, C. M., Thompson, C. B., McManus, B. M., and Hunt, D. W. Early release of mitochondrial cytochrome c and expression of mitochondrial epitope 7A6 with a porphyrin-

derived photosensitizer: Bcl-2 and Bcl-xL overexpression do not prevent early mitochondrial events but still depress caspase activity. Lab Invest, *79*: 953-965, 1999.

145.   Granville, D. J., Carthy, C. M., Jiang, H., Shore, G. C., McManus, B. M., and Hunt, D. W. Rapid cytochrome c release, activation of caspases 3, 6, 7 and 8 followed by Bap31 cleavage in HeLa cells treated with photodynamic therapy. FEBS Lett., *437*: 5-10, 1998.

146.   Granville, D. J., Shaw, J. R., Leong, S., Carthy, C. M., Margaron, P., Hunt, D. W., and McManus, B. M. Release of cytochrome c, Bax migration, Bid cleavage, and activation of caspases 2, 3, 6, 7, 8, and 9 during endothelial cell apoptosis. Am.J.Pathol., *155*: 1021-1025, 1999.

147.   Houge, G., Robaye, B., Eikhom, T. S., Golstein, J., Mellgren, G., Gjertsen, B. T., Lanotte, M., and Doskeland, S. O. Fine mapping of 28S rRNA sites specifically cleaved in cells undergoing apoptosis. Mol.Cell Biol., *15*: 2051-2062, 1995.

148.   Cudd, A. and Fridovich, I. Electrostatic interactions in the reaction mechanism of bovine erythrocyte superoxide dismutase. J.Biol.Chem., *257*: 11443-11447, 1982.

149.   Huie, R. E. and Padmaja, S. The reaction of no with superoxide. Free Radic.Res.Commun., *18*: 195-199, 1993.

150.   Radi, R. Peroxynitrite reactions and diffusion in biology. Chem.Res.Toxicol., *11*: 720-721, 1998.

151.   Gilaberte, Y., Pereboom, D., Carapeto, F. J., and Alda, J. O. Flow cytometry study of the role of superoxide anion and hydrogen peroxide in cellular photodestruction with 5-aminolevulinic acid-induced protoporphyrin IX. Photodermatol.Photoimmunol.Photomed., *13*: 43-49, 1997.

152.   Issels, R. D., Fink, R. M., and Lengfelder, E. Effects of hyperthermic conditions on the reactivity of oxygen radicals. Free Radic.Res.Commun., *2*: 7-18, 1986.

153.   Yusof, M., Yildiz, D., and Ercal, N. N-acetyl-L-cysteine protects against delta-aminolevulinic acid-induced 8-hydroxydeoxyguanosine formation. Toxicol.Lett., *106*: 41-47, 1999.

154.   Coutier, S., Bezdetnaya, L., Marchal, S., Melnikova, V., Belitchenko, I., Merlin, J. L., and Guillemin, F. Foscan (mTHPC) photosensitized macrophage activation: enhancement of phagocytosis, nitric oxide release and tumour necrosis factor-alpha-mediated cytolytic activity. Br.J.Cancer, *81*: 37-42, 1999.

155. Gupta, S., Ahmad, N., and Mukhtar, H. Involvement of nitric oxide during phthalocyanine (Pc4) photodynamic therapy-mediated apoptosis. Cancer Res., *58*: 1785-1788, 1998.

156. Hall, D. M., Buettner, G. R., Matthes, R. D., and Gisolfi, C. V. Hyperthermia stimulates nitric oxide formation: electron paramagnetic resonance detection of .NO-heme in blood. J.Appl.Physiol, *77*: 548-553, 1994.

157. Grune, T., Blasig, I. E., Sitte, N., Roloff, B., Haseloff, R., and Davies, K. J. Peroxynitrite increases the degradation of aconitase and other cellular proteins by proteasome. J.Biol.Chem., *273*: 10857-10862, 1998.

158. Souza, J. M., Choi, I., Chen, Q., Weisse, M., Daikhin, E., Yudkoff, M., Obin, M., Ara, J., Horwitz, J., and Ischiropoulos, H. Proteolytic degradation of tyrosine nitrated proteins. Arch.Biochem.Biophys., *380*: 360-366, 2000.

159. Stamler, J. S., Simon, D. I., Jaraki, O., Osborne, J. A., Francis, S., Mullins, M., Singel, D., and Loscalzo, J. S-nitrosylation of tissue-type plasminogen activator confers vasodilatory and antiplatelet properties on the enzyme. Proc.Natl.Acad.Sci.U.S.A, *89*: 8087-8091, 1992.

160. Kamisaki, Y., Wada, K., Bian, K., Balabanli, B., Davis, K., Martin, E., Behbod, F., Lee, Y. C., and Murad, F. An activity in rat tissues that modifies nitrotyrosine-containing proteins. Proc.Natl.Acad.Sci.U.S.A, *95*: 11584-11589, 1998.

161. Kuo, W. N., Kocis, J. M., and Webb, J. Protein denitration/modification by Escherichia coli nitrate reductase and mammalian cytochrome P-450 reductase. Front Biosci., *7:A9-A14.*: A9-A14, 2002.

162. Crow, J. P. Peroxynitrite scavenging by metalloporphyrins and thiolates. Free Radical Biology and Medicine, *28*: 1487-1494, 2000.

163. Estevez, A. G., Spear, N., Manuel, S. M., Barbeito, L., Radi, R., and Beckman, J. S. Role of endogenous nitric oxide and peroxynitrite formation in the survival and death of motor neurons in culture. Prog.Brain Res., *118:269-80.*: 269-280, 1998.

164. Gomer, C. J., Ryter, S. W., Ferrario, A., Rucker, N., Wong, S., and Fisher, A. M. Photodynamic therapy-mediated oxidative stress can induce expression of heat shock proteins. Cancer Res., *56*: 2355-2360, 1996.

165. Ewing, J. F., Raju, V. S., and Maines, M. D. Induction of heart heme oxygenase-1 (HSP32) by hyperthermia: possible role in stress-mediated elevation of cyclic 3':5'-guanosine monophosphate. J.Pharmacol.Exp.Ther., *271*: 408-414, 1994.

166.   Tyrrell, R. M. Approaches to define pathways of redox regulation of a eukaryotic gene: the heme oxygenase 1 example. Methods, *11*: 313-318, 1997.

167.   Thews, O., Kelleher, D. K., Lecher, B., and Vaupel, P. Effect of cell line and differentiation on the oxygenation status of experimental sarcomas. Adv.Exp.Med.Biol., *428:123-8.*: 123-128, 1997.

168.   Doi, K., Akaike, T., Fujii, S., Tanaka, S., Ikebe, N., Beppu, T., Shibahara, S., Ogawa, M., and Maeda, H. Induction of haem oxygenase-1 nitric oxide and ischaemia in experimental solid tumours and implications for tumour growth. Br.J.Cancer, *80*: 1945-1954, 1999.

169.   Sawa, T., Wu, J., Akaike, T., and Maeda, H. Tumor-targeting chemotherapy by a xanthine oxidase-polymer conjugate that generates oxygen-free radicals in tumor tissue. Cancer Res., *60*: 666-671, 2000.

170.   Xue, L. Y., Agarwal, M. L., and Varnes, M. E. Elevation of GRP-78 and loss of HSP-70 following photodynamic treatment of V79 cells: sensitization by nigericin. Photochem.Photobiol., *62*: 135-143, 1995.

171.   Vargas-Roig, L. M., Gago, F. E., Tello, O., Aznar, J. C., and Ciocca, D. R. Heat shock protein expression and drug resistance in breast cancer patients treated with induction chemotherapy. Int.J.Cancer, *79*: 468-475, 1998.

172.   Barnes, J. A., Dix, D. J., Collins, B. W., Luft, C., and Allen, J. W. Expression of inducible Hsp70 enhances the proliferation of MCF-7 breast cancer cells and protects against the cytotoxic effects of hyperthermia. Cell Stress.Chaperones., *6*: 316-325, 2001.

173.   Li, C. Y., Lee, J. S., Ko, Y. G., Kim, J. I., and Seo, J. S. Heat shock protein 70 inhibits apoptosis downstream of cytochrome c release and upstream of caspase-3 activation. J.Biol.Chem., *275*: 25665-25671, 2000.

174.   Atlante, A., Passarella, S., Quagliariello, E., Moreno, G., and Salet, C. Carrier thiols are targets of Photofrin II photosensitization of isolated rat liver mitochondria. J.Photochem.Photobiol.B, *7*: 21-32, 1990.

175.   Jiang, F., Lilge, L., Belcuig, M., Singh, G., Grenier, J., Li, Y., and Chopp, M. Photodynamic therapy using Photofrin in combination with buthionine sulfoximine (BSO) to treat 9L gliosarcoma in rat brain. Lasers Surg.Med., *23*: 161-166, 1998.

Curriculum Vitae

Name:	Christine Lambert
Date of birth:	August 1st, 1971
Place of birth:	Schwäbisch Gmünd, Germany
Nationality:	German

1978-1982	Primary School: Grundschule Böbingen, Germany
1982-1988	Secondary School: Realschule Heubach, Germany School leaving qualification: Mittlere Reife
1988-1991	Secondary School: Hauswirtschaftliches Gymnasium, Schwäbisch Gmünd, Germany School leaving qualification: Abitur
1991-1992	Work experience with handicapped persons Vincent-von-Paul-Werkstätten, Schwäbisch Gmünd, Germany
1992-1998	Study of Nutrition Science, University of Hohenheim, Germany
1997-1998	Diploma thesis: Prof. Dr. H.K. Biesalksi, Institute of Biological Chemistry and Nutrition Science, University of Hohenheim, Germany *Modulation der Calreticulinexpression durch ? - und ? -Tocopherol*
1999-2002	Doctoral thesis: Priv. Doz. Dr. J. Frank, Institute of Biological Chemistry and Nutrition Science, University of Hohenheim, Germany

Declaration/Erklärung

I hereby certify that this thesis is entirely my own work. All materials and references which were required for this work are indicated.

Hiermit erkläre ich, daß ich die vorliegende Dissertation selbständig und unter Verwendung der angegebenen Quellen und Hilfsmittel angefertigt habe.

Stuttgart, den 17.07.2002